Epigenetic control of DNA replication dynamics in mammals

Vom Fachbereich Biologie der Technischen Universität Darmstadt

zur

Erlangung des akademischen Grades

eines Doctor rerum naturalium

genehmigte Dissertation von

Dipl. Biol. Corella Susana Casas Delucchi

aus Lima, Peru

Referent: Prof. Dr. M. Cristina Cardoso

Koreferent: Prof. Dr. Adam Bertl

Tag der Einreichung: 08. April 2011

Tag der mündlichen Prüfung: 10. Juni 2011

Darmstadt 2011

D 17

Una vez más, para el Pápele.

Y para la Mámele, su compañera inseparable.

My three golden rules:

"An experiment worth doing is an experiment worth doing right." (JS)

"Date your theories, never marry them!" (TC)

"Nicht alles wird so heiß gegessen, wie es gekocht wird." (FW)

Index

1. Summary

One of the most critically important processes in any living organism, essential for development and reproduction, is that of the accurate replication of its genome before each cell division. The process of DNA replication can take place millions of times in a single organism and any mistake, if left unrepaired, is potentially transmitted into the next generation. Errors during replication can result in genetic mutations or karyotype aberrations, both of which can lead to disease or death.

The duplication of the genome happens in a well-conserved spatio-temporal manner, a phenomenon implicated in development and disease. This fact indicates that DNA replication needs to be tightly regulated. Further, its precise coordination suggests that distinct genomic regions undergo replication at specific times during S-phase. On the other hand, the regulation of replication is a flexible process throughout development and is, therefore, proposed to be controlled epigenetically. However, the complexity of the mammalian nucleus has hampered the elucidation of how chromatin structure can regulate replication timing. In fact, our understanding of the regulation of replication timing in mammals is restricted to only a few studies with, in part, seemingly contradicting results.

In the context of the present thesis, I set out to study the epigenetic mechanisms that control DNA replication dynamics in mammalian cells. To this end, I took advantage of the most prominent example of facultative heterochromatin, the epigenetically silenced X chromosome (Xi) of female mammalian cells, as well as of the mouse chromocenters, formed by clusters of constitutive heterochromatin. To study their particular replication dynamics and the epigenetic mechanisms controlling them, I used a set of genetic (conditional) knockouts, chemical inhibitory treatments and differentiation assays. The latter allowed me to control whole-chromosome inactivation and the subsequent establishment of the corresponding replication pattern, as well as to distinguish the contribution of different epigenetic markers in this process. I visualized the epigenetic changes and their effects on the replication program *in situ* by immunostainings, also in combination with fluorescence *in situ* hybridization (FISH), confocal and super resolution light microscopy, as well as *in vivo* by time-lapse microscopy over periods of up to two days. This approach prompted the development of several tools for live-cell analysis.

Using established and new tools, I comprehensively assessed the Xi replication dynamics and the effects of modulating different epigenetic modifications of heterochromatin, their cross-talk and the subsequent effects on DNA replication timing and was able to show that histone hypoacetylation, a common mark of the Xi and chromocenters, is responsible for the delayed initiation in replication of both heterochromatic regions. Consequently, I propose that histone hyperacetylation, probably due to its opening effect on chromatin structure, renders some genomic regions prone to be bound by initiation factors earlier and / or more abundantly. This preferential binding, e.g. by replication initiation factors, would thus lead to earlier and concomitantly more efficient replication origin firing. Moreover, I discuss the causal relation between transcriptional inactivity and synchronous replication dynamics, a common feature of developmentally opposite systems, such as the mammalian Xi and the embryos of flies and frogs.

Zusammenfassung

Einer der wichtigsten Prozesse in jedem lebenden Organismus, essenziell für Entwicklung und Fortpflanzung, ist die präzise Duplikation des Genoms vor jeder Zellteilung. Der Prozess der DNA Replikation kann millionenfach in einem einzigen Organismus statt-finden und jeder Defekt, wenn nicht repariert, kann an die nächste Generation weitervererbt werden. Fehler während der DNA Replikation können genetische Mutationen oder karyoty-pische Aberrationen verursachen, die zu Krankheiten bis hin zum Tod führen können.

Die Duplikation des Genoms findet auf eine stark konservierte Weise statt und ihre Organisation spielt eine wichtige Rolle sowohl bei der Entwicklung, als auch bei der Entstehung von Krankheiten. Dieses Phänomen deutet darauf hin, dass die DNA Replikation eng reguliert werden muss. Ferner suggeriert diese genaue Koordination, dass spezifische genomische Regionen an definierten Zeitpunkten der S-phase repliziert werden. Auf der anderen Seite ist die Regulation der Replikation ein flexibler Prozess, der sich entwicklungsbedingt verändern kann. Dies deutet darauf hin, dass die Replikation auf einer epigenetischen Ebene kontrolliert wird. Dennoch hat die Komplexität des Säugerkerns die Aufklärung der Mechanismen erschwert, bei denen die Chromatinstruktur die Replikationsdynamik regulieren kann. In der Tat beschränkt sich unser Verständnis über die zeitliche Regulierung der Replikation in Säugern bis dato auf sehr wenige Studien mit sich scheinbar widersprechenden Ergebnissen.

Im Rahmen dieser Dissertation habe ich mich mit den epigenetischen Mechanismen auseinandergesetzt, die die DNA Replikationsdynamik in Säugerzellen kontrollieren. Zu diesem Zweck habe ich das bedeutendste Beispiel von fakultativen Heterochromatin genutzt, das epigenetisch inaktivierte X Chromosom (Xi) in weiblichen Säugerzellen, sowie Chromozentren aus Mauszellen, die durch Zusammenlagerung von konstitutivem Heterochromatin entstehen. Um die spezifische Replikationsdynamik dieser Regionen und die jeweiligen Kontrollmechanismen zu erforschen, habe ich konditionelle Knockout Zellen, chemisch inhibitorische Behandlungen und Differenzierungsuntersuchungen angewandt. Die Letzteren ermöglichten, die Inaktivierung eines ganzen Chromosoms und die Etablierung des darauffolgenden Replikationsmodus zu steuern. Ferner konnte ich hiermit den Beitrag der verschiedenen epigenetischen Markern in diesem Prozess bestimmen. Die epigenetischen Veränderungen in den verschiedenen Systemen, sowie die entsprechenden Effekte auf das Replikationsprogramm, habe ich mit verschiedenen Methoden visualisiert: *in situ* durch Immunofärbungen, auch in Kombination mit Fluoreszenz *in situ* Hybridisierung, mit konfokaler und superauflösender Lichtmikroskopie, sowie *in vivo* mit Hilfe mikroskopischer Beobachtungen von lebenden Zellen über mehrere Tage. In diesem Rahmen veranlasste die Anwendung der o.g. Ansätze die Entwicklung mehrerer Werkzeuge für eine effizientere Lebendzellanalyse.

Mittels etablierter und neuer Methoden habe ich eine umfangreiche Analyse der Xi Replikationsdynamik durchgeführt. Ich erforschte die Effekte von Manipulationen der epigenetischen Modifikationen von Heterochromatin und untersuchte potentiellen Crosstalk zwischen den verschiedenen Markern, sowie die Auswirkung auf das Replikationstiming der betroffenen Regionen. Ich konnte zeigen, dass die Histonacetylierung, eine gemeinsame epigenetische Modifikation des Xi und der Chromozentren, für die verzögerte Replikation beider heterochromatischen Regionen verantwortlich ist. Aus diesem Grund schlage ich vor, dass Histonacetylierung, vermutlich durch Erhöhung der Chromatinakzessibilität, bestimmte Regionen im Genom dafür anfällig macht, von Initiationsfaktoren früher und / oder besser gebunden zu werden. Die begünstigte Bindung durch z.B. Replikationsaktivierungsfaktoren, könnte demzufolge zu einer früheren und dabei effizienteren Aktivierung von Replikationsursprüngen führen. Weiter diskutiere ich die kausale Beziehung zwischen transkriptioneller Inaktivität und synchroner Replikationsdynamik, eine Gemeinsamkeit vom Säuger-Xi und den Embryonen von Fliegen und Fröschen, in der Entwicklung entgegengesetzten Systemen.

2. Introduction

In prokaryotes, a smaller genome size allows a whole genome to be replicated in a timely fashion from a single replication origin. As genome size and complexity increase, a fast enough replication of the whole genome becomes more difficult to achieve, so that eukaryotic chromosomes possess a large number of origins of replication. In human cells, for instance, the number of origins that fire each cell cycle was estimated to reach a number of 50,000 (Huberman and Riggs, 1966). While in some single cell eukaryotes with less complex genomes, such as *Saccharomyces cerevisiae* (budding yeast), replication origins are defined genetically and their time of firing is constant, already in *Schizosaccharomyces pombe* (fission yeast) replication origins are defined far less stringently. When it comes to metazoan, the search for genetically defined origins has proven elusive and, in spite of great efforts, no consensus sequence defining origins of replication has been identified (Gilbert, 2001).

With the increase in the number of sites of replication initiation, also the regulation of their firing becomes an issue. The cell needs not only to ensure the error-free duplication of the DNA strand in a timely fashion, but it needs as well to avoid the re-replication of any region, that might result from uncoordinated origin firing. To make matters yet more complex, the process of replication cannot be taken out of the nuclear context and thus needs to be coordinated with other chromatin-based processes, particularly that of transcription and the concomitant chromatin remodeling (Schwaiger and Schubeler, 2006). Hence, control and organization of origin firing are of critical importance.

At a global scale, the eukaryotic genome replicates in an organized, non-random manner, meaning that defined genomic regions replicate at distinct S-phase stages, as first described over 50 years ago (Taylor, 1960). In other words: first, not all origins fire at the same time and second, synchronously firing origins are not homogenously distributed throughout the genome. These dynamics result in the appearance of replication patterns that change in a well-conserved manner as S-phase progresses and can be visualized at the light microscopy level (Nakamura et al., 1986). On the other hand, at a single origin level, the firing process is believed to be a stochastic one: not every potential origin fires in every cell cycle (Patel et al., 2006), but can have a rather higher or lower firing efficiency (Raghuraman et al., 2001; Weinreich et al., 2004). What is more, the regulation of DNA replication is not a static process. On the contrary, it is a flexible undertaking that changes throughout development and with differentiation (Calvi et al., 1998; Hatton et al., 1988; Hiratani and Gilbert, 2009; Hyrien et al., 1995; Norio et al., 2005). This observation, as well as the unsuccessful search after an origin defining sequence in metazoan, has led to the proposal that the regulation of DNA replication

cannot be explained at a genetic level alone. Plausible candidates to control replication are epigenetic factors that influence the chromatin state of different genomic regions. Already shown to influence processes such as transcription, epigenetic modifications including DNA methylation, histone modifications, non-coding RNAs, among others, intrinsically define chromatin structure and potentially play a role in any chromatin-based event. Indeed, over the last decades, correlations between certain epigenetic modifications and the particular replication timing of a region have been demonstrated in different organisms (Aran et al., 2011; Eaton et al., 2011; Karnani et al., 2007; Lucas et al., 2007). Furthermore, manipulation of the chromatin state at different regions has been shown to result in changes in replication timing (Table 1).

Still, the influence of epigenetics on the process of origin firing and its regulation, particularly in mammals, is far from being completely elucidated and therefore the role of distinct epigenetic modifications therein is a matter of fervent research. This quest has, however, been complicated by the fact that epigenetic mechanisms seldom exert their influence on chromatin independently from each other, but are characterized by a strong crosstalk. This fact represents a particularly high hurdle in the case of higher eukaryotes with a more complex epigenetic constitution than unicellular eukaryotes or lower metazoans. Moreover, the flexibility epigenetic marks offer as regulatory mechanisms to the cell and their concomitant variability within a population further increase the experimental difficulty in studying their effects on any process. It is, therefore, of extreme importance to combine high-throughput and *in vitro* biochemical methods with single cell *in vivo* studies. While the former are powerful tools and have extensively elucidated the involved molecular players and their interactions, they intrinsically average out the cell-to-cell variability in a population and lack any information on nuclear context, the latter permit a detailed view into cellular processes in high time resolution without losing the biological variability inherent to them. To date, however, live-cell imaging methods are to a great extent limited, partly at the acquisition step, partly at the data analysis step, to rather low to medium throughput. Therefore, the development of tools to increase the efficiency of live-cell analyses constitutes an important component of the present work.

2.1 The molecular process of DNA replication:
From determining replication origins to completing a replication round.

The first steps toward the elucidation of the molecular factors and processes involved in DNA replication were carried out *in vitro*, using bacteriophage T4 and, later, SV40 as models of prokaryotic and eukaryotic replication, respectively (Li and Kelly, 1984; Nossal, 1992). We

owe to these pioneer studies the basis of our understanding on the essential factors, their interactions and the enzymatic processes involved in DNA replication. A further milestone in the DNA replication field was the transition to an *in vivo* eukaryotic system with the establishment of yeast genetics as a tool to study DNA replication (Bell and Dutta, 2002; Dutta and Bell, 1997). Studies in yeast have, without any doubt, been an extremely powerful tool in dissecting the different biochemical components of the replication process in the vast sense, which includes setting up the replication program, the origin firing process as well as DNA synthesis itself. However, it is important to mention that, when it comes to the spatio-temporal regulation of the replication of the genome, intrinsic differences between *S. cerevisiae* and metazoans make it dangerous to generalize conclusions arising from studies carried on in yeast. Nevertheless, the biochemical players of the processes of initiation and replication are well conserved from yeast to mammals and, in general terms, seem to act following the same principles (Figure 1).

Pre-replicative complex assembly: it all starts without a nucleus

Before the actual DNA synthesis process can start during S-phase, the cell has to determine where the next round of replication will, or more precisely, can potentially start. The process of origin determination starts even before G1, during the end of mitosis and thus, in metazoan organisms, without the presence of a nuclear membrane. The first well known step is the binding of the origin recognition complex (ORC, (Palzkill and Newlon, 1988)), six related proteins, conserved from yeast to humans, which bind to potential replication origins during telophase. Their targeting mechanism, however, varies between different eukaryotes (Gilbert, 2001). Whether the ORC subunits form a complex before their binding to chromatin or whether they actually change their association to chromatin throughout the cell cycle or, in turn, are constitutively bound to chromatin is matter of debate. Most likely there are variations in the diverse organisms concerning the binding behavior of the different ORC subunits (DePamphilis, 2005; Ohta et al., 2003; Wu and Nurse, 2009). Conserved throughout eukaryotes is the fact that during the transition from mitosis to G1 the ORC recruits, independently from each other, the initiation factors Cdc6 and Cdt1 (Figure 1). Cdc6, an AAA+ ATPase, might thereby modulate ORC binding to chromatin (Harvey and Newport, 2003) and inhibits ORC binding to non-specific DNA (Mizushima et al., 2000). The main function of the ORC, Cdc6 and Cdt1 is to load the Mcm2-7 complex (MCM) onto chromatin and to thereby complete the licensed pre-replication complex (pre-RC, Figure 1). This is demonstrated by the observation that, after MCM loading, the ORC, Cdc6 and Cdt1 become dispensable for origin firing (Donovan et al., 1997; Harvey and Newport, 2003; Maiorano et al., 2000). In fact, structural studies

have shown that ORC and Cdc6 may function together as a clamp loader complex for opening and closing MCM around at origins (Shin et al., 2003). Recent studies have shown that Cdt1 recruits HBO1 (human acetylase binding to Orc1), a histone H4 acetyltransferase (HAT) to origins and that the HAT activity of HBO1 is required for MCM loading (Miotto and Struhl, 2010). Interestingly, no yeast homologue for HBO1 has been identified so far. Moreover, HBO1 is inhibited by Cdt1 interaction with Geminin (McGarry and Kirschner, 1998; Miotto and Struhl, 2010), another specific factor of metazoan replication. These mechanisms represent an additional origin regulatory step and emphasize the differences of metazoan from unicellular organisms. The MCM renders an origin licensed for replication in the subsequent S-phase. *In vitro*, the MCM has a helicase activity and is therefore considered the putative replication helicase (Forsburg, 2004; Labib and Diffley, 2001), able to unwind origins (Walter and Newport, 2000) and has furthermore even been proposed to stay bound to the replication fork (Aparicio et al., 1997). However, there are several observations that do not immediately fit to this hypothesis. The so-called MCM paradox refers to the seemingly dictory observations of the excess of nuclear MCM and its accumulation far from active replication foci and its proposed role as the replicative helicase (Hyrien et al., 2003; Laskey and Madine, 2003). Nevertheless, a fraction of MCM was recently shown to colocalize with sites of active DNA replication (Masata et al., 2011), supporting their role as replicative helicases. All in all, while the overall principles of the many initiation steps are supported by observations in different organisms, the recruitment of the different factors to origins still need to be elucidated in their molecular details.

Origin firing: transition from the pre-RC to the replication fork

Before the actual process of synthesizing DNA can start, the pre-RC complex must be activated by cyclin-dependent kinase (CDK) and Dbf4-dependent kinase (DDK) activities (Bousset and Diffley, 1998; Donaldson et al., 1998; Pasero et al., 1999; Sheu and Stillman, 2010). Phosphorylation of the pre-RC leads to the recruitment of additional factors to the replication origin, such as Cdc45, Mcm10, Sld3 and GINS (Figure 1, (Gambus et al., 2006; Kamimura et al., 2001; Kanemaki and Labib, 2006)). These initiation factors are necessary for the unwinding of the replication origins and recruitment of the replicative DNA polymerases. The result is an open replication bubble containing two replication forks that will progress in opposite directions as both leading and lagging strands are replicated.

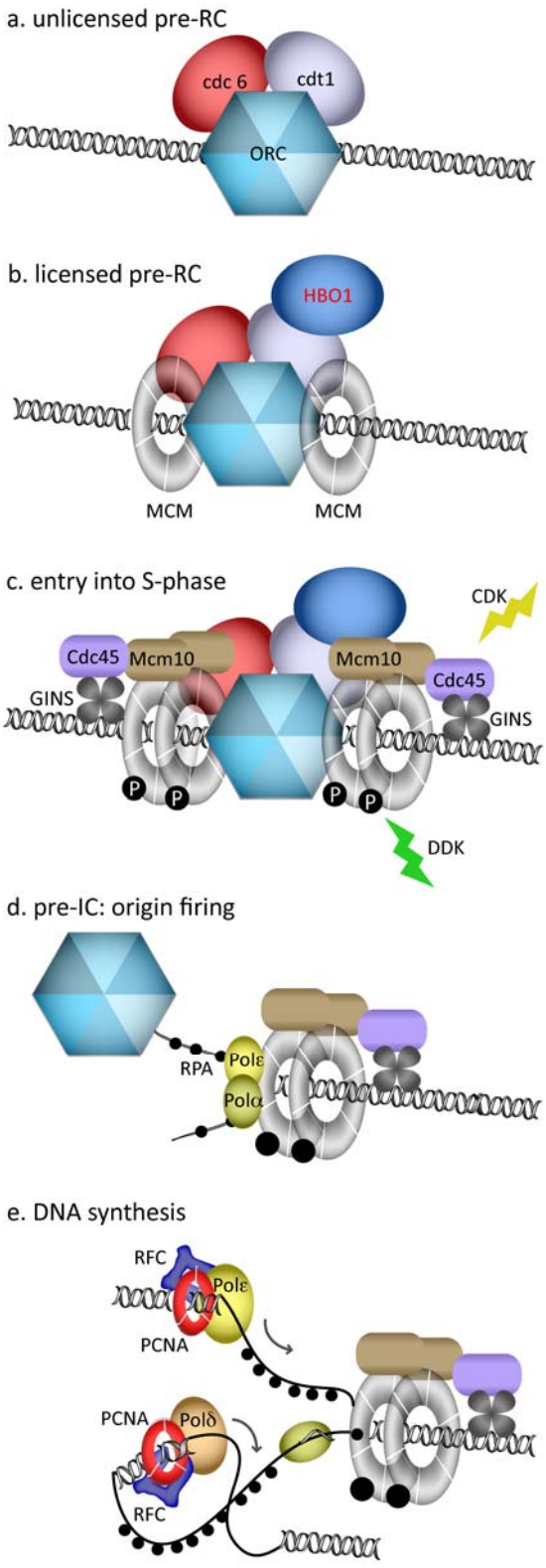

Figure 1 | Schematic representation of the molecular factors involved in (a) replication origin determination, (b) licensing, (c - d) activation and (e) the actual DNA synthesis.
The origin recognition complex (ORC) is either constitutively bound to chromatin or binds during late mitosis. ORC recruits Cdc6 and Cdt1. (b) In metazoan, Cdt1 binds to the histone acetyltransferase HBO1, necessary for pre-RC licensing via MCM loading. (c) DDK and CDK phosphorylation of MCM result in pre-IC (pre-initiation complex) assembly, including bind of Mcm10, Cdc45 and GINS. (d) Origin activation results in unwinding of the double helix. Single stranded DNA is stabilized by the replication protein A (RPA) and DNA polymerases α and ε are recruited. DNA pol α has also a primase activity and is thus able to synthesize RNA primers on single stranded DNA. (e) Processive DNA synthesis is achieved after a polymerase switch to DNA pol δ and the loading of the proliferating cell nuclear antigen (PCNA) sliding clamp by the replication factor C (RFC). Duplication of the lagging strand happens in a discontinuous manner, with several rounds of Okazaki fragments, starting each with the synthesis of a new RNA primer.

In detail, the transition from the pre-RC to the elongating state is initiated by interaction of Mcm10 with Orc2 and various Mcm2-7 subunits (Homesley et al., 2000; Merchant et al., 1997). Cdc45 is then recruited to this complex (Aparicio et al., 1999; Aparicio et al., 1997) and stimulates the helicase activity of the Mcm2-7 complex (Pacek et al., 2006; Zou and Stillman, 2000). Single stranded DNA configuration is stabilized by replication protein A (RPA), which further stimulates origin unwinding (Walter and Newport, 2000). Cdc45 and RPA binding results in the recruitment of the actual DNA synthesis machinery, including the replicative DNA polymerases ε and α to the now open origins (Masumoto et al., 2000), forming the pre-initiation complex (pre-IC, Figure 1). DNA polymerase α (pol α), also a primase, is the only DNA polymerase that can start de novo synthesis on single-stranded DNA and is recruited to origins to synthesize short RNA primers for leading and

lagging strand. After primer synthesis, DNA polymerases are exchanged and DNA pol α is replaced by DNA pol δ or DNA pol ε, which have a higher processivity and proofreading exonuclease activity (Hubscher et al., 2002). This enhanced processivity however requires association to the proliferating cell nuclear antigen (PCNA), a homotrimeric ring that serves as a loading platform for various elongation factors (Görisch and Cardoso, 2006). PCNA is loaded by the replication factor C (RFC) and moves with the replication fork along active sites of replicating DNA. Additionally, the MCM, Cdc45 and GINS also move away from replication origins as part of the replication fork machinery (Gambus et al., 2006), arguing for a role in elongation besides their initiation function.

Thus, one licensed pre-RC, if activated, is unwound and results in the assembly of two replication forks that will progress in opposite directions, normally until they collide with a replication fork originated from a neighboring replication origin (Campbell, 1986). The replicon, or unit of DNA that is replicated from one single replication origin, is generally a symmetric structure with the origin lying in the middle and has an average size of approximately 100 - 200 kb in somatic cells (Lebofsky et al., 2006). The molecular replication machinery, in charge of duplicating a replicon, is termed the replisome.

How replication propagates:
the molecular dynamics of the replisome and the domino model

Once replication has initiated at a limited number of particular loci, it needs to expand throughout the entire genome, so that replication of the entire genome can be achieved in a timely fashion. To reach this goal, further origins need to be activated. Analyses of the molecular dynamics of the replisome have shown that neighboring chromatin foci are not replicated by the same machinery, but rather a new replisome is assembled, preferentially close to already active replication sites (Sporbert et al., 2002). The observation that new sites of DNA replication almost always appear in close proximity to active sites (Leonhardt et al., 2000) has led to the proposal of a domino model, with a “next-in-line” mechanism determining the temporal order of origin activation (Sporbert et al., 2002). Fitting to this proposal, it has been shown in human cells that the spatial continuity of replication foci correlates with their genomic continuity along chromosomes (Maya-Mendoza et al., 2010). This model is further supported by the fact that neighboring replication domains tend to initiate replication at the similar time points on human chromosomes (Woodfine et al., 2004), as well as by the observation that the temporal order of replication of some regions correspond to their linear order in the genome (Braunstein et al., 1982). It has been proposed that this “replication wave” is most likely transmitted by local destabilization or changes in chromatin structure resulting

from replication activity itself. Such structural changes, caused by active replication, would render neighboring regions more prone to replication initiation and result in the self-propagation of replication (Figure 2). What the exact mechanism is, by which initiation of DNA replication is propagated along the genome, is a matter of current research.

Strikingly, this spatio-temporal propagation of replication sites does not happen in a random manner throughout the nucleus. As discussed in the following section, the continuous assembly and disassembly of active replication sites throughout S-phase results in highly conserved nuclear patterns of replication that clearly differ between early , mid and late S-phase.

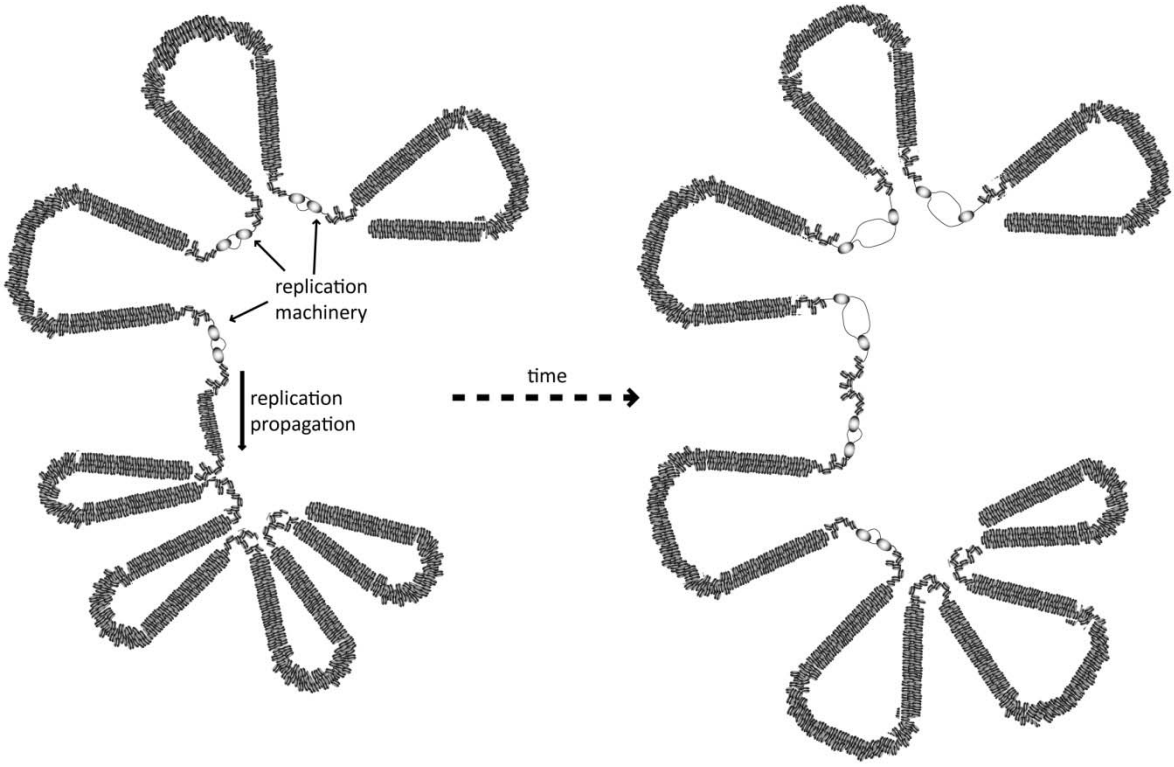

Figure 2 | Spreading of active replication along the genome.
Schematic drawing of how DNA replication might spread along chromatin according to the domino model. Active replication might destabilize higher order structures, rendering replication origins in neighboring chromatin regions more prone to fire. This spreading feature might be an intrinsic effect of the replication machinery, possibly of the replicative helicases or, alternatively, a replication-independent factor might precede the replication machinery and change chromatin conformation as a preparation and thereby positively influence origin firing.

2.2 Organization of DNA replication: a 4D-matter.

DNA replication dynamics

In metazoan cells, *in situ* visualization of sites of active replication results in distinct replication patterns that change as S-phase progresses and are typically divided into early, mid and late (O'Keefe et al., 1992). These patterns are conformed by replication foci, structures of approximately 150 nm in size that are stably maintained throughout the cell cycle (Baddeley et

al., 2010). Each replication focus represents a series of coordinately activated sites of replication that are in close spatial proximity. As replication begins, in early S-phase (Se) many small foci can be observed throughout the nucleus, with exception of the nucle(ol)ar periphery. These regions become populated by somewhat better defined foci during mid S-phase (Sm). Finally, during the second half of S-phase (Sl), larger clusters of active replication foci accumulate into fewer, but bigger structures (Figure 3)(Maison and Almouzni, 2004; O'Keefe et al., 1992).

These replication dynamics are conserved from hydra to mammals (Alexandrova et al., 2003; Pope et al., 2010) and reflect the higher order 3D organization of chromatin in the nucleus (Cremer and Cremer, 2001; Sadoni et al., 2004): early foci correspond to euchromatic regions or R bands, characterized by a high gene density and mostly found in the nuclear interior, mid foci represent facultative heterochromatin, accommodated in the nucle(ol)ar periphery and late foci mark constitutive heterochromatin (Craig and Bickmore, 1993). The existence of such patterns demonstrates that clusters of replication origins are activated in a highly coordinated manner, with some nuclear regions being specifically activated earlier than others. Furthermore, these replication dynamics raise the question of how specific replication origins are selected to fire at a particular S-phase stage.

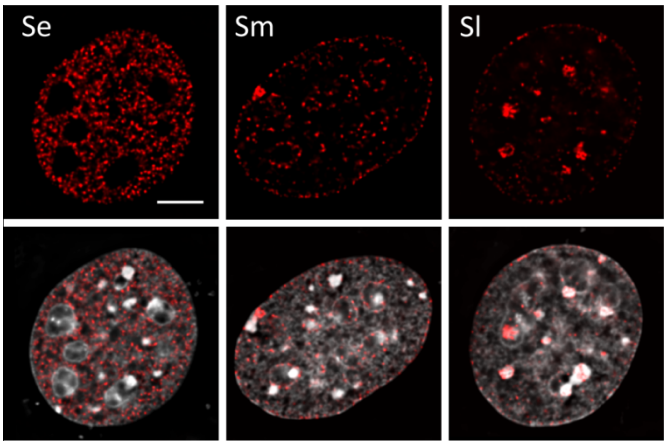

Figure 3 | DNA replication follows at a global level well-conserved spatio-temporal dynamics.
Here, super resolution images of three cells exhibiting the characteristic early (Se), mid (Sm) and late (Sl) S-phase patterns are presented. Sites of nascent DNA were visualized by short pulse incorporation of modified nucleotides and chemical detection after fixation (red). The bottom row shows and overlay of the replication staining (red) and DNA staining by DAPI (grey). Scale bar: 5 µm.

Replication origin definition: from yeast to man

In *S. cerevisiae*, replication origins were identified as those sequences that are able to replicate autonomously when inserted into a plasmid (Autonomous Replication Sequences, ARS), all sharing an ~11 bp long conserved sequence, the autonomous consensus sequence (ACS, (Stinchcomb et al., 1979; Theis et al., 2007). The ACS alone is, however, not sufficient to predict a functional origin. In fact, a region of helical instability close to the ACS is also necessary for origin activity (Eaton et al., 2010), demonstrating that sequence is, even in yeast, not the only determinant of active replication origins.

In higher eukaryotes the sequence elements defining replication origins are much weaker, suggesting that the role of DNA structure and chromatin is crucial (Mechali, 2010). Indeed, in metazoan no consensus sequence defining origins has been found. In fact, any DNA injected into *Xenopus* egg extracts replicates well (Stanojcic et al., 2008) and replications orgins seem to be selected every cell cycle anew (Li et al., 2003).

Probably one of the most striking examples of the flexibility of DNA replication dynamics and origin choice in metazoan is observed in *Xenopus* and *Drosophila* embryos. In these organisms, during early embryogenesis, replication starts at the same time, randomly all over the nucleus. This replication mode results in a very short inter-origin distance of approximately 15 kb (Hyrien et al., 1995; Hyrien and Mechali, 1993). During the mid blastula transition (MBT), there is a re-arrangement in replication dynamics that correlates with the onset of transcription and global changes in chromatin structure and results in much longer inter-origin distances. In mammals, re-programming of mouse somatic cells to a pluripotent state is accompanied by the reduced size of replication domains (Hiratani et al., 2008). These developmental changes clearly illustrate that replication origins are not defined at a sequence level and its selection can adapt throughout cell differentiation.

A series of studies have led to the proposal that there is a correlation between transcription sites and replication origins. For instance, the presence of a promoter or transcription factors can affect replication origin localization and activation in different systems (Cheng et al., 1992; Danis et al., 2004; Ghosh, 2005; Maric et al., 2003; Minami et al., 2006). Nevertheless, the correlation between sites of active transcription and replication origins is not always a positive one: active transcription in a gene silences origins inside that gene (Haase et al., 1994; Mesner and Hamlin, 2005; Sasaki et al., 2006) or reduces the size of the initiation zone and abolishing transcription by deletions in the promoter region allows the body of the gene to become a template for initiation (Danis et al., 2004; Lunyak et al., 2002; Saha et al., 2004). While in some organisms transcriptionally active genes have more efficient origins (Cadoret et al., 2008; Norio et al., 2005; Sequeira-Mendes et al., 2009), this is not always the case (Hiratani et al., 2008; Schwaiger et al., 2009). Studies showing a clear segregation between sites of active replication and active transcription (Wei et al., 1998) have made it clear that transcription activity per se is not a requisite for replication. It has, therefore, been suggested that transcription permissiveness or the chromatin structure that corresponds to it, rather than transcription itself, might facilitate origin activity (Danis et al., 2004; Lunyak et al., 2002).

In general, open chromatin is considered to be a better substrate for both transcription and replication initiation: replication origins are usually enriched in open chromatin structures (Audit et al., 2009; Field et al., 2008; Zhou et al., 2005). Transcriptionally active promoters are

usually H3/H4 hyperacetylated (Berger, 2007), resulting in an open chromatin conformation and making such regions into favorable substrates for DNA replication. Nucleosome positioning has also been involved in origin activity. Although only shown in yeast, ORC might facilitate pre-RC formation by influencing nucleosome positioning (Lipford and Bell, 2001) and placing a nucleosome at DNA replication origin inhibits initiation (Crampton et al., 2008; Simpson, 1990). In *Xenopus* development, the massive rearrangement of replication dynamics that takes place during the MBT is accompanied by histone H1 incorporation, which results in inhibition of pre-RC formation (Lu et al., 1998).

The influence of chromatin structure on defining metazoan replication origins is further strengthened by studies in human cells proposes H4K20m1 to regulate replication origin firing and shows that deficient degradation of PR-Set7, the enzyme responsible for H4K20m1, and the resulting abnormally high levels of H4K20m1 at origins, caused significant re-replication (Tardat et al., 2010). In addition, in *Drosophila* as well as in *Xenopus*, histone acetylation seems to play a role in defining origins of replication (Aggarwal and Calvi, 2004; Danis et al., 2004). Supporting the positive role of histone acetylation levels on replication in human cells, Cdt1-mediated recruitment of the human HBO1, before the onset of S-phase, plays a role in replication by increasing H4 acetylation, chromatin decondensation and subsequently enhancing MCM recruitment (Wong et al., 2010). Indeed, HBO1 knockdown results in a decrease in DNA synthesis and affects progression through S-phase. Importantly, it is the acetylating activity of HBO1 what was necessary for MCM recruitment (Iizuka et al., 2006; Miotto and Struhl, 2010). This effect is counteracted by HDAC11, another partner of Cdt1, which is active during S-phase, prevents MCM recruitment and thereby avoids re-replication (Wong et al., 2010).

Interestingly, transcription and the corresponding open chromatin have been proposed to correlate better to early replication timing rather than replication activity itself. In fact, early origins correlate with actively transcribed genes, while late origins are located in non-transcribed regions (Donaldson, 2005; Gilbert, 2002; Schwaiger and Schubeler, 2006).

Determining DNA replication timing

In *S. cerevisiae*, the time of origin firing is, just like origins themselves, determined to a great extend genetically: the order in which the pre-RC are activated is determined by proximal cis-activity chromosomal elements, telomeres and other DNA sequences for subtelomeric and non-telomeric late-firing origins (Ferguson and Fangman, 1992; Friedman et al., 1996). In *S. pombe*, the definition of early and late replication origins is less clear. However, some genetic

elements have been identified that seem to enforce late replication (Yompakdee and Huberman, 2004) and relocation of an inefficient origin to the early replicating segment leads to earlier replication timing (Hayashi et al., 2007).

Considering the extent of the differences in the epigenetic constitution of unicellular and higher eukaryotes, already obvious in the definition itself of replication origins, observations on replication timing made in yeast cannot be directly transferred to higher organisms. The same is true for lower metazoan, such as *Drosophila*, an important model organism, however lacking major epigenetic modifications found in mammals. Therefore, the structural elements proposed to play a role in yeast and *Drosophila* replication timing are summarized in Table 1, but will not be further discussed here. In the context of the present thesis, I set out to study the mechanisms that are involved in controlling the replication timing of mammalian organisms.

Just like the process of origin selection itself, the determination of replication timing in multicellular organisms is a dynamic process, regulated by developmental and tissue-specific signals (Gregoire et al., 2006; Norio et al., 2005; Zhou et al., 2002). The rearrange of replication dynamics undergone by *Xenopus* embryos during the MBT (see above) is a clear example of this flexibility: before the MBT all origins fire synchronously, so there is no temporal discrimination. After the MBT, with the increase in S-phase length, some origins start firing later than others. In mammals, at least 20% of the genome undergoes changes in replication timing during directed differentiation of ES cells to neural progenitor cells (Hiratani et al., 2008). These examples of developmental regulation demonstrate, similar as for origin selection, that replication dynamics cannot be defined at a sequence level and suggests chromatin structure to play a role in the regulation of replication timing.

The notion of replication timing being controlled by a mechanism beyond the level of DNA sequence first appeared in the 1960's, when it was observed that in female mammalian cells, one of the X chromosomes is randomly inactivated and replicates with drastically different dynamics than its active homologue, clearly showing that genetics alone cannot determine replication timing.

Unlike in yeast, in metazoan there is some correlation between transcription, early replication and open chromatin structure. Already decades ago, the correlation between replication and Giemsa banding patterns was recognized: the usually actively transcribed R-bands replicate early, while gene-poor G-bands are late replicating (Craig and Bickmore, 1993; Drouin et al., 1990). But early replication is not a straightforward consequence of transcriptional activity (Hiratani and Gilbert, 2009). Changes in replication timing are not directly influenced by transcription or influence transcription but rather results from a level of higher-order organiza-

tion of the genome, which in turn affects transcription competence (Hiratani and Gilbert, 2009; McNairn and Gilbert, 2003). For instance, in human erythrocytes, the 100kb ß-globin gene cluster is active, early replicating and histone hyperacetylated. In non-erythrocytes, ß-globin is inactive, late replicating and histone hypoacetylated. Tethering a histone deacetylase (HDAC) to the active promoter causes a shift to late replication. On the other hand, targeting a HAT to the inactive promoter results in advanced replication timing. Importantly, this happens without affecting transcription (Goren et al., 2008).

Table 1 | Summary of recent studies on the epigenetic control of replication timing in lower eukaryotes

Organism	Factor	Publication	Outcome
Yeast	Transcription	(Raghuraman et al., 2001)	No correlation between transcription activity and origin selection.
	Histone acetylation	(Vogelauer et al., 2002)	HDAC Rpd3 KO or HAT Gcn5 recruitment to late origin result in earlier origin firing and concurrent Cdc45 binding.
		(Zappulla et al., 2002)	Sir proteins are sufficient to reprogram an origin from early to late.
		(Knott et al., 2009)	> 100 late origins regulated by Rpd3L.
		(Crampton et al., 2008)	HDAC Sir2 (H4K16 deacetylation) inhibits pre-RC assembly at late origins by promoting unfavorable structures and inhibiting MCM binding.
		(Unnikrishnan et al., 2010)	Multiple acetylated residues are required for efficient origin activation.
	Histone methylation	(Pryde et al., 2009)	HMT Set2: H3K36m1 (with H.ac.) advance binding time of Cdc45, while H3K36m3 and histone deacetylation delay it.
Drosophila	Histone acetylation	(Aggarwal and Calvi, 2004)	Histone hyperacetylation at origins affects ORC binding.
	HP1	(Schwaiger et al., 2010)	HP1 knockdown > 5-10% of genome affected in replication timing, advance replication of centromeric repeats, BUT delayed replication of unique sequences embedded in repeats (targets of HP1).
	Chromatin modifiers / modifications at ORC sites	(Eaton et al., 2011)	ORC binding sites enriched in ISWI, WDS, GAF; early ORI regions enriched in H3K4me, H3K18ac, H3K27ac. Chromatin environment acts as a tunable rheostat to regulate replication initiation events.

As a result of these observations, it has been proposed that the open chromatin structure that permits active transcription is most likely involved in determining replication timing by turning specific chromatin domains into favorable substrates for DNA replication. This might be a

consequence of increased chromatin accessibility to initiation factors resulting, for instance, preferential ORC binding (MacAlpine et al., 2004), or other downstream initiation factors. Consequently, reasonable candidates to control replication timing are epigenetic modification defining chromatin constitution.

2.3 Epigenetics and DNA replication timing in mammals: Orchestrating genome duplication.

Even though epigenetic mechanisms are generally accepted to play a role in determining replication timing, it has proven a difficult task to elucidate which of the many candidates really play a direct role in this process. Especially in higher eukaryotes, which exhibit a more complex epigenetic constitution (Figure 4), such studies have been complicated by the fact that epigenetic modifications exhibit a high level of crosstalk and often act synergistically (Csankovszki et al., 2001). The search after the epigenetic determinant of replication timing in mammals has yielded a series of results that clearly show that chromatin structure plays a major role in determining the spatio-temporal organization of DNA replication. However, the actual direct mechanism responsible for such regulation is far from being clear.

Particularly suitable systems to study the role of epigenetic modifications in controlling replication timing are both the inactive X chromosome in mammals and the mouse chromocenters. These regions are the most prominent examples of facultative and constitutive heterochromatin, respectively, and have been extensively described in their epigenetic constitution (Figure 4). In principle, any epigenetic modification that discriminates between euchromatic and heterochromatic regions is a potential candidate responsible for differential replication timing, ranging from DNA methylation, to histone modifications and higher order chromatin structure. While the manipulation of certain modifications, such as histone H3 trimethylation at lysine 9 (H3K9m3 (Peters et al., 2001)) has been demonstrated to not affect global replication timing (Wu et al., 2006), other epigenetic modifications, such as DNA methylation and histone acetylation are proposed to be involved in controlling replication dynamics.

DNA methylation refers to the covalent addition of a methyl group to the 5' position of the cytosine pyrimidine ring, a modification that, in mammals, takes place only at CpG dinucleotides. CpG islands at promoter regions are usually demethylated. On the other hand, CpGs in constitutive heterochromatin are characterized by high levels of DNA methylation (Lewis et al., 1992). The same is true for promoter regions of the inactive X chromosome in female mammalian cells, as well as of imprinted genes (Li et al., 1993; Pfeifer et al., 1990). All of these regions have a characteristic replication pattern, differing from that of demethylated euchro-

matic regions. Therefore, DNA methylation would be a reasonable candidate to influence replication timing.

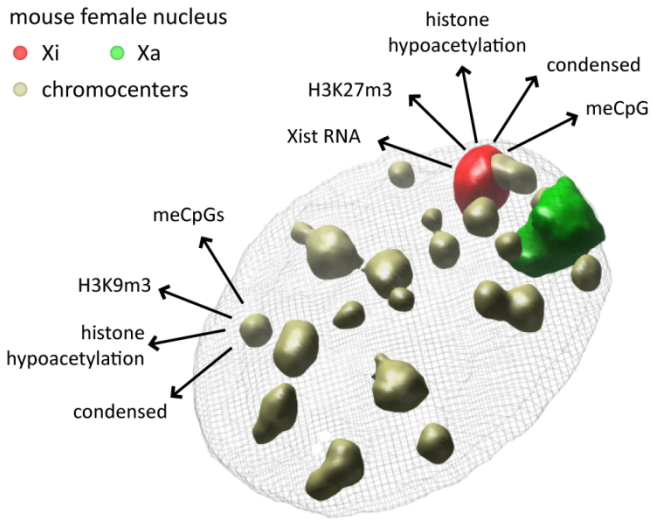

Figure 4 | Epigenetics of hetetochromatin. 3D-reconstruction of a female mouse fibroblast nucleus showing the active and inactive X chromosomes (Xa in green and Xi in red, respectively) and the clusters of pericentric heterochromatin (chromocenters, beige). The epigenetic markers characteristic for the most prominent facultative (Xi) and constitutive (chromocenters) heterochromatic regions are annotated.

Nevertheless, studies on differential replication at imprinted regions have shown that treating cells with the demethylating agent 5-azacytidine did not change replication timing of imprinted foci in relation to the earlier replicating homologous regions (Bickmore and Carothers, 1995). Moreover, it has been postulated that asynchronous replication of imprinted loci is independent of DNA methylation but consistent with differential subnuclear localization (Gribnau et al., 2003). Additionally, DNA methylation is not enough to promote late replication, as shown by *in vitro* methylated DNA inserted into specific genomic sites. Interestingly, these sequences remained early replicating even though transcription was blocked (Schubeler et al., 2000).

In contrast, in mouse F9 terratocarcinoma cells the heterochromatic major satellite repeats are abnormally demethylated and replicate earlier. Moreover, treating RAG fibroblasts with 5-azacytidine causes demethylation of major satellites and subsequently earlier replication (Selig et al., 1988). Furthermore, a study on the replication of the inactive X chromosome has shown that its methylated CpG islands replicated later than the unmethylated ones on the active homologue (Gomez and Brockdorff, 2004). However, the mechanism maintaining the silenced state of the Xi is composed of many layers of partially redundant epigenetic mechanisms (Csankovszki et al., 2001) and it is therefore difficult to ascertain whether the delayed replication timing is actually a consequence of higher DNA methylation. All in all, these studies make it difficult to clearly state the role of DNA methylation in replication timing. On this context, preliminary results from our laboratory have shown that the mammalian Xi exhibits strikingly different replication dynamics than the active homolog, with what appears to be a

synchronous activation of replication sites throughout most of the Xi territory (Figures 5 and 6).

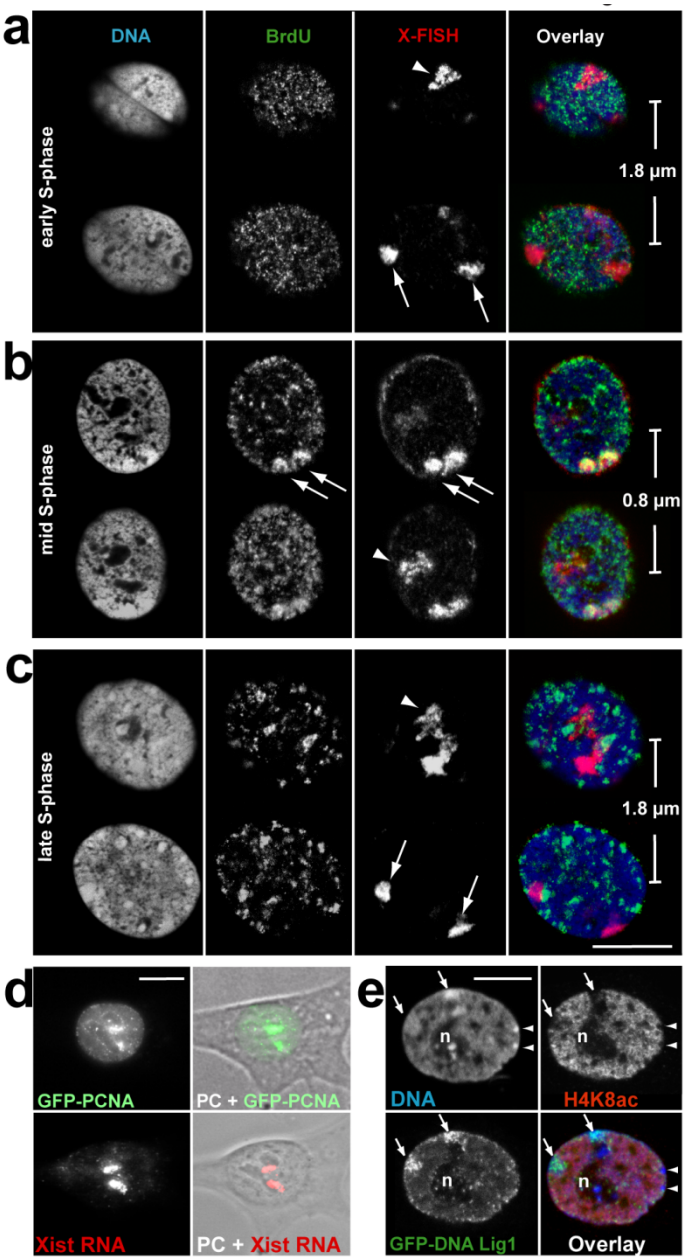

Figure 5. Large mid S-phase replication structures represent bulk chromatin of the inactive X chromosome

C2C12 cells were BrdU pulse-labeled (10 µM, 30 minutes) to visualize actively replicating DNA, while the X chromosome was detected by FISH. DNA was counterstained using TO-PRO 3. Panels show two mid-confocal optical sections of three cells during (a) early, (b) mid or (c) or late S-phase. Arrows point to the Xi territories. Arrowhead points to the Xa territory. Perpendicular scale bars indicate section distances in Z direction. (d) C2C12 cells expressing GFP-PCNA grown on photoetched coverslips featuring an alpha-numerical grid. Individual cells were pre-imaged for characteristic mid S-phase replication structures and post-processed for FISH. After hybridization and detection of a Xist specific probe, cells were re-imaged to compare the localization of the GFP-PCNA and the Xist label. Xist and GFP-PCNA labeled the same chromatin regions within the nucleus. PC: phase contrast. (e) Mid S-phase replication structures are hypoacetylated for histone H4 at lysine 8. Confocal microscopy images of a C2C12 cell stably expressing GFP-DNA Ligase 1 show the characteristic large mid S-phase replication structures (arrows). The cell was stained with an antibody specific for H4K8ac. Note that the replication structures are clearly hypoacetylated, while the DNA staining by TO-PRO 3 indicates a dense, heterochromatic constitution, both hallmarks of the inactive X chromosome. Other heterochromatic regions show likewise reduced H4K8 acetylation levels (arrowheads). n: nucleolus. Scale bars: 10 µm. This figure was kindly provided by Alessandro Brero, Hans-Peter Rahn and Irina Solovei[1].

[1] Published in Casas-Delucchi CS, Brero A, Rahn HP, Solovei I, Wutz A, Cremer T, Leonhardt H, Cardoso MC (2011) Histone acetylation controls the inactive X chromosome replication dynamics. Nature Communications 2:222, doi 10.1038/ncomms1218

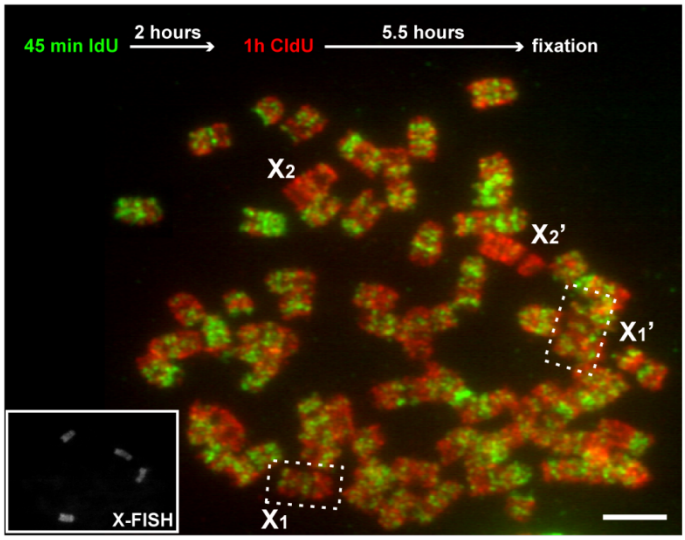

Figure 6. Differential replication dynamics of Xa and Xi visualized in double replication labeled mitotic chromosomes

Mitotic spread of a C2C12 cell double labeled with IdU and CldU in order to simultaneously visualize DNA replicated at two time points with an interval of two hours (see labeling scheme). X chromosomes were identified by FISH (see inset). Two X chromosomes show intense staining of most of their DNA, while having incorporated essentially only the second, i.e. later label (X_2 and $X_{2'}$). The other two X chromosomes (X_1 and $X_{1'}$) show a banded pattern of both labels, with only a limited incorporation of the later label. Scale bar: 10 µm. This figure was kindly provided by Alessandro Brero.[2]

On the other hand, hyperacetylation by trichostatin A (TSA) is, unlike DNA demethylation by 5-azacytidine, able to abolish replication timing imprinting, causing the later loci to replicate earlier when compared to the homologous active regions (Bickmore and Carothers, 1995). Histone hypoacetylation is an epigenetic hallmark of heterochromatic regions (Jeppesen et al., 1992; Kohlmaier et al., 2004) and has indeed been proposed to possibly be the best candidate to determine replication timing (Donaldson, 2005) since high levels of histone acetylation correlate with euchromatin, transcriptional activity and an open chromatin structure.

A study on the tandem ribosomal genes in mouse cells (rDNA) has brought about interesting results regarding chromatin structure and replication timing (Li et al., 2005): 60% of rDNA is actively transcribed, located in the nucleolar interior and early replicating; 40% are inactive, prefer the nuclear periphery and replicate late. The promoter region of active rDNA is demethylated and histone hyperacetylated, while in inactive rDNA the same region is methylated and histone deacetylated (Santoro et al., 2002). The ATP-dependant chromatin remodeling complex NoRC recruits histone modifying and DNA methylating enzymes to the rDNA promoter and functions as a scaffold, coordinating activity of various macromolecular complexes and resulting in the formation of heterochromatin structures. Overexpression of NoRC results

[2] Published in Casas-Delucchi CS**,** Brero A, Rahn HP, Solovei I, Wutz A, Cremer T, Leonhardt H, Cardoso MC (2011) Histone acetylation controls the inactive X chromosome replication dynamics. Nature Communications 2:222, doi 10.1038/ncomms1218

in silencing of active rDNA and shift from early to late replication, suggesting that the heterochromatinization of rDNA delays its replication timing. These results illustrate the extent crosstalk between different mechanisms defining chromatin structure and the concomitant difficulty in discerning which one is directly responsible for the temporal regulation of DNA replication.

Altogether, these studies point out to the fact the epigenetic modifications are somehow involved in determining the replication timing of specific genomic regions. However, their apparently contradictory results show that we have but scratched the surface when it comes to the intricacy of the mammalian epigenetic network regulating replication timing.

2.4 Studying these processes *in vivo* and in real time: A short note on the importance of developing new tools.

In the last years, high-throughput and whole-genome methods based on the analysis of bulk DNA, such as ChIPseq (highthroughput sequencing of immuno-precipitated chromantin) and genomic tiling arrays, have increased our insights into the organization of the eukaryotic genome replication immensely (Schepers and Papior, 2010; Watanabe et al., 2002; Woodfine et al., 2004). Thanks to these studies we have a much more complete view on the distribution of replication origins throughout the genome, as well as on their correlation with transcriptional activity, promoter regions, histone modifications and much more. Such studies have also provided valuable insights on how these parameters change in development, as well as on the degree of conservation / difference between different species and even cell lines (Hiratani and Gilbert, 2009; Schwaiger et al., 2009). On the other hand, single cell based *ex vivo* methods, such as single DNA / chromatin fiber analysis (Cohen et al., 2009; Schwob et al., 2009), which do not average out biological variation in a population, have provided with important information on the one dimensional-distribution of replication sites, as well as on the dynamics of the replication fork.

However, key aspects of the replication program still remain unresolved, in part because most of these methods are intrinsically based on the analysis of populations of cells and on fixed cell or *ex situ* work. The observations and interpretations of such results therefore represent what the bulk of the cells are doing and for the most part do not show what individual cells may be doing (Raghuraman and Brewer, 2010). For instance, a peak in a replication profile shows the location of an origin initiation at that chromosomal location, but it does not give any information on whether the origin fired in all cells or only a subset of them. Another important shortcoming of high throughput sequencing methods is their limitation when it

comes to the analysis of repetitive sequences. Other parameters extracted from bulk DNA analysis, such as the replication half time (the time at which an origin has fired in half of the cells in a population), extracted from 2D gel analyses, is a composite value reflecting those cells in the population that actually fire the origin and those in which the origin was replicated passively by an incoming fork. This kind of data cannot differentiate whether an origin fires early but inefficiently or late but efficiently. *Ex vivo* and *ex situ* single cell experimental methods are further limited in the extent to which they can allow us to make conclusions on dynamics processes that are regulated both spatially and temporally. For instance, in the case of DNA or chromatin fiber analyses, while cell can be synchronized and particular sequence identified, any information on the 3D higher chromatin order is intrinsically lost. Moreover, while the 1D spatial information gained from such methods is by far superior to that of microscopy-based approaches, their temporal resolution is limited by the fact that synchronization of a cell population is not a 100% efficient process. This means that even after synchronizing a population not all cells will indeed go through the same cell cycle stage at the exact same time and the longer the time interval between release and measurement the higher the variability within the population. In addition, most synchronization strategies imply the use of chemical substances that are likely to affect normal cell progression, even after release from the blockage. Therefore, synchronization represents at best an enrichment of cells going through a particular cell cycle stage of a few hours and by no means results in the temporal resolution in a range of milliseconds, as can be achieved by live-cell microscopy techniques.

For these reasons, *in vivo* studies based on single cell experiments are extremely valuable as a complement to high-throughput bulk and *ex vivo* data. In the recent years, time-lapse microscopy has already been presented as a very promising tool in the field of replication (Gorisch et al., 2008; Leonhardt et al., 2000; Sporbert et al., 2002). Developments in this area over the last decade have provided exciting new insights into the dynamics of DNA replication and its regulation. To really take advantage of the technical improvements that allow the observation of living cells and the visualization of the processes taking place in them over periods of up to days, the available biological tools, as well as the computational resources for data analysis, have been challenged to redefine themselves continuously. And so, advances in the field of live-cell microscopy, either by improved imaging techniques, by new molecular ways of visualizing live-cell processes, or by better automated and more robust ways of data analysis, are directly related to advances in our knowledge of cell biology in general and of DNA replication dynamics, in particular.

Within the present thesis, great effort was invested into the development of new, more efficient and reliable ways of visualizing cellular processes and analyzing live-cell microscopy data, laying special emphasis on the power of computational methods. The results of these

efforts are a recurrent theme throughout this work and played an essential role in the biological insights gained from it.

3. Aims of this study

Striking examples of the flexibility of the spatio-temporal DNA replication dynamics throughout development have led to the conclusion that this process cannot be regulated at a genetic level alone. In fact, these observations have pointed to epigenetic mechanisms as possible candidates to regulate replication timing. In mammals, the elucidation of this control mechanism has proven particularly challenging because of the extensive crosstalk between the several layers of epigenetic regulation.

In this study, I attempt to elucidate in a comprehensive manner the contribution of different epigenetic mechanisms in defining replication timing in mammals. To this end, I have taken advantage of the most prominent and epigenetically best defined chromatin regions, namely the inactive X chromosome and the pericentric heterochromatin of mouse cells. I particularly assessed the interaction between the different epigenetic modifications of each region and dissected this extensive crosstalk to ascertain which mechanisms regulate replication timing.

As an essential complement to the whole-genome, high throughput data and other *ex vivo* methods, I put especial effort on the development of tools that allow observations of replication-related processes in single cells *in vivo*. Importantly, the tools developed in the context of this thesis are suited for the study of a vast range of nuclear processes using live-cell imaging techniques.

4. Materials and methods

Cells

To study replication dynamics of the Xi, female mouse myoblasts (C2C12) were grown at 37˚C / 5% CO_2 in DMEM supplemented with 20% FCS and 1 µm/ml gentamycin (Cardoso et al., 1993). A stable cell line expressing GFP-PCNAL2 (Leonhardt et al., 2000) or GFP-DNA Ligase 1 (Cardoso et al., 1997) was selected by a combination of FACSorting, antibiotic selection and screening for GFP positive clones via fluorescence microscopy. To induce histone hyperacetylation C2C12 myoblasts, as well as mouse and human primary fibroblasts, were treated with TSA (Sigma-Aldrich, Steinheim, Germany) at a final concentration of 20 nM for four days.

To study the replication timing of constitutive heterochromatin, wild-type mouse fibroblasts, *Suv39h*1/2 double null, *p53*$^{-/-}$ as well as *p53*$^{-/-}$ and *dnmt1*$^{-/-}$ double knockout cells (MEF-WT, MEF-D15, MEF-P, MEF-PM respectively) were grown at 37˚C / 5% CO_2 in DMEM supplemented with 15 % FCS as previously described (Lande-Diner et al., 2007; Peters et al., 2001). Cells used for immunofluorescence analysis were grown on glass coverslips (#1.5 for high resolution imaging). TSA treatment of wild-type and KO MEFs was performed with a final concentration of 20 nM over 72 hours changing medium with fresh TSA changing medium every day. To analyze replication patterns, cells were pulse-labeled with 100 µM BrdU or 5 µM EdU for 30 min.

Isolation and cultivation of primary cells: Mouse primary fibroblasts were isolated from adult mouse (C57BL/6) ear tissue by cutting the ear tip with a scalpel. The tissue was shaken at 37˚C with 2 mg/ml collagenase NB8 (Serva Electrophoresis, Heidelberg, Germany) in DMEM supplemented with antibiotics for several hours and vortexed repeatedly. Single cells were plated on a dish and cultivated in DMEM supplemented with 20 % FCS at 37˚C / 5% CO_2. As human diploid female cells we used fetal lung fibroblasts WI-38 (Hayflick, 1961) and fibroblasts established from a skin biopsy obtained from a young healthy female, kindly provided by the University of Amsterdam, as well as primary coronary artery smooth muscle cells (Cell System Biotechnologie Vertrieb GmbH, St. Katharinen, Germany; Cat.# CC-2583, Lot.# 15524).

Inactivation of feeder cells and embryonic stem cell culture: Primary MEF cells were expanded until passage 5 and inactivated with mitomycin C at a final concentration of 10 µg/ml for 2.5 h. Inactivated MEF cells can no longer replicate but can be frozen and thawed when needed. Feeders were seeded on culture dishes one day before splitting ES cells on them to allow them to form a monolayer.

ES cells carrying a doxycycline-inducible *Xist* gene in chromosome 11 were cultured as described in (Wutz and Jaenisch, 2000). In short, ES cells were kept in an undifferentiated state by growing them on a feeder cell monolayer and adding 1000 U/ml LIF to the medium. Fresh medium was added daily. The ectopic *Xist* gene was induced by 10 µg/µl doxycycline for six days. To differentiated ES cells, they were grown without feeders and LIF. Additionally, 100 nM retinoic acid was added to the medium freshly every day. Differentiation was visualized on the base of morphological changes.

Adenovirus amplification and infection of mouse cells: Replication incompetent adenovirus expressing Cre recombinase tagged with GFP (AdV-Cre-GFP, Vector Laboratories Inc., Burlingame, USA) was amplified in transgenic HEK293 cells that express the E1 gene missing in the virus genome. Under these conditions, the otherwise unable to proliferate adenovirus is able to replicate and does so very efficiently. HEK293 were grown to a confluency of 60%. On the day of infection fresh medium containing a concentration of 7 x 10^6 U/ml Adenovirus-Cre-GFP was given to the cells (day 0). Cells were incubated under standard growing conditions for 48 h. Successful viral infection was controlled by GFP fluorescence and cell morphology (day 2). Infected cells that produce the adenovirus inflate and eventually detach from the surface. Cells were incubated for further 24 h under standard conditions, without changing the virus-containing medium. At day three cells detached from the growing surface and were collected with the growing medium. The cell suspension was centrifuged for 10 minutes at 900 rpm to pellet the cells and most of the supernatant discarded. Cell pellets were frozen at -80°C, thawed to 37°C in a water bath, froze again in liquid nitrogen and thawed twice. The centrifugation step was repeated under the same conditions, so that the cell debris was pelleted and the supernatant contained the free virus particles. Caesium chloride gradient centrifugation was performed at 30,000 rpm for 2 h at 21°C. The adenovirus particles gathered at a density of ~1.34g/cm^2 and were carefully collected with a syringe by piercing the tube. A second centrifugation step was performed with a gradient of 1.4 – 1.25 g/cm^2 for 16 h under otherwise the same conditions and collected with a syringe. The suspension was run through a column to extract salts. The virus titer was determined by the OD(260), resulting in a concentration of 2x10^7 particles/ml. Aliquots of the adenovirus were then frozen at -80°C and thawed when needed.

Mouse embryonic fibroblasts (MEFs) carrying two conditional knockout ("floxed") alleles of Ezh2 were cultured and recombined using Adeno-Cre or Adeno-Cre-GFP virus as described (Su et al., 2003). In short, on the day of infection fresh medium without FCS was given to the cells at approximately 60% confluency. The volume was kept as low as possible with the cells still well covered. The multiplicity of infection (MOI) was calculated to 50. After 2 hours incubation, medium complete was added to the virus-containing medium. On the next day, suc-

cessful infection was determined by GFP signal. A successful infection gave typically > 90% green fluorescent cells. The supernatant was removed 48 h after infection and cells further cultivated under standard conditions for five more days to get rid of the H3K27m3 mark on the Xi. Female SV40 T-antigen transformed MEFs with a *Xist* deletion on one X chromosome and a "floxed" allele on the other are described in (Csankovszki et al., 2001) and were cultured accordingly and recombined using Adeno-Cre virus as for Ezh2 MEFs[3].

Western Blot analysis and quantification

Control, treated and KO MEFs were harvested, boiled in 1x Laemmli sample buffer and analyzed on Western blots using the following primary antibodies: rabbit-anti-H3 (1/5000, Upstate, Cat #: 07-690), rabbit-anti-H4 (1/1000, Upstate, Cat #: 07-108), rabbit-anti-H3ac (1/500, Upstate, Cat #: 06-599), rabbit-anti-H3K9ac (1/500, Upstate, Cat #: 06-942), rabbit-anti-H4K8ac, dilution 1/1000 (Upstate, Cat #: 06-790), rabbit-anti-H4K12ac (1/1000, provided by T. Jenuwein). The following secondary antibodies were used: anti-rabbit IgG-Alexa Fluor 647 and anti-rabbit IgG-Alexa Fluor 680 (1/4000, Invitrogen). Blots were imaged using 700 nm excitation and quantified on a LI-COR Odyssey Infrared Imaging System using Odyssey V1.2.15 software (Biosciences, Lincoln). Integrated pixel intensity was measured for each band and the respective background signal was subtracted. Signals were normalized to the respective loading control (histone H3 or histone H4) and the fold difference to the respective control cells was calculated using Excel software (Microsoft, Redmont, USA).

Bisulfite treatment and pyrosequencing

Genomic DNA extraction of 4 x 10^6 per condition was performed using QIAmp DNA extraction kit (Qiagen, Valencia, USA) according to the manufacturer's instructions. In short, cells were trypsinized, pelleted and resuspended in PBS. Cells were lysed in the presence of proteinase K for 10 minutes at 56°C. DNA was extracted by ethanol precipitation, run through a QIAamp mini spin column, washed and eluted at room temperature for 2 minutes. The extraction yielded between 30 and 60 µg genomic DNA. Bisulfite conversion of 1.5 µg DNA per sample was performed using EpiTect (Qiagen). Major satellite repeats were amplified by polymerase chain reaction using the following primers: AAAATGAGAAATATTTATTTG (forward) and CCATGATTTTCAGTTTTCTT (reverse), adding 25 mM betaine (Sigma-Aldrich) and 100 mM tetramethyl ammonium chloride (TMAC, Sigma-Aldrich) to the standard reaction to get a specific band of the repetitive sequences containing only one repeat. DNA of three amplification reactions was concentrated by vacuum, pooled together in 50 µl ddH_2O. These step was performed in duplicate and pooled to get 100 µl amplified DNA. This was sent for pyrosequenc-

[3] Adenovirus infection of Xist conditional KO MEFs was performed by A. Brero

ing to Varionostic (Ulm, Germany). Two pyrosequencing reactions, from the 3' and 5' end respectively, were performed per sample in order to cover the eight CpGs on each major satellite unit.

Plasmids and cloning strategy

The MBD domain of MeCP2 (pMeCP2Y.5; (Brero et al., 2005)) was cut with restriction enzymes NheI and BamHI, resulting in the 308 bp insert 1. The GBP of pGFPbinderLacI (Rothbauer et al., 2008) was cut by BglII and HindIII, resulting in the 384 bp insert 2. pEGFP-C2 (Clontech) was cut with NheI and HindIII, resulting in a 3980 bp fragment without the eGFP coding sequence. The compatible ends of BamHI and BglIII allowed for double ligation to insert MBD-GBP into the pEGFP-C2 backbone (pMBD-GBP, 4662bp)[4].

pEGFP-HBO1 was kindly provided by Dr. A. Ehrenhofer-Murray. In short, human HBO1 from pET11cGST-HBO1 (provided by Dr. B. Stillman) was cloned into pEGFP-C1 vector (Clontech), resulting in pEGFP-HBO1. Site-directed mutagenesis at G485A was performed to create a catalytically inactive HBO1, with the following primers: ATGCCTCAGTACATGAGACAGGCCTATGGCAAGATGCTTA (forward) and TAAGCATCTTGCCATAGGCCTGTCTCATGTACTGAGGCAT (reverse). Mutation was confirmed by restriction analysis and DNA sequencing.

Immunofluorescence

Cells were grown on glass coverslips, fixed in 4 % paraformaldehyde (10 minutes at RT) and permeabilized for 20 minutes at RT in 0.5 % triton / PBS. Immunofluorescence staining was performed in 4 % BSA / PBS for 1 h at RT (primary antibodies) and 45 minutes at RT (secondary antibodies). Following primary antibodies were used: anti-DNA Ligase 1 antibody (1/100, (Cardoso et al., 1997)), anti-acetylated histone H3 (1/200, Upstate, Lake Placid, USA, Cat. no. 06-599), anti-acetylated histone H4 (1/200, Abcam, Cambridge, UK, Cat. no. 06-866), anti-acetylated lysine 8 on histone H4 (1/500,(Jeppesen and Turner, 1993) Upstate, Lake Placid, USA, Cat. no. 06-760) and anti-H3K27m3 (1/400, Upstate, Lake Placid, USA, Cat. no. 05-851). For detection of PCNA, incubation for 10 min in ice-cold methanol after formaldehyde fixation was necessary.

***In situ* replication labeling**

To visualize replicating DNA cells were pulse labeled with 5-bromo-2'-deoxyuridine (see respective figures for pulse length, Sigma-Aldrich, Steinheim, Germany) or 5-ethynyl-2'-deoxyuridine (5 µm EdU, Invitrogen, Carlsbad, USA) or double pulse labeled using 5-iodo-2'-deoxyuridine (20 µM IdU, 30 minutes, Sigma-Aldrich, Steinheim, Germany) and 5-chloro-2'-

[4] pMBD-GBP was cloned by Jennifer Völger

deoxyuridine (20 µM CldU, 30 minutes, Sigma-Aldrich, Steinheim, Germany) with a chase of two to three hours after each pulse.

Incorporated BrdU was recognized by mouse anti-BrdU/IdU antibody (5 µg/ml, Becton Dickinson, Franklin Lakes, USA) and anti-BrdU/CldU (1/50, clone BU1/75, Serotec, Oxford, UK) antibodies in conjunction with 10 µg/µl DNase for 1h at 37°C in 1% BSA / 30 mM Tris HCl (pH 8.1) / 0.33 mM $MgCl_2$ / 1 mM Mercaptoethanol. Cells were then washed with 0.5% BSA/1mM EDTA/PBS + 0.01% Tween to stop DNase digestion. EdU was detected using ClickIT chemistry (Invitrogen, Carlsbad, USA) as described in (Salic and Mitchison, 2008). Following secondary antibodies were used: Streptavidin-Alexa 488, 1/500 (Invitrogen), donkey-anti-mouse IgG-Cy3 and donkey-anti-rabbit IgG-Cy3 1/200 (The Jackson Laboratory, Bar Harbor, USA), goat-anti-mouse IgG-Alexa 488 1/200 (Invitrogen). Nuclear DNA was visualized by Hoechst 33258 (1 µg/ml), DAPI (0.05 µg/ml, Sigma-Aldrich, Steinheim, Germany) or TO-PRO-3 (1 µM, Invitrogen, Carlsbad, USA). Cells were mounted in Vectashield antifade (Vector Laboratories Inc., Burlingame, USA).

Fluorescence *in situ* hybridization (FISH) and immuno-FISH

3D-FISH and metaphase FISH with mouse chromosome paints (Rabbitts et al., 1995) were performed according to standard protocol (Cremer et al., 2006). For 3D-FISH cells were, additionally to the fixation steps described for immunostaining, incubated in 20% glycerol for 45 minutes, frozen and thawed in liquid N_2 four times, treated with 0.1 N HCl for five minutes and kept in 50% formamide / 2x SSC over night. For RNA FISH with Xist probes, 0.1 N HCl treatment was omitted. The probe for mouse Xist RNA detection was a PCR product of exon 1 and 6 from a cosmid-cloned *Xist* gene(Herzing et al., 1997). Full-length human *Xist* cDNA was purchased from Origene (Rockville, MD, US, cat. no SC312039). Combination of FISH and halogenated nucleotide detection was performed by sequential detection of the modified nucleotides without additional denaturation after standard FISH detection. C2C12 cells expressing GFP-PCNA were sub-cultured on coverslips engraved with a photoetched alpha numerical grid (Bellco, Vineland, USA) in order to identify and image the same cells *in vivo* (for GFP signal) and after FISH procedure to identify the inactive chromosome.

Immuno-FISH was performed as described (Zinner et al., 2007) using mouse-anti-PCNA (1/200, Dako, Carpinteria, USA), rabbit-anti-H4K8ac (1/200, Upstate (Lake Placid, USA), Cat. no. 06-760) antibodies and DNA probes against mouse repetitive sequences that were labeled with biotinylated dUTPs by nick translation. FISH signal was detected using Streptavidin-Cy5 1/500 (Amersham Biosciences, Piscataway, USA).

Microscopy

Wide-field microscopy: Epifluorescence images were obtained using Zeiss (Zeiss, Jena, Germany) Axiophot II and Axiovert 200 microscopes equipped with Zeiss Plan-Apochromat 63x/1.4 NA oil immersion objective lenses and 12-bit CCD cameras. The Axiovision software was used for image acquisition.

Confocal and spinning disc microscopy: Confocal images were collected using an UltraVIEW VoX spinning disc system on a Nikon Ti microscope equipped with an oil immersion Plan-Apochromat 60x/1.45 NA objective lens (pixel size in XY = 111nm, Z-step = 0.3 – 1 µm) or a Leica TCS SP1 or SP5 confocal laser scanning microscope (Leica, Wetzlar, Germany) equipped with an oil immersion Plan-Apochromat 63x/1.4 NA objective lens (pixel size in XY set to 50 nm, Z-step = 200 nm). Laser lines used were: 405 nm for DAPI detection, 488 nm for GFP / FITC / Alexa488 detection, 561 nm for Cy3 / Rhodamin / mRFP detection and 640 nm for Cy5 detection. Axial chromatic shift was corrected and corresponding RGB-stacks, montages and maximum intensity projections were created using ImageJ (http://rsb.info.nih.gov/ij/). To accurately compare the treated cells between different experiments, all images were taken using identical settings.

High resolution microscopy: To study the structure of constitutive heterochromatin in TSA-treated and KO cells versus wild-type MEFs, DAPI images were acquired at the OMX microscope and reconstructed with 3D structured illumination microscopy as described in (Schermelleh et al., 2008).

Deconvolution microscopy: For additional colocalization analysis of early replication sites and chromocenters, 3D z-stacks of cells were collected using a Delta Vision Olympus widefield microscope with a 60x/1.4 Plan-Apochromatic oil objective (Olympus Corp., Tokyo, Japan) and post-processed by deconvolution (Applied Precision, Issaquah, USA). For this I used a radially averaged PSF recorded on the microscope under comparable image conditions.

Live cell microscopy and mitotic shake-off

Prior to live observation, C2C12 cells stably expressing GFP-PCNA were synchronized via mitotic shake-off. Growing medium was replaced by PBS/EDTA and the adherent growing cells were shaken until most mitotic cells had detached from the substrate, as monitored on the bright field microscope. The detached cells were pelleted and re-plated on a microscopy dish and incubated under standard conditions for five hours. G1 cells were then imaged on the spinning disc microscope. Unsynchronized MEFs were transfected with mRFP-PCNA (Sporbert et al., 2005) and MaSat-GFP (Lindhout et al., 2007) or pMBD-GBP and pEGFP-HBO1 (2 µg total plasmid DNA for 5 x 10^5 cells) using Amaxa (Lonza, Cologne, Germany) nucleofection

(solution V, program B-032) and thereby plated on 35µ optical dishes (Ibidi, Munich, Germany). Transfected cells were incubated under standard growth conditions for 15 h and either used for live cell microscopy or fixed as described above.

4D time lapse experiments were carried out on a UltraVIEW VoX spinning disc confocal system (PerkinElmer, UK) in a closed live cell microscopy chamber (ACU control, Olympus, Japan) heated to 37°C, with 5% CO_2 and 60% air humidity control, on either a Nikon Ti microscope (Nikon, Japan) or a Zeiss Microscope. Image acquisition was performed using a 60x/1.45 NA Planapochromat oil immersion objective lens or a 63x/1.4 Plan-Apochromatic oil (Zeiss). Images were obtained with a cooled CCD camera. Maximum intensity projections were assembled onto QuickTime videos and annotated using ImageJ and Adobe Photoshop.

Image analysis and quantification

Quantification of the effects of drug treatment / virus infection / expression of *Xist* on replication mode was assessed by comparing the frequency of the characteristic Xi replication pattern after BrdU incorporation. The levels of histone acetylation at the inactive territory were quantified by selecting the H3K27m3 accumulation as a ROI and measuring the mean intensity of the acetylation signal in the respective region. For Ezh2 conditional KO, the total nuclear histone acetylation signal was quantified as the Xi lost its H3K27m3 accumulation.

Fluorescence intensity histogram quantifications were performed using ImageJ (http://rsb.info.nih.gov/ij/). A ROI was selected around each nucleus and the fluorescence intensity histogram of each nucleus, its mean value and standard deviation were measured. To quantify the levels of histone acetylation of MEFs the mean values of the histograms of approx. 25 cells per condition were averaged and normalized to untreated cells. These measurements were performed in triplicates.

For ES cells and differentiated cells, the (anti)correlation between histone acetylation and methylation signals at the inactivated autosome was determined by plotting the normalized signal intensities at each pixel along a line through the inactive territory 11, as defined by accumulation of H3K27m3. The Pearson correlation coefficient was calculated using ImageJ within a region of interest containing the inactive chromosome and surrounding nucleoplasmic signal.

To quantify the decondensation of pericentric heterochromatin the standard deviation of DAPI histograms of approx. 25 cells per condition were averaged and normalized to the control (Figure 7). The same analysis was repeated on three independent experiments and averaged.

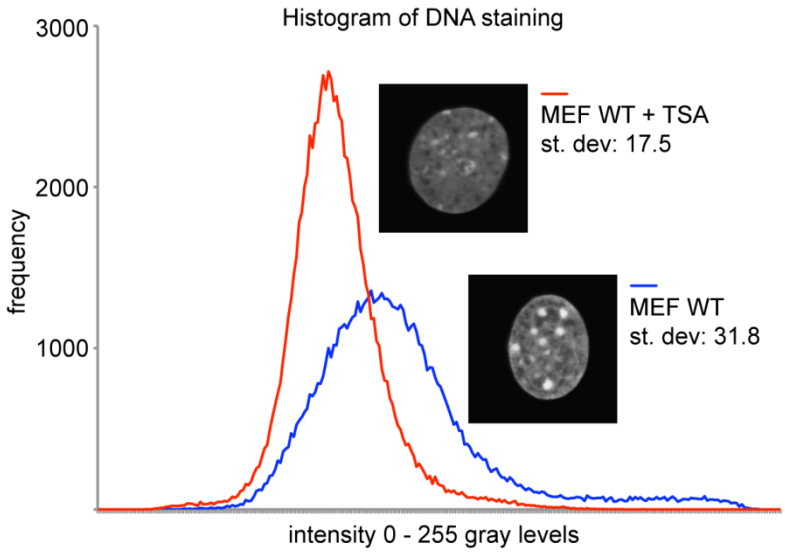

Figure 7. Decondensation results in a decreased standard deviation of the fluorescence intensity distribution of DNA stainings.
Histograms of the DNA staining of a wildtype control MEF and a treated MEF are presented to illustrate the effects of DNA decondensation on the fluorescence intensity distribution. In control cells, the highly condensed, bright chromocenters result in a broader intensity distribution and, therefore, in a higher standard deviation than treated cells with decondensed heterochromatin and a more homogenous DNA staining.

The frequency of early versus late replicating patterns was quantified on the wide-field microscope after staining of incorporated modified nucleotides by counting only early and late replicating cells (sum of both equals n) and calculating the percentage of early or late patterns, respectively.

Colocalization of major satellites and early replication sites was calculated using custom written software in the Priithon image analysis platform (http://code.google.com/p/priithon/)[5]. Images were processed using a 3D median filter for chromocenters and 3D Gaussian-of-Laplace filter for replication foci. Filtered images were thresholded automatically using the Otsu algorithm (Otsu, 1979). The thresholded images were used to calculate the colocalization percentage. For this, the number of all overlapping voxels was divided by the total number of voxels corresponding to chromocenter signals.

The total histone acetylation signal at the chromocenters was quantified as described above, but I adapted the code so that after obtaining a mask for the acetylation channel this was multiplied by the raw acetylation image, as to obtain the integrated value of histone acetylation signal at the chromocenters by summing up the intensity of all remaining voxels.

[5] Code written by Sebastian Haase.

Colocalization of replication foci and major satellites on live cell data was assessed by the H-coefficient, using the following formula[6]:

$$H_{coeff} = \frac{N_p \sum_{i=1}^{N_p} Ir_i \; Ig_i}{\left(\sum_{i=1}^{N_p} Ir_i \right) \left(\sum_{i=1}^{N_p} Ig_i \right)},$$

where Ir_i and Ig_i is the intensity of the channels r and g in the pixel i and Np is the total number of pixels.

Statistical analysis

To assess the statistical significance of the different results presented throughout this work, I tested the different sets of data either by the double-tailed t-test or by the Fisher's exact test, as described in the corresponding figures. Differences were considered significant if $p < 0.05$.

[6] Algorithm developed by Henry D. Herce and is part of the following manuscript: Herce HD, Casas-Delucchi CS, Cardoso MC. Image co-localization and spatial correlation of objects in multicolor images as a measure of interactions between bio-molecules. *In preparation*.

5. Results

5.1 Histone acetylation controls the inactive X chromosome replication dynamics[7]

To dissect the control mechanisms of the replication of diverse chromatin states we chose the inactive X chromosome (Xi), the most prominent facultative heterochromatic region in mammals. Xi in female somatic cells is a well-known example for epigenetically silenced chromatin(Lyon, 1961). In embryonic stem (ES) cells the *Xist* gene is transcribed at low levels from both X chromosomes, while in somatic cells it is transcribed exclusively from the inactive homologue, where it coats the chromosome territory(Brockdorff et al., 1991; Clemson et al., 1996). Xist RNA accumulation, shown to be dispensable for maintaining the inactive state(Csankovszki et al., 1999), is initially followed by tri-methylation of lysine 27 on histone H3 (H3K27m3) (Plath et al., 2003; Silva et al., 2003) and later by histone hypoacetylation(Jeppesen and Turner, 1993), DNA methylation(Norris et al., 1991) and the formation of the Barr body(Barr and Bertram, 1949). These modifications form a multi-layer silencing mechanism proposed to maintain the Xi's silenced state (reviewed, e.g., in (Chow and Heard, 2009)). Interestingly, the replication timing of Xi has been shown to differ from that of its active homologue (Xa), based on early studies using modified nucleotides to label replicating DNA of human blood cells (German et al., 1962; Gilbert et al., 1962; Morishima et al., 1962) and post-implantation mouse embryonic cells (Takagi, 1974; Takagi et al., 1982). Analyzing chromosomes in the subsequent mitosis revealed that one of the two X chromosomes in female cells replicated later than all other chromosomes (Gilbert et al., 1962). The "late replication" of Xi has been referred to many times ever since, and is to date thought to be an important factor for the maintenance of the silenced state(Chadwick and Willard, 2003).

In this study I assessed the dynamics of Xi replication in living cells. Furthermore, I elucidate the epigenetic factors that determine this replication mode. To address these questions I utilized GFP-tagged DNA replication factors in order to analyze the precise progression of S-phase *in vivo* with high temporal and spatial resolution. I found Xi to replicate within a limited time period during early-mid S-phase and corroborated these results using classical nucleotide incorporation detection. I was further able to show that an autosome silenced by ectopic *Xist* expression acquires the same replication mode as Xi. Finally, I demonstrate that the level of histone acetylation is the critical factor controlling the maintenance of the replication timing of Xi. I conclude that in female mammalian cells the Xi replicates in a synchronous man-

[7] The work described in this chapter is included in the following publication: Casas-Delucchi CS, Brero A, Rahn HP, Solovei I, Wutz A, Cremer T, Leonhardt H, Cardoso MC (2011) Histone acetylation controls the inactive X chromosome replication dynamics. Nature Communications 2:222, doi 10.1038/ncomms1218

ner, before constitutive heterochromatin, and these replication dynamics are controlled by histone hypoacetylation.

Xi replicates synchronously during early-mid S-phase

To analyze the replication dynamics of Xi in living cells, I followed GFP-PCNA dynamics during S-phase progression (1 frame/20 minutes; Supplementary Movies Xi 1 - 4) I was able to visualize cells in the first half of S-phase with the same prominent replication structures as the previously observed in our lab in fixed cells (see Figure 5 in introduction). These structures persisted for one to two hours (Figure 8a) and coexisted with a replication pattern constituted by small replication foci at the nucle(ol)ar periphery, usually referred to as a mid S-phase replication pattern (Nakayasu and Berezney, 1989).

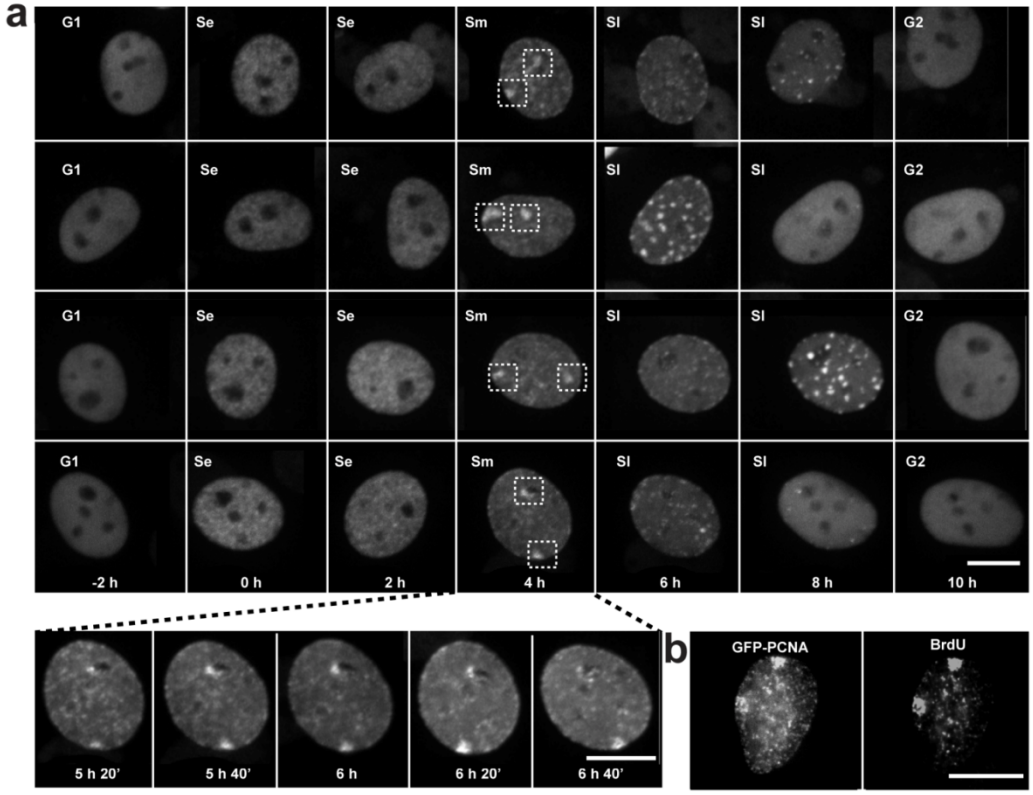

Figure 8. The inactive X chromosome replicates synchronously during early-mid S-phase
(a) Selected frames of time lapse imaging movies (Supplementary Movies Xi 1 – 4) of C2C12 myoblasts stably expressing GFP-PCNA. Z-stacks were collected every 20 minutes over a time period of up to 15 h. GFP-PCNA (Leonhardt et al., 2000) marks S-phase progression. Note the two large, synchronously replicating chromatin structures that appear during early-mid S-phase and persist for 60-120 minutes. (b) Epifluorescent micrographs of C2C12 cells stably expressing GFP-tagged PCNA. Cells were pulse-labeled with 10 µM BrdU for 30 minutes to visualize actively replicating DNA. Note that the large synchronously replicating DNA regions marked by PCNA were active sites of DNA synthesis as shown by the colocalization with incorporated nucleotide. Scale bars: 10 µm.

It should be noted that the pericentric heterochromatin region belonging to Xi was replicated later in S-phase, concomitantly to the pericentric heterochromatin of the autosomes. I confirmed that the large structures visualized by GFP-tagged PCNA indeed represented sites of actively replicating DNA by pulse labeling nascent DNA in the transgenic C2C12 cells with BrdU (Figure 8b).

Xi replication mode is conserved in mammals

If the Xi replication pattern described above were a general feature of mammalian cells, one should be able to observe it in different species and cell types. To test this possibility, we examined whether this replication pattern would also be found in diploid primary cells, in cells of different tissues and in other species. Figure 9 presents the results of a triple replication labeling experiment of primary mouse male and female fibroblasts. Cells were double labeled using short 10-minute pulses of IdU and CldU separated by a three hours chase period, followed by a further three hours chase period before they were fixed and immunostained for incorporated IdU, CldU and DNA Ligase 1, with the latter highlighting the state of DNA replication at the time of fixation (Cardoso et al., 1997). Typically, cells that stained positively for all three replication markers displayed an early IdU, mid CldU and late DNA Ligase 1 replication pattern and exhibited one prominent replication structure equivalent to the ones shown in Figures 8, but only in the second, i.e. mid replication label and exclusively in female cells (Figure 9a). These data confirmed and extended the validity of our previous results in established mouse myoblast lines to primary diploid mouse fibroblasts. I further co-stained sites of active replication and H3K27m3, a Xi hallmark, in mouse and human primary diploid fibroblasts to unequivocally demonstrate that the prominent replication structure corresponds to the Xi (Figure 9b). BrdU labeling of female diploid human vascular smooth muscle primary cells also revealed the presence of the large early-mid replication structure, further substantiating the universality of the described Xi replication mode (Figure 9c). Based on these observations, I conclude that the synchronous replication of Xi during the first half of the S-phase is a phenomenon common to mammalian female cells and is not restricted to immortalized, aneuploid cell lines.

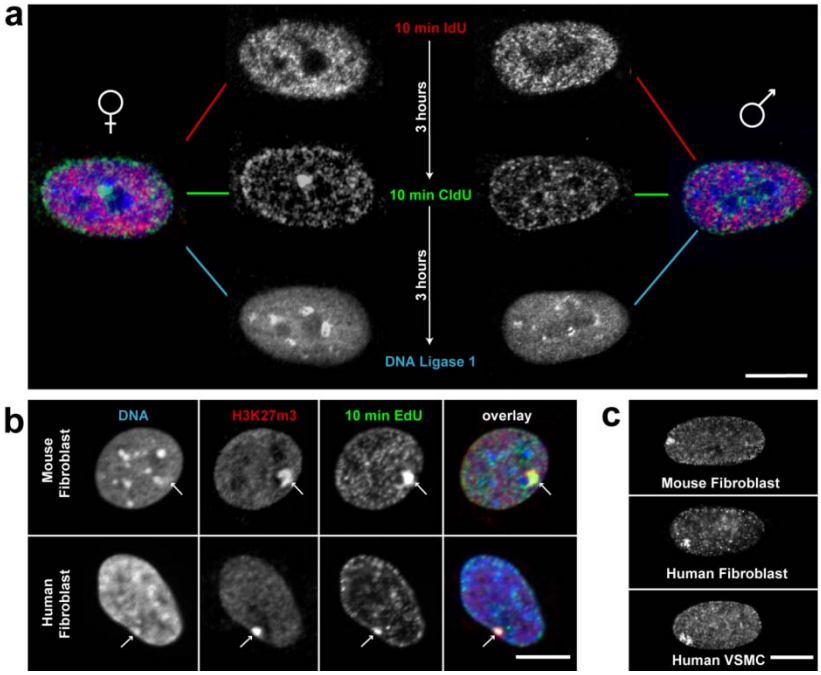

Figure 9. Synchronous replication of Xi during early-mid S-phase is conserved in different types of cells and mammalian species[8]

(a) Male and female primary mouse ear fibroblasts were triple-labeled to mark DNA replicated at three distinct time points during S-phase. The first two labels were accomplished by IdU and CldU incorporation respectively, while the third time point was visualized by staining of DNA Ligase 1. The chase time between the labels was three hours. Shown are epifluorescent micrographs of a female and a male fibroblast exhibiting representative early (red), mid (green) and late (blue) replication pattern. (b) Co-staining of H3K27m3 and replication sites after 15 minutes of 10 µM EdU incorporation in female primary mouse ear fibroblasts and human adult skin fibroblasts. (c) Xi replication pattern (see also (a)) in BrdU-labeled (100 µM, 20 minutes) female primary mouse ear fibroblasts, human fetal lung fibroblasts and human vascular smooth muscle cells (VSMC). Note that the characteristic Xi replication pattern coincides with the onset of the typical perinuclear mid S-phase replication pattern. Scale bars: 10 µm.

Xi replication timing is epigenetically controlled

I have described a massive difference in the replication dynamics of Xa and Xi, homologous chromosomes that differ from each other only epigenetically. To examine the extent to which different epigenetic modifications define their replication dynamics, I disrupted individually three epigenetic hallmarks of Xi: accumulation of Xist RNA, H3K27m3 and histone hypoacetylation.

To assess the role of *Xist* expression in the synchronous Xi replication mode, I used mouse embryonic fibroblasts (MEF) carrying a *Xist* null allele on one homologue and a conditional knockout ("floxed") allele on the other chromosome (G19SV(Csankovszki et al., 2001; Csankovszki et al., 1999)). This system allowed us to test whether the synchronous replication pattern would remain unchanged after disruption of *Xist* expression, or whether accumula-

[8] Figure 9 parts a and c were assembled from stainings from Hans-Peter Rahn.

tion of Xist RNA has an effect on the Xi replication dynamics. Upon infection with Cre recombinase expressing adenoviruses (Adeno-Cre), I observed a complete loss of *Xist* expression in essentially all G19SV MEFs but not in control mock-infected cells, as shown by RNA FISH with a Xist specific probe (data not shown). Loss of *Xist* expression had no influence on cellular proliferation (Figure 10) in agreement with published observations (Csankovszki et al., 1999). In contrast, a clear reduction in the percentage of Xi replication patterns (visualized by nucleotide incorporation) was seen in *Xist* deficient cells compared to control cells (4.7% vs. 11.2%; Figure 11). The fact that the Xi replication mode was decrease by only 50% although Xist was absent in 100% of the cells argues against Xist being essential for the Xi replication dynamics.

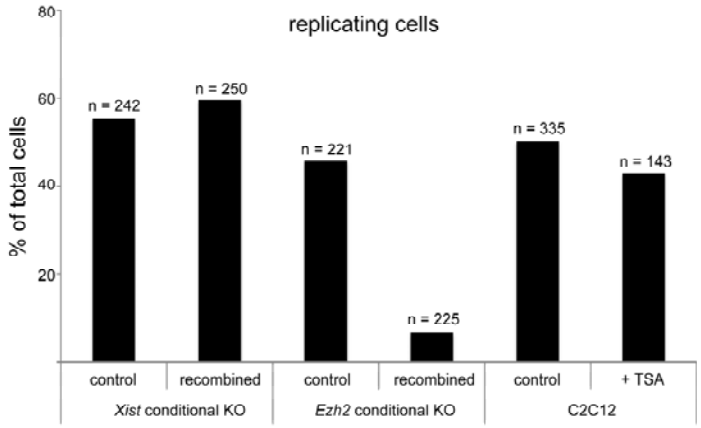

Figure 10. Effects of loss of Xist RNA, H3K27m3 accumulation and histone hypoacetylation on cell cycle progression[9]
BrdU incorporation was used to identify the S-phase cells. The percentage of replicating cells in the population was quantified in control and recombined *Xist* conditional KO and Ezh2 conditional KO, as well as in control and TSA treated C2C12. While knocking out *Xist* and treating cells with TSA did not significantly disturb the relative S-phase duration, Ezh2 KO cells show a strong impairment in cell cycle progression.

On the other hand, H3K27m3 is known to accumulate at the Xi, yielding a characteristic staining pattern. In the Xist knockout MEFs, a comparable 50% reduction was observed for the frequency of H3K27m3 Xi patterns (Figure 11a), suggesting a connection between Xi replication pattern and downstream epigenetic modifications of the Xi. Indeed, I observed that in all Xist deficient cells still displaying the typical Xi replication pattern, H3K27m3 was still accumulated on Xi (Figure 12). Moreover, knocking out *Xist* resulted in a significant increase of histone acetylation (Figure 11b), supporting the idea of a possible interdependency between the changes in the Xi replication dynamics and the downstream effects of the loss of Xist RNA accumulation. Consequently, I was interested in assessing the relationship between H3K27m3 and Xi replication dynamics. To this end, I used MEFs carrying two conditional knockout alleles of the histone methyltransferase enhancer of zeste2 (*Ezh2*(Su et al., 2003)), the enzyme responsible for the H3K27m3 modification on Xi (Plath et al., 2003; Silva et al., 2003). To induce recombination, the cells were incubated with the Adeno-Cre followed by an additional

[9] Adenovirus-Cre infection of Xist conditional KO and replication staining of Ezh2 conditional KO were performed by Alessandro Brero.

growth period of seven days before fixation. Successful recombination of the floxed Ezh2 genes was quantified by the frequency of H3K27m3 Xi patterns in virus-treated cells versus control-infected cells. As shown in Figure 11a, this frequency dropped from 81.4% to 12.4%.

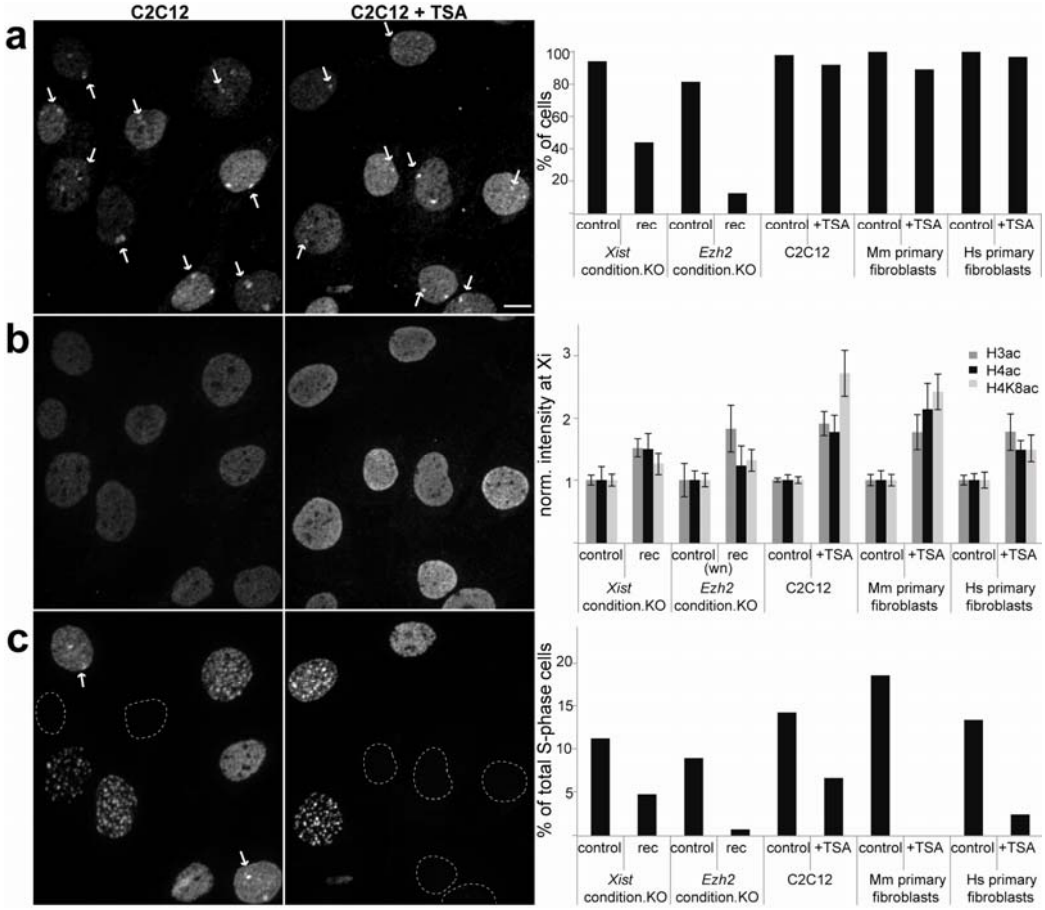

Figure 11. Influence of *Xist*, H3K27m3 and histone acetylation on the Xi replication dynamics
Conditional knockout (KO) mouse embryonic fibroblasts (MEF) for *Xist* (G19SV) and for the histone methyltransferase *enhancer of zeste 2* (*Ezh2*) were used to determine the influence of *Xist* and H3K27m3 on the replication timing of Xi. The effect of hyperacetylation of Xi on its replication timing was analyzed by treatment of C2C12 mouse myoblasts as well as mouse and human primary fibroblasts with 20 nM trichostatin A (TSA) over four days. Maximum intensity projections of control (left) and TSA treated (right) C2C12 cells are presented to illustrate the quantification method. (a) Confocal images of cells immunostained with antibodies specific for H3K27m3. Arrows point to cells scored as positive for H3K27m3 accumulation at Xi. Histogram shows the quantification of positive cells, n > 220 for immortalized cell lines, n > 34 for primary cells. (b) Confocal images of cells immunostained for H4K8ac. Histogram shows the intensity of Xi histone acetylation at H3ac, H4ac and H4K8ac, normalized to the respective control. In control and recombined *Ezh2* conditional KO cells the whole nuclear (wn) histone acetylation was plotted. Error bars represent 95% C.I. (c) Cells were labeled for 15 minutes with 10 µM EdU and incorporated nucleotide detected. Arrows point to cells exhibiting the Xi replication pattern. Histogram shows the percentages of Xi replication pattern plotted relative to the total number of S-phase cells, n > 85 for immortalized cell lines, n > 20 for primary cells. Scale bar: 10 µm.

A significant decrease was also observed for the percentage of Xi replication pattern in virus-infected S-phase cells (0.7% vs. 8.9% in control cells; Figure 11c), indicating that, independently of *Xist* expression, H3K27m3 accumulation has an influence on Xi replication. However, it should be noted that, in contrast to loss of *Xist* expression, loss of *Ezh2* had a dramatic effect

on the proliferation of the cells, as revealed by the reduction of actively replicating cells from 45.7% to 6.7% (Figure 10) suggesting that decrease of H3K27m3 levels impedes normal cell cycle progression.

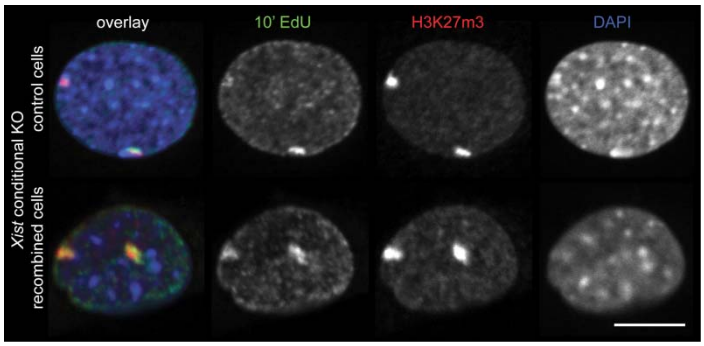

Figure 12. *Xist* conditional KO cells showing the Xi replication pattern before and after recombination
Xist conditional KO (control and recombined) cells after 15 minutes incorporation of 10 µm EdU were co-stained for replication and H3K27m3. *Xist* KO cells still show a clear synchronous replication pattern during mid S, demonstrating that Xist RNA coating the Xi is dispensable to maintain the Xi replication dynamics. Scale bar: 10 µm.

On the other hand, loss of H3K27m3 resulted in an increase in histone acetylation, especially at histone H3 (Figure 11b). Therefore, the question arose whether H3K27m3 itself, being an early modification of Xi, is a direct determinant of the Xi replication dynamics or whether the possible concomitant loss of modifications downstream of H3K27m3, such as histone hypoacetylation, might be the actual cause for the decrease of Xi replication patterns in Ezh2 conditional knockouts. To test the latter, I interfered with histone hypoacetylation (Keohane et al., 1996). This was accomplished by treating C2C12 mouse myoblasts, as well as mouse and human primary fibroblasts, with the HDAC inhibitor trichostatin A (TSA), which leads to global histone hyperacetylation. As shown in Figure 11b, 20 nM TSA treatment for four days, while not having a significant effect on the percentage of cells going through S-phase (Figure 10), caused hyperacetylation of chromatin, globally and directly at the Xi (Figure 13). Concomitantly, I observed a clear decrease in the percentage of S-phase cells with Xi replication pattern, which dropped from 13.3-18.6% in control cells to 0-6.6% in treated cells (Figure 11c), suggesting that low acetylation levels on the X chromosome are required to maintain the synchronous early-mid replication timing of Xi. Importantly, TSA treatment did not cause loss of H3K27m3 (Figure 11a) or Xist RNA on Xi (Figure 14), arguing for a direct role of hypoacetylation in controlling Xi replication dynamics, independently of Xist and H3K27m3.

I conclude that high H3K27m3 and histone hypoacetylation play a role in maintaining the characteristic synchronous early-mid replication timing of Xi, with histone hypoacetylation being the most likely to play a direct role. Nevertheless, disrupting any of the Xi epigenetic modifications might have some influence on the other modifications (Csankovszki et al., 2001). To clarify this situation I utilized a system that allowed us to artificially control chromosome inactivation and to follow the appearance of the distinct epigenetic modifications

that accompany *Xist*-dependent whole chromosome silencing and their relation to the shift in the replication mode of the inactivated chromosome.

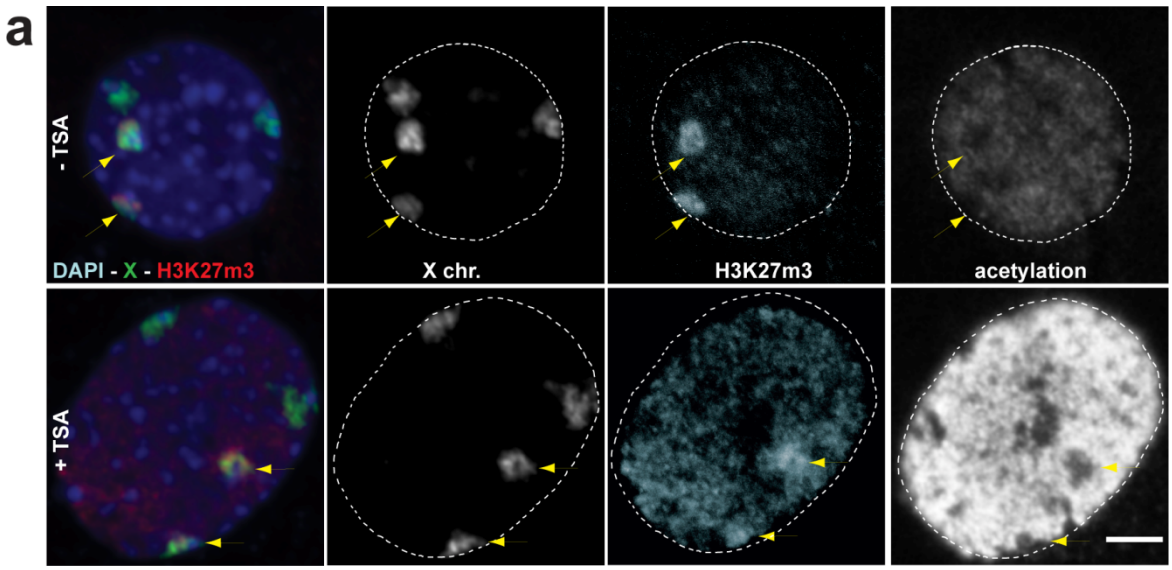

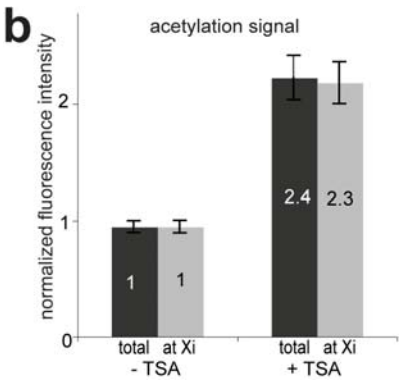

Figure 13. Global and Xi specific hyperacetylation after TSA treatment

(a) C2C12 cells were treated with 20 nM TSA for four days, fixed and double stained with anti-H4K8ac and anti-H3K27m3 specific antibodies followed by FISH with a chromosome X specific probe(Zinner et al., 2007). DNA was counterstained with DAPI. Confocal microscopy images showing the X chromosome territories and H3K27m3 marking the two Xi chromosomes (left panels, maximum intensity projections) and corresponding acetylation signal (single mid section). Arrows point at Xi chromosomes. Scale bar: 5 µm. (b) The integrated histone acetylation signal intensity over the whole nucleus or exclusively at the Xi territory was measured in confocal mid sections of TSA treated and untreated cells (n = 34) by measuring the integrated acetylation signal intensity at the whole nucleus/inactive territory as defined by the X chromosome FISH signal and H3K27m3 accumulation. The results were normalized to the value in control cells. Statistical analysis was performed using Microsoft Excel. Results are plotted relative to control untreated cells. Error bars represent 95% confidence interval.

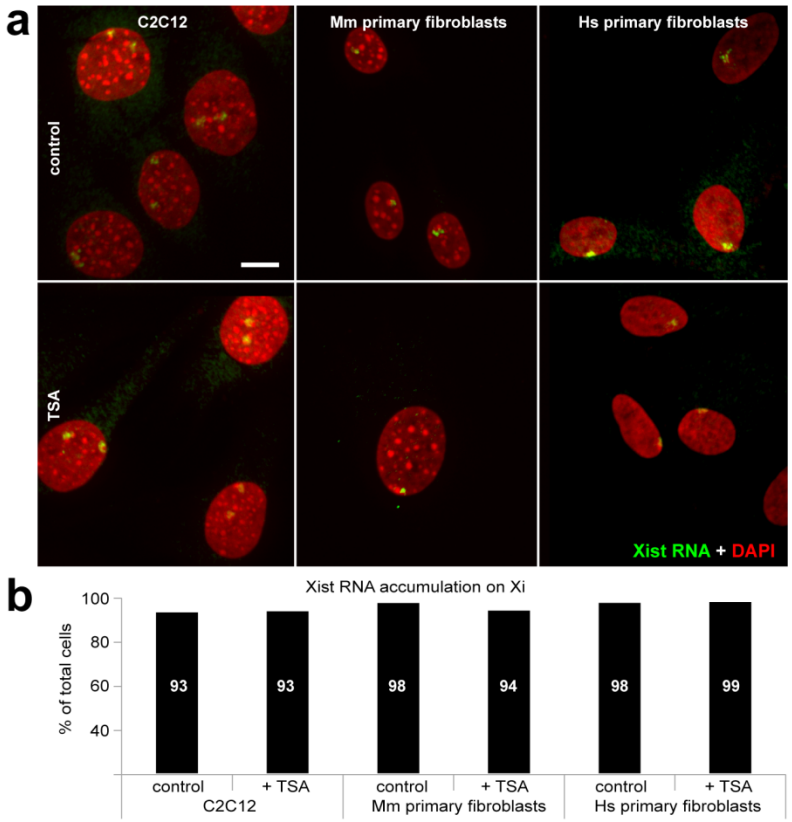

Figure 14. Effect of TSA treatment on Xist RNA accumulation
(a) Maximum intensity projections of confocal images of Xist RNA FISH (green) and DAPI (red) on C2C12, mouse and human female primary fibroblasts, with and without TSA. Scale bar: 10 µm. (b) Quantification of the percentage of cells showing accumulation of Xist RNA on the Xi territories with and without TSA (20 nM TSA for four days); n > 78.

Inactive autosomes replicate as Xi upon cell differentiation

Artificially inducing chromosome inactivation allowed us to address two questions: 1. is ectopic expression of *Xist* from an autosome sufficient to establish the characteristic synchronous, early-mid replication timing; and 2. can we temporally discriminate between the contribution of histone methylation and hypoacetylation to the inactive chromosome and their relation to synchronous replication? To this end, I took advantage of a male mouse transgenic ES cell line that carries a doxycycline-inducible *Xist* gene on chromosome 11. Previous studies have shown that *Xist*-expressing, silenced autosomes acquire a delayed replication timing only after cellular differentiation(Wutz and Jaenisch, 2000). Thus, ES cells were induced to express *Xist* by adding doxycycline, and either differentiated using retinoic acid, or kept in an undifferentiated state (Figure 15a). Six days after induction of *Xist* cells were BrdU labeled to allow visualization of the Xi replication pattern and RNA FISH with a Xist specific probe was performed to visualize the silenced autosome (Figure 15b). While we observed the typical synchronous early-mid replication pattern shown for Xi (compare BrdU signal Figure 15b "differentiated cell" with, e.g., Figure 8) in differentiated cells, we were unable to find such a

replication structure in undifferentiated ES cells, though we did observe early-mid S-phase cells, with the characteristic perinuclear and perinucleolar replication pattern (Figure 15b "ES cell"). Therefore, we conclude that *Xist* expression from an autosome is sufficient to trigger all downstream mechanisms that are necessary to establish the synchronous early-mid replication pattern in differentiated cells.

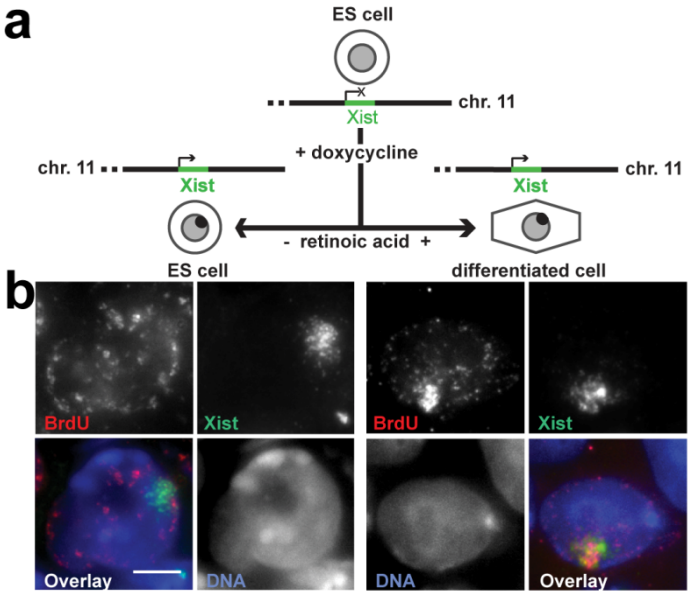

Figure 15. *Xist*-dependent autosome inactivation induces synchronous, early-mid replication in differentiated cells

(a) Mouse ES cells carrying an ectopic, doxycycline-inducible *Xist* gene on one chromosome 11 were either treated for six days with doxycycline and retinoic acid (differentiated, *Xist* expressing) or singly with doxycycline (undifferentiated, *Xist* expressing). (b) Cells were BrdU pulse labeled (10 minutes), fixed and stained to detect incorporated nucleotide followed by RNA-FISH to detect Xist. DNA was counterstained with DAPI. Epifluorescence micrographs show representative mid S-phase *Xist* expressing ES (left) and differentiated (right) cells, as revealed by perinuclear BrdU specific staining. The characteristic Xi replication pattern was only observed in differentiated cells, but never in undifferentiated ES cells. Scale bar: 5 µm.

Histone acetylation regulates synchronous replication timing

Since cellular differentiation was required to establish the synchronous replication pattern of the inactivated autosome, I next examined the epigenetic differences before and after differentiation. Consistent with published data for Xi (Plath et al., 2003; Silva et al., 2003) and for the *Xist*-inactivated autosome(Kohlmaier et al., 2004; Wutz and Jaenisch, 2000) accumulation of H3K27m3 was observed shortly after *Xist* induction (Figure 16a) but before the appearance of the synchronous replication pattern. This result clearly indicates that H3K27m3 is not sufficient to induce the shift in replication dynamics. Hence, I next quantified the levels of histone acetylation at the inactivated autosome. I first selected the *Xist* expressing autosome by the accumulation of H3K27m3 and analyzed the histone acetylation level by plotting the variation of fluorescence intensity along a line across the inactivated chromosome territory (Figure 16b). In addition, I performed a Pearson correlation analysis comparing the level of H3, H4 and H4K8 acetylation at the inactivated Xi relative to the surrounding chromatin in ES versus differentiated cells. In all cases this resulted a significantly stronger anticorrelation (Table 2). With both analyses, I could observe a clear decrease of histone acetylation level at the inactivated autosome upon differentiation. This decrease correlated with the appearance of synchronous replication patterns (Figure 16b). Altogether, these observations (summarized in Figure 16c) confirmed our findings in somatic female cells and demonstrate that histone hypoacetylation directly promotes the rearrangement in replication dynamics of the inactive chromosome, whereas the Xist RNA coating and H3K27m3 per se are not sufficient to determine synchronous replication dynamics.

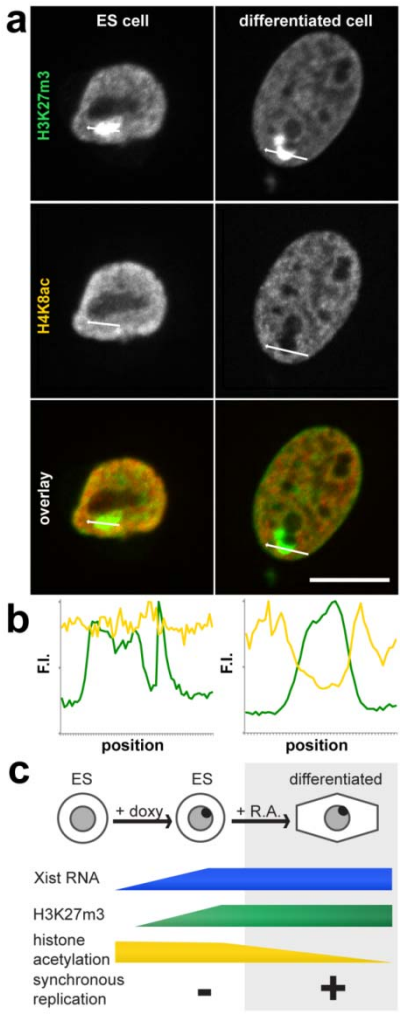

Figure 16. Early-mid Xi replication pattern in differentiated cells correlates with global histone hypoacetylation on the inactivated autosome

(a) Undifferentiated ES or differentiated cells were fixed after induction of *Xist* and then double stained with antibodies to H3K27m3 and H4K8ac. While accumulation of H3K27m3 at the inactivated autosome is already seen very clearly in undifferentiated cells (left), global histone hypoacetylation of this chromosome only appears upon differentiation (right). (b) Line intensity plots of H3K27m3 (green) and H4K8ac (orange) distribution through the inactivated autosome showing an increased anticorrelation of both epigenetic marks upon cellular differentiation. F.I.: fluorescence intensity. (c) Summary of the interplay between the different epigenetic modifications and their relationship to synchronous, early-mid replication before and after differentiation.

Table 2: Pearson correlation coefficient for different acetylated residues in ES and differentiated cells

Modification	ES cells	differentiated cells	t-test
H3ac	-0.25 (n = 34)	-0.52 (n = 25)	$p < 0.001$
H4ac	-0.24 (n = 11)	-0.59 (n = 18)	$p < 0.001$
H4K8ac	-0.23 (n = 27)	-0.47 (n = 22)	$p < 0.001$

The Pearson correlation coefficient for H3K27m3 versus histone acetylation signal results represent the mean value for n (as indicated) cells. p-value calculated by 2-tailed t-test.

Movies Xi 1 – 4. Dynamics of DNA replication visualized by GFP-PCNA.
Time lapse analyses of GFP-PCNA throughout S-phase in living C2C12 myoblasts after mitotic shake-off, starting acquisition during G1. Confocal 3D images were collected every 20 minutes over a time period of up to 18 h. GFP–PCNA behaves as a characteristic S-phase progression marker: the typical punctuated pattern in early S-phase, the perinucleolar and perinuclear distribution of replication foci in early-mid S-phase, the donut-like pattern in late S-phase and intermediate steps are visible. Frame rates: 4/sec.

Contributions to this chapter

The work described in this chapter is included in the following publication: "Histone acetylation controls the inactive X chromosome replication dynamics" by Casas-Delucchi CS, Brero, A., Hahn H.P., Solovei, I., Wutz, A., Cremer, T., Leonhardt, H. and Cardoso M.C., published in 2011 in Nature Communications 2:222 (doi:10.1038/ncomms1218).

I performed the live-cell microscopy experiments to follow cell cycle progression and replication of the inactive X chromosome in synchronized C2C12 cells, did the data acquisition and analysis, as well as figure preparation (Figure 8 and corresponding movies). I extracted and cultivated primary fibroblasts from wild-type female and male mice and cultivated primary human cells. I performed the stainings of replication and epigenetic markers of the inactive X-chromosome and prepared the corresponding figure (Figure 9). I performed the adenovirus amplification and infection of *Ezh2* conditional knockouts, as well as the TSA-treatment of immortalized and primary human and mouse cells. I performed histone methylation and histone acetylation stainings of these cells and of the *Xist* conditional KO cells, as well as replication staining of *Xist* conditional KO MEFs, TSA-treated primary and C2C12 cells and all Xist-RNA FISH experiments. I did the data acquisition, analysis and quantification and prepared the corresponding figure (Figure 10, 11, 12, 13, 14). I inactivated primary MEFs to make feeder cells, cultivated the *Xist*-transgenic ES cells, induced chromosome inactivation and differentiation and performed replication stainings (Figure 15). I performed histone acetylation and methylation stainings on ES cells and differentiated cells, acquired the data, analyzed it by line plots and Pearson's correlation coefficient and prepared the corresponding figure (Figure 16). I wrote the major part of the manuscript.
Contribution from others: Alessandro Brero, Hans-Peter Rahn and Irina Solovei performed replication staining in combination with FISH (Figure 5, Introduction) and double replication staining on metaphase chromosomes (Figure 6, Introduction). Part of these experiments was done in the laboratory of Thomas Cremer. Karyotype analysis of the transgenic cell lines was performed by Isabel Jentsch (data not shown). Alessandro Brero performed the adenovirus experiments experiments on *Xist* conditional KO cells, the replication staining of recombined *Ezh2* conditional KO cells and supported the manuscript writing. Anton Wutz provided the *Xist*-transgenic ES cells. Heinrich Leonhardt and M. Cristina Cardoso gave advice throughout the work and read the manuscript critically.

5.2 Histone acetylation controls replication timing of constitutive heterochromatin[10]

To address how epigenetic modifications influence replication timing, I focused on the replication of constitutive heterochromatin (Heitz, 1928). Constitutive heterochromatin exhibits a complex epigenetic landscape, marked by high levels of DNA methylation, H3K9m3 and histone hypoacetylation. These modifications help define a highly condensed nature, and in mouse cells these regions assemble into higher order aggregates known as chromocenters (Jones, 1970). These structures are composed of approximately 10^5 major satellite repeats (Vissel and Choo, 1989) and can be visualized by DNA staining with DAPI as round, highly condensed structures. Because of their prominent structure, chromocenters represent an identifiable landmark within the nucleus that can be easily visualized throughout the cell cycle. It is thus possible to directly image the interactions of the replication machinery with the chromocenters during S-phase.

I have undertaken a comprehensive study investigating the role of epigenetic markers in defining the late replication timing of constitutive heterochromatin. The late replication timing of chromocenters was assessed by quantification of replication patterns and colocalization of early replication foci with chromocenters by immuno-FISH. I also perfomed live cell imaging using fluorescently tagged proteins to label the replication machinery and major satellite repeats and followed chromocenter replication in real time. I manipulated the epigenetic state of constitutive heterochromatin by altering all three of its epigenetic hallmarks: histone hypoacetylation, accumulation of H3K9m3, and DNA methylation. These manipulations allowed us to identify several conditions in which constitutive heterochromatin underwent hyperacetylation. This increase was associated with an earlier onset of replication. I therefore conclude that hypoacetylation, but not DNA methylation or accumulation of H3K9m3, plays a critical role in defining late-replicating regions of the genome. Our results put into context observations from different model systems, as well as from *in situ* and *in vitro* experiments and conclusively demonstrate that histone acetylation is the most direct epigenetic determinant of replication timing.

Manipulation of the epigenetic composition of constitutive heterochromatin

In order to investigate the connection between epigenetic markers and replication timing, I used drug treatment and genetically modified cell lines to manipulate the main features of

[10] This work is part of the following manuscript: Casas-Delucchi CS, van Bemmel JG, Haase S, Herce HD, Nowak D, Meilinger D, Stear JH, Leonhardt H, Cardoso MC. Histone acetylation controls replication timing of constitutive heterochromatin. Under revision.

constitutive heterochromatin: histone hypoacetylation, accumulation of H3K9m3, and DNA methylation. I treated wild type mouse embryonic fibroblasts (MEF-WT) with TSA to inhibit HDACs (Taddei et al., 2001), thereby elevating histone acetylation. To modulate the levels of H3K9m3 on constitutive heterochromatin, I performed experiments in *Suv39h*1/2 double knock-out cells (Lehnertz et al., 2003), which lack the enzymes responsible for this modification. Finally, I used *dnmt1*$^{-/-}$ cells (Lande-Diner et al., 2007), with low levels of DNA methylation. Since *dnmt1*$^{-/-}$ somatic cells do not proliferate normally, these experiments were performed in homozygous *p53*$^{-/-}$ cells to increase their viability. As a control for the *p53*$^{-/-}$ / *dnmt1*$^{-/-}$ double knock-out cells, I used *p53*$^{-/-}$ cells (Lande-Diner et al., 2007).

Changes in the levels of epigenetic markers were assessed by Western Blot analysis of cell extracts (Figure 17A), as well as immunofluorescence stainings *in situ* (Figure 17B) using antibodies specific to the histone modifications of interest. These data confirmed that TSA treatment promoted an increase of histone acetylation and that *Suv39h*1/2$^{-/-}$ cells have a decreased level of H3K9m3. *Dnmt1*$^{-/-}$ cells lost DNA methylation at major satellite repeats, as shown by pyrosequencing analysis after bisulfite conversion (Figure 17C and 18). In the case of TSA treatment and *Suv39h*1/2$^{-/-}$ cells, the effects on the epigenetic modifications were specific; TSA-treatment only affected histone acetylation and *Suv39h*1/2$^{-/-}$ cells exhibited only significant alterations in histone methylation. In contrast, *dnmt1*$^{-/-}$ cells, in addition to a drastic decrease in DNA methylation, also exhibited an increase in global histone acetylation (Figure 17B and see below). This result is consistent with the idea that cross-talk exists between epigenetic markers at constitutive chromatin, and that disrupting one modification may promote alterations in the overall chromatin composition and state of the region (Felsenfeld and Groudine, 2003).

Moreover, I predict that disruption of these three epigenetic modifications may also influence the condensation levels of chromocenters (Popova et al., 2009). Figure 17D illustrates that chromocenters in control cells exhibit the characteristic round, condensed structure described above. In contrast, this pattern is disrupted after TSA treatment, as well as in *Suv39h*1/2$^{-/-}$ and *dnmt1*$^{-/-}$ cells.

Chromocenters in these cells appeared more open and lacked the distinct, highly condensed appearance of control cells. Because the decondensation of constitutive heterochromatin results in a more homogenous DNA staining throughout the nucleus, I measured the standard deviation of the respective DAPI histograms to quantify the degree of decondensation in treated and mutant cells (Figure 17D). Since all three treatments influence chromatin condensation, any differences in the effects on replication timing resulting from TSA treatment or knocking out *dnmt1* or *Suv39h*1/2 would exclude condensation as a primary determinant of replication timing.

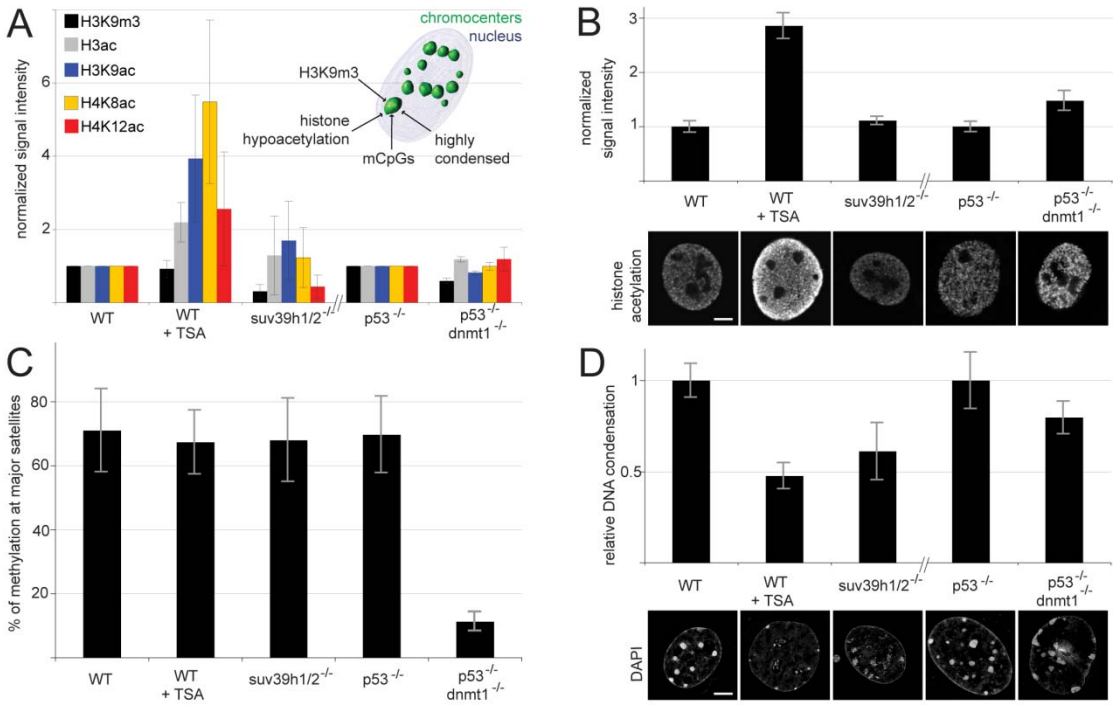

Figure 17. Manipulation of epigenetic marks and organization of constitutive heterochromatin.[11] Global histone acetylation levels were assessed by (A) Western Blot analysis of H3, H3ac, H3K9ac, H4, H4K8ac and H4K12ac, as well as (B) immunofluorescence *in situ* using antibodies against H4K8ac. Confocal mid sections of *in situ* stainings were imaged and the mean value of the fluorescence signal was plotted as a ratio to control cells (MEF WT and *p53*$^{-/-}$, respectively). For Western Blot analysis, the fluorescence signal of histone modifications was double normalized to the amount of histone signal itself (H3 and H4, respectively), as well as to control cells. While TSA treatment resulted in a clear increase of histone acetylation, *dnmt1*$^{-/-}$ showed a slight increase in the level of global histone acetylation (B). On the other hand, *suv39h1/2*$^{-/-}$ exhibited, as expected, decreased levels of H3K9m3 (A). (C) Pyrosequencing analysis after bisulfite conversion demonstrated that exclusively *dnmt1*$^{-/-}$ had abnormal levels of DNA methylation at major satellites, decreased from 70% to 10%. (D) Mid confocal sections of cells stained with DAPI were used to quantify the standard deviation of DAPI histograms, as a measure for the homogeneity of DNA compaction over the nucleus (see Figure 7 in Materials and methods). The results, presented as a ratio to control cells, showed the effect of the different modifications on condensation of constitutive heterochromatin. High resolution 3D-SIM images are presented to illustrate how the disruption of all three factors, histone hypoacetylation, H3K9m3 and DNA methylation, resulted in changes in the structural conformation of chromocenters, with TSA having the most prominent effect, as seen by a more homogeneous DAPI staining. Error bars represent (A) standard deviation, (B - D) 95% CI.

[11] The Western Blots of MEF WT, TSA-treated and suv39h1/2 KO cells were performed by Danny Nowak. Andreas Meisner acquired the high resolution data at the OMX.

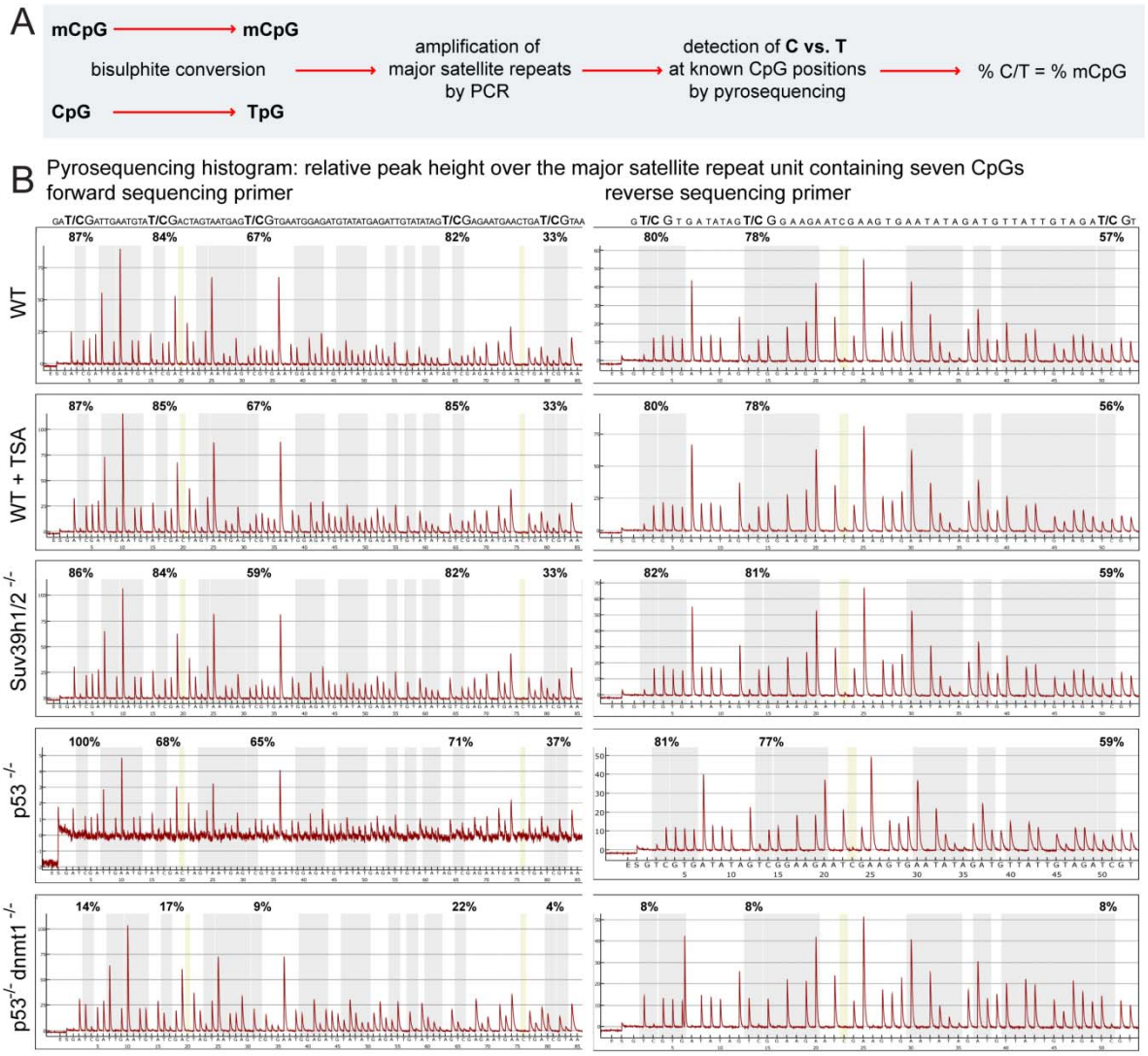

Figure 18. Histograms of pyrosequencing reaction showing the relative frequency of methylated versus unmethylated cytosines at CpG dinucleotides in the major satellite repeats[12]

(A) The sequence of major satellite repeats, amplified by PCR after bisulfite conversion, was determined by pyrosequencing. The relative frequency of cytosine (protected from bisulfite conversion due to methylation) vs. thymidine (resulting from unmethylated cytosines) was quantified at all CpG dinucleotides present in each major satellite repeat unit and represents the percentage methylation at each CpG. (B) Histograms of pyrosequencing reactions showing the ratio of C vs. T at all CpGs through the major satellite repeat unit. All control and treated cells exhibit high levels of DNA methylation, with exception of *dnmt1* KO cells.

Manipulating chromatin epistate affects late replication of constitutive heterochromatin

If changes in the epigenetic make-up of constitutive heterochromatin promote alterations in its replication timing, I predict that the stereotypical late replication timing exhibited by constitutive heterochromatin would be disrupted. To test this model, I quantified the percentage of late replication patterns in S-phase cells. Modified nucleotides, either 5-bromo-2-

[12] Pyrosequencing experiments were performed under instructions from Daniela Meilinger.

deoxyuridine (BrdU) or 5-ethynyl-2′-deoxyuridine (EdU), were added to proliferating populations of cells and incorporated into newly synthesized DNA for 30 minutes prior to fixation. Detection of these nucleotides allowed us to quantify the percentage of replicating cells going through late S-phase, as defined by the characteristic pattern formed by large replication structures as compared to early S-phase patterns (Figure 19A). One caveat of this experiment is that several of the treatments I use increase the time required for the cells to complete the cell cycle. To ensure that the increased duplication time in mutant and treated cells does not result in a change of the replication pattern distribution, I cultivated wild-type fibroblasts under decreased temperature and serum concentration (30°C, 5% FCS). While these cells progressed much slower through the cell cycle, similarly to TSA treated cells, I did not observe any difference in the distribution of replication patterns when compared to the control cells grown under standard conditions (Figure 19B). In an untreated wild type population approximately 40% of replicating cells exhibited staining patterns consistent with late replication (Figure 19B). While *Suv39h*1/2$^{-/-}$ did not show a significant change in this distribution, in agreement with previous data (Wu et al., 2006), both TSA-treated cells and *dnmt1*$^{-/-}$ cells exhibited a clear decrease (down to 16%) in the frequency of late replication patterns. These results demonstrate that manipulation of either histone acetylation or DNA methylation leads to an alteration in the distribution of late replication patterns, suggesting a possible change in the replication timing of heterochromatic regions.

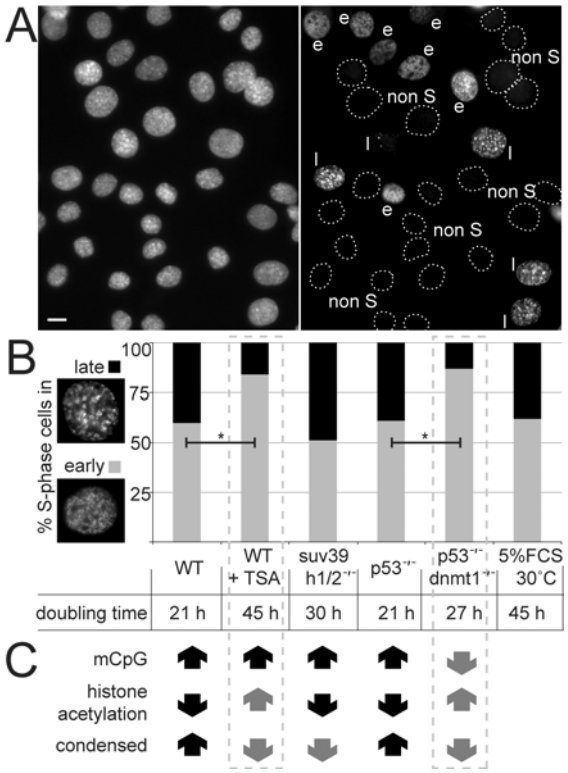

Figure 19. Effects of histone hyperacetylation, loss of H3K9 trimethylation and DNA methylation on late replication.

Modified nucleotides (BrdU or EdU) were given to the cells for 30 minutes before fixation. Detection thereof and epifluorescence microscopy allowed the quantification of early versus late replication patterns. (A) shows an exemplary field in a control cell population, with cells going through early (e), late (l) S-phase, as well as not replicating (non S). (B) shows the distribution of early versus late replication patterns. In control cells, around 40% of replicating cells are going through late S. While *Suv39h*1/2$^{-/-}$ did not show any significant effect on this distribution, both TSA-treated cells and *dnmt1*$^{-/-}$ exhibited a significant decrease in the frequency of late patterns down to approx. 15%. Statistical significance was tested using the Fisher's exact test. The doubling time of the control, mutant and treated cells are shown below the histogram. Cells grown under starvation conditions have a similar doubling time as TSA treated cells, even though the replication pattern distribution of the former is unchanged. (C) summarizes the epigenetic changes in the different cells. Red arrows indicate differences to the respective control cells. Scale bar: 10 µm.

Before investigating how these two epigenetic modifications are related to the regulation of replication timing, it was important to dissect the relationship between histone acetylation and DNA methylation at chromocenters (Nan et al., 1998). I show that TSA had no effect on DNA methylation at heterochromatic sequences (Figure 17C), while *dnmt1*$^{-/-}$ cells exhibited increased levels of global histone acetylation (Figure 17A and B). It is therefore possible that the effect of reducing DNA methylation on replication timing is directly related to the accompanying effect on histone acetylation (Rountree et al., 2000). However, since the increase in the global level of histone acetylation in *dnmt1*$^{-/-}$ cells was not as pronounced as in TSA-treated cells (Figure 17 A and B), I refined the analysis to directly examine the levels of histone acetylation at heterochromatic regions.

I used immuno-FISH to measure changes in histone acetylation levels specifically at chromocenters, simultaneously detecting histone acetylation by immunostaining, and chromocenters by FISH. Subsequent collection of 3D confocal stacks allowed us to quantify the total acetylation signal at chromocenters (Figure 20). TSA treatment resulted in a clear increase of histone acetylation at heterochromatic regions with no change in DNA methylation. Strikingly, *dnmt1*$^{-/-}$ cells showed the same degree of hyperacetylation at chromocenters. Furthermore, treating *dnmt1*$^{-/-}$ cells with TSA as done for WT MEF did not reduce the frequency of late replicating patterns (Figure 21). The fact that TSA treatment of *dnmt1*$^{-/-}$ cells does not result in additional effects on their replication timing indicates that chromocenters in *dnmt1*$^{-/-}$ cells have lost normal histone hypoacetylation. It further suggests that the hyperacetylation observed in *dnmt1*$^{-/-}$ cells may be functionally equivalent to that in TSA-treated cells.

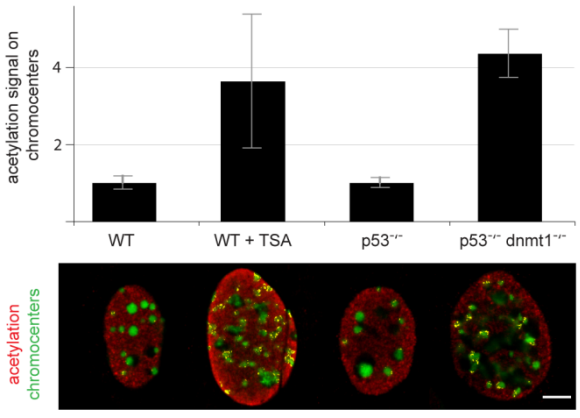

Figure 20. *Dnmt1*$^{-/-}$ have increased levels of histone acetylation at chromocenters. Co-staining of histone acetylation and chromocenters by immuno-FISH and confocal imaging (top) allowed us to quantify the total histone acetylation signal on the chromocenters (bottom). As expected, TSA treatment resulted in a clear increase of histone acetylation in these regions. Interestingly, lowering the levels of DNA methylation at chromocenters by knocking out *dnmt1*$^{-/-}$ had the same effect on histone acetylation, suggesting that this modification is likely to control late replication of constitutive heterochromatic regions. Error bars: 95% CI. Scale bar: 5 µm.

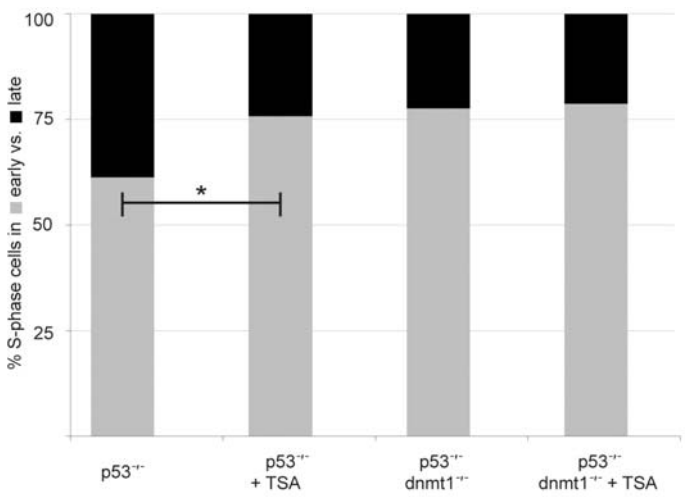

Figure 21. TSA treatment of *dnmt1*$^{-/-}$ cells does not further decrease the frequency of late replication patterns
S-phase patterns were quantified as described in Figure 19. Contrary to control *p53*$^{-/-}$cells, TSA treatment did not further decrease the frequency of late S-phase patterns in *dnmt1*$^{-/-}$ cells. These results support the fact that in *dnmt1*$^{-/-}$ chromocenters have already lost their normal levels of histone hypoacetylation. Statistical significance was tested using the Fisher's exact test.

Dnmt1$^{-/-}$ cells provide a drug-free system in which histone acetylation is specifically increased at otherwise methylated regions, such as pericentromeric heterochromatin. I have thus utilized two distinct approaches to promote the hyperacetylation of constitutive heterochromatin. In both cases I observe a decrease of late replication patterns, raising the question of when these hyperacetylated heterochromatic regions are being replicated. Therefore, one possible model would be that hyperacetylation of heterochromatin promotes earlier onset of replication.

Histone hyperacetylation of constitutive heterochromatin increases its replication during early S-phase

To test the hypothesis that hyperacetylated heterochromatic sequences are replicated during early S-phase, I examined whether there was an increase of replication sites at heterochromatic regions during early S-phase. To this end I used immuno-FISH to co-stain replication sites and chromocenters and directly examine their interaction during early S-phase. In control cells, as expected, I detected very little association between heterochromatin and sites of early DNA replication. In contrast, both TSA-treated and *dnmt1*$^{-/-}$ cells exhibited increased colocalization between chromocenters and early replication foci (Figure 22). These results support the notion that constitutive heterochromatic regions are being replicated in parallel to euchromatin, i.e. during early S-phase.

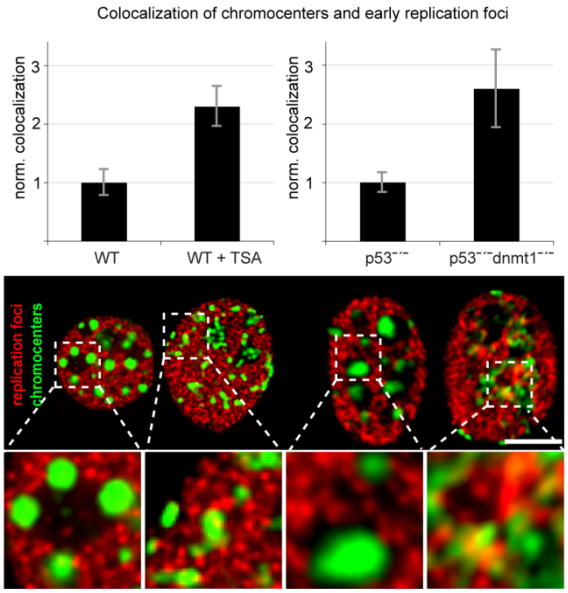

Figure 22. Histone hyperacetylation at heterochromatic regions increase their replication concomitant to euchromatin[13]
Immuno-FISH was performed to co-stain replication structures (by either PCNA or EdU) and chromocenters. Early patterns were selected and imaged by 3D confocal microscopy, as well as deconvolution microscopy. ROIs were defined automatically in the chromocenter channel by the Otsu algorithm and used to quantify the replication signal at chromocenters. The percentage of chromocenter material colocalizing with early replication foci was plotted as ratio to control cells. Both, TSA-treated and *dnmt1*$^{-/-}$ cells showed a significant increase of replication of heterochromatic sequences during early S-phase. Error bars: 95% CI. Scale bars: 5 µm.

To further investigate the idea that increased histone acetylation shifts the replication timing of heterochromatin, I monitored S-phase progression in living cells, focusing again on the association between constitutive heterochromatin and the replication machinery.

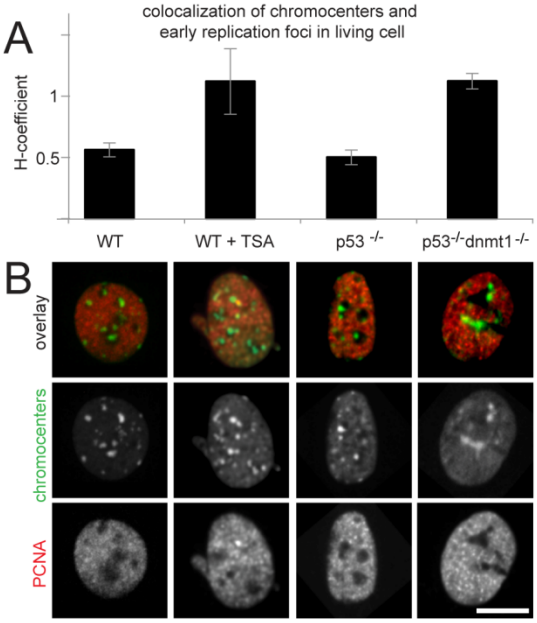

Figure 23. Histone acetylation causes earlier onset of replication of constitutive heterochromatic regions[14]
Progression of S-phase followed by time-lapse microscopy of living cells transfected with mRFP-PCNA, marking sites of active replication, and MaSat-GFP, labeling major satellite repeats. The temporal information allowed us to unequivocally select early S-phase cells and quantify the colocalization of constitutive heterochromatic regions and replication structures prior to the onset of late replication. (A) Hyperacetylated chromocenters showed a signify-cantly increased colocalization with PCNA during early S-phase when compared to untreated wild type cells. (B) Exemplary images of wild type cells going through early S-phase. The TSA-treated cell shows colocalization of chromocenters and TSA, quantified in (C). Error bars: 95% CI. Scale bars: 5 µm.

Cells were transfected with mRFP-PCNA, a central component of the replication machinery (Leonhardt et al., 2000; Sporbert et al., 2005), and MaSat-GFP, a polydactyl zinc finger protein which binds to major satellite repeats (Lindhout et al., 2007) and is a live-cell marker for pe-

[13] Analysis tool developed by Sebastian Haase
[14] Algorithm developed by Henry D. Herce, Herce HD, Casas-Delucchi CS, Cardoso MC. Image co-localization and spatial correlation of objects in multicolor images as a measure of interactions between bio-molecules. *In preparation*.

ricentromeric heterochromatin. Series of time-lapse images were collected in 30-minute intervals for up to 45 hours (Movies CC 1 – 2 and Figure 23A).

Observation over such long periods allowed us to distinguish between the different stages of S-phase in the same cell and to unequivocally identify cells in early S-phase. I analyzed the level of colocalization between replication foci and major satellites and observed a clear increase of colocalization between early replication foci and major satellites as a consequence of TSA treatment and in *dnmt1*$^{-/-}$ cells (Figure 23 and 24). Based on these results, I conclude that increasing histone acetylation at constitutive heterochromatic regions, results in an earlier onset of replication. I therefore propose that histone hypoacetylation is the major determinant for late-replication of heterochromatin.

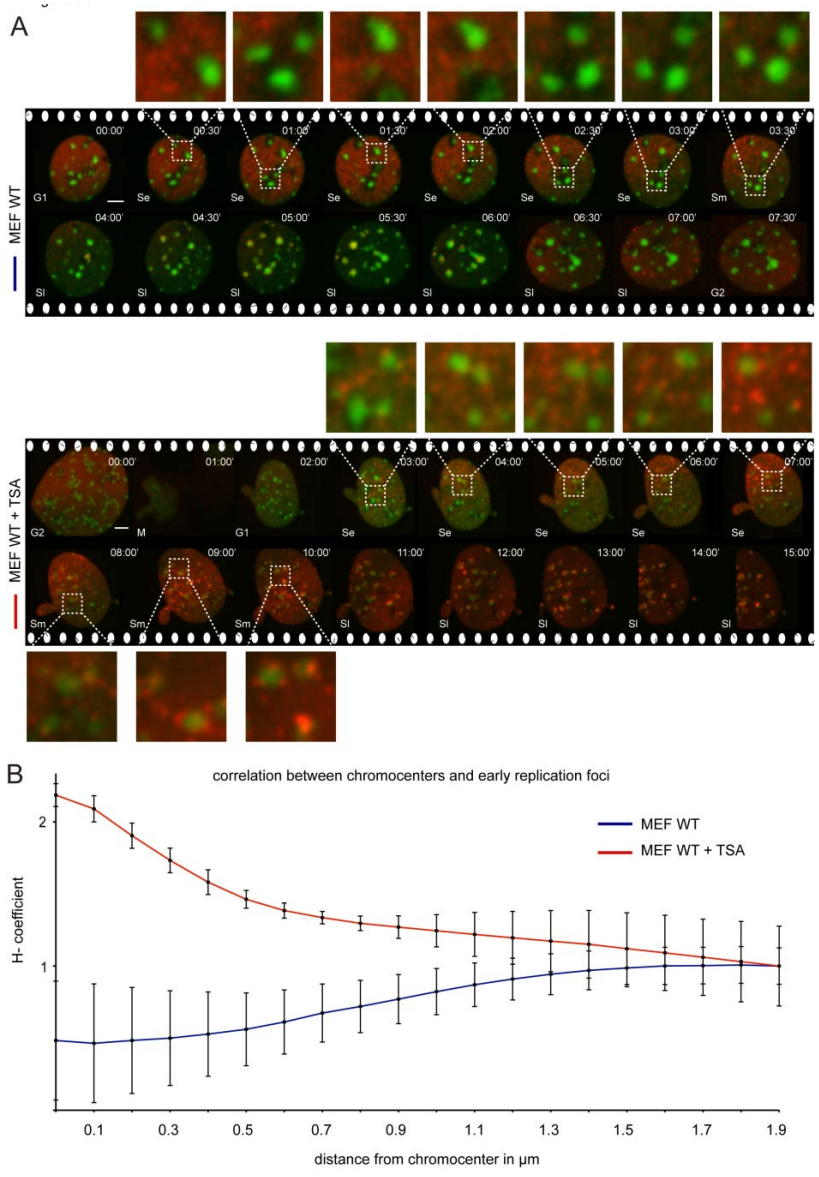

Figure 24. Early replication foci are depleted from heterochromatic regions in control cells but accumulate in hyperacetylated chromocenters[15]

(A) Time-lapse observation of control and TSA-treated replicating cells. (B) The correlation of replication foci to chromocenters during S-phase was assessed by the H-coefficient (Herce et al. in prep) showing that in control cells, the accumulation of early foci outside the chromocenter (right part of the x-axis) is higher than in the chromocenters. In TSA treated cells, on the contrary, the correlation reaches its peak at 0 µm from the reference signal (chromocenters), showing an accumulation of replication foci in heterochromatic regions during early S-phase.

[15] Algorithm developed by Henry D. Herce. Algorithm developed by Henry D. Herce, Herce HD, Casas-Delucchi CS, Cardoso MC. Image co-localization and spatial correlation of objects in multicolor images as a measure of interactions between bio-molecules. *In preparation*.

Movies CC 1 – 2.

Time lapses of control (Supplementary Movie 1) and treated (Supplementary Movie 2) WT MEF progressing through S-phase. Chromocenters were labeled by a GFP-tagged zinc finger protein (MaSat) and active replication foci by mRFP-PCNA. Images were taken with a spinning disc confocal microscope with temperature, CO_2 and humidity control every 30 min. Note the increased colocalization between chromocenters and replication foci in treated cells prior to the onset of late S-phase. Frame rate: 3 fps. Scale bars: 10 µm.

Contributions to this chapter

This work is part of the following manuscript: Casas-Delucchi CS, van Bemmel JG, Haase S, Herce HD, Nowak D, Meilinger D, Stear JH, Leonhardt H, Cardoso MC. Histone acetylation controls replication timing of constitutive heterochromatin. *Under revision.*

I cultivated all cells and performed all cell culture treatments for all experiments. I performed the Western Blots for *p53* and *p53*, *dnmt1* double knockouts. For all cell lines / treatments I performed the *in situ* histone acetylation stainings, the preparation of samples for high-resolution imaging (3D-SIM), the confocal data acquisition and all data analysis and statistical tests. I performed the genomic DNA extraction, bisulfite conversion and amplification for pyrosequencing with instructions from Daniela Meilinger. I prepared the corresponding figures (Figure 7, 17, 18). I performed the doubling time measurements, replication pulse labeling and staining, data acquisition and quantification. I prepared the corresponding figure (Figure 19 and 21). I performed the immuno-FISH experiments, data acquisition, analysis, statistical tests and prepared the corresponding figure (Figure 20). I performed replication stainings in combination with major satellite FISH, acquired the data in the confocal microscope, as well as in the deconvolution microscope, programmed imaged analysis routines in Python to streamline analysis of large amounts of live-cell data, performed the data analysis and statistical tests and prepared the corresponding figure (Figure 22). I performed the double transfection / nucleofection of wild type, TSA-treated and mutant cells, the live-cell microscopy experiments, data analysis and preparation of the corresponding figure (Figure 23 and 24 and corresponding movies). I designed the model figure (Figure 29) and wrote the manuscript.
Contributions from others: Joke van Bemmel performed preliminary experiments on the effects of TSA on replication pattern distribution, Sebastian Haase and Henry D. Herce developed and implemented software data analysis tools for colocalization in fixed and living cells, respectively (Figure 22, 23, 24). Danny Nowak performed Western Blots of TSA treated cells and *Suv39h*1/2$^{-/-}$, Daniela Melinger helped with pyrosequencing. Andreas Meisner acquired high resolution images at the OMX microscope. Jeffrey H. Stear, Heinrich Leonhardt and M. Cristina Cardoso gave advice throughout the work and read the manuscript critically.

5.3 Establishing targeted manipulation of chromatin epistates

Studies attempting to manipulate epigenetic marks at defined particular genomic regions are often based on genetic manipulations or drug treatment, such as (conditional) knockouts of chromatin modifiers, trichostatin A (TSA) or 5-azacytidine (5-aza) treatment (Bickmore and Carothers, 1995; Casas-Delucchi et al., 2011; Kemp et al., 2005; Selig et al., 1988). However, the epigenetic marks manipulated are usually not exclusive to a single genomic region. Thus, these powerful tools have the disadvantage of not being specific regarding the chromatin regions they affect.

Consequently, I was interested in developing tools that would allow the specific manipulation of the epistate of particular genomic regions. In a first stage, I was interested in targeting chromatin modifiers to mouse chromocenters. However, this strategy can similarly be implemented for other targets, such as the inactive X chromosome, as well as for different factors.

To test the effect of histone hyperacetylation on replication timing specifically at pericentric heterochromatin, I decided to target HBO1, a histone H4 acetyltransferase implicated in MCM loading (Miotto and Struhl, 2010). Chromocenters are bound by many different factors, among others MeCP2 and HP1, via different protein domains that recognize specific chromatin modifications characteristic of these regions. In the case of HP1, its chromodomain mediates binding to H3K9m3 (Aasland and Stewart, 1995), one of the hallmark modifications at pericentric heterochromatin. On the other hand, MeCP2, as well as most other members of the MBD protein family, binds via its MBD domain to highly methylated DNA (Hendrich and Bird, 1998; Lewis et al., 1992), another epigenetic mark of chromocenters. I chose the MBD domain of MeCP2 as a carrier to target chromocenters because of its well-characterized and strong accumulation at these regions (Brero et al., 2005).

Direct targeting to chromocenters could be achieved by fusing this domain to our enzyme of interest HBO1. This strategy would result in a single construct, hence experiments on the effects of further chromatin modifiers would have required generation of new expression constructs. Therefore, to make this tool more flexible, I decided to use an indirect approach that would allow the targeting of any GFP-tagged nuclear protein to chromocenters using the same carrier. To this end, I took advantage of the GFP-binding protein (GBP, (Rothbauer et al., 2008)). This nanobody binds to GFP with high affinity *in vivo* and *in vitro*. I reasoned that this interaction might be strong enough to recruit not only GFP, but also GFP-tagged proteins and could thereby be useful to direct potentially any protein fused to GFP. Consequently, I developed a strategy to target any GFP-tagged protein to chromocenters by co-transfection with a fusion construct containing the MBD and the GBP (Figure 25).

I used GFP-HBO1 and created a catalytically inactive HBO1 G485A using site-directed mutagenesis. This mutation was previously described to result in a catalytically inactive enzyme

(Iizuka and Stillman, 1999) and, therefore, was used here as a negative control for HBO1 WT. In addition, we generated an MBD fused to GBP expression construct

Co-transfection of MBD-GBP and GFP-HBO1, but not GBP and GFP-HBO1 or GFP-HBO1 alone, resulted in accumulation of HBO1 at distinct nuclear regions in living cells, instead of the homogeneous nuclear distribution observed for untargeted HBO1 (Figure 26a).

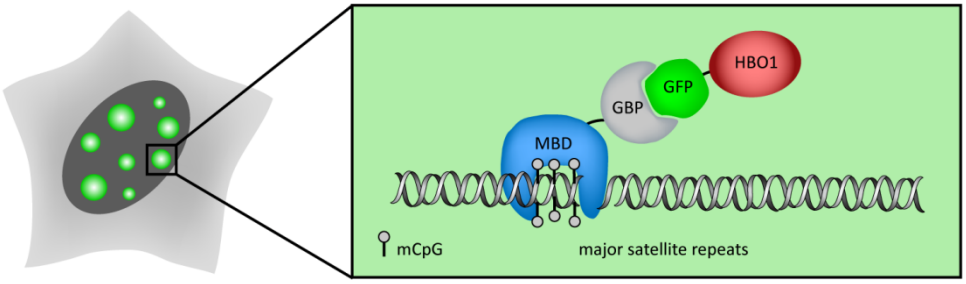

Figure 25 | Schematic outline of the strategy to target chromatin modifiers to chromocenters
Here we take advantage of the strong binding between the GBP nanobody and GFP to target overexpressed GFP-tagged HBO1, a histone H4 acetyltransferase, to chromocenters (green dots in cell nucleus). The same strategy can be used changing either the carrier or the recruited factor.

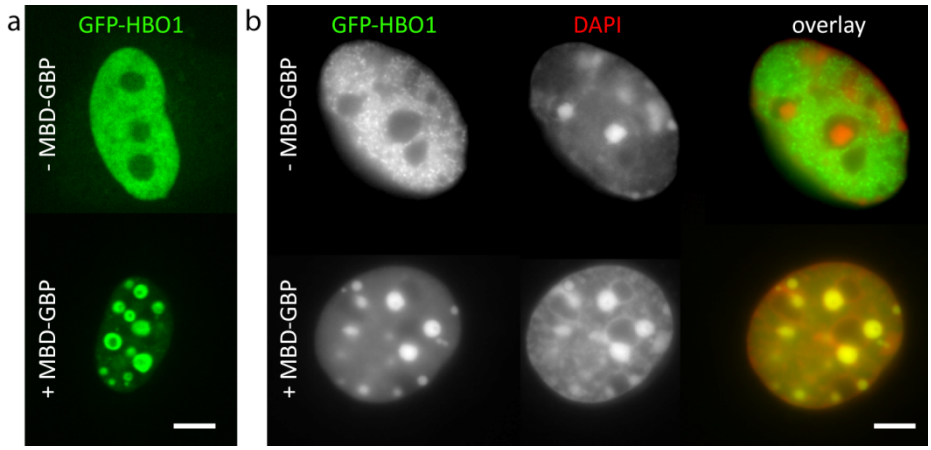

Figure 26 | MBD-GBP targets GFP-HBO1 to chromocenters[16]
a. GFP-HBO1 is homogenously distributed throughout the nucleus. When co-transfected with MBD-GBP, GFP-HBO1 accumulates into structures resembling chromocenters, demonstrating that MBD-GBP causes GFP-HBO1 to accumulate in chromocenter-like structures. **b.** DAPI staining of GFP-HBO1 -/+ MBD-GBP transfected cells showed that the clusters of GFP-HBO1 seen in double transfected cells correspond to chromocenters.

To assess whether the GFP-HBO1 structures seen in living cells after co-transfection with MBD-GBP indeed represented chromocenters, I fixed cells expressing GFP-HBO1 and MBD-GBP and stained them with DAPI. Colocalization of the GFP signal with the DAPI highlighted chromocenters (Figure 26b), demonstrated that MBD-GBP is indeed able to direct GFP-HBO1 to pericentric heterochromatin.

[16] The pMBD-GBP construct was cloned by Jennifer Völger.

These results demonstrate here that a MBD-GBP fusion protein is able to recruit GFP-tagged chromatin modifiers to chromocenters. I thus propose that this tool can be used in combination with a variety of nuclear proteins to specifically modify pericentric heterochromatic regions. Moreover, I propose that an equivalent strategy, with other proteins or domains as a carrier, can be used to target enzymatic activities to other genomic regions, such as the Xi via fusion of GBP to macroH2A (Costanzi and Pehrson, 1998).

Similarly to the fluorescent two hybrid assay (Zolghadr et al., 2008), this assay could be expanded to visualize interaction partners, while at the same time recruiting them to the genomic regions of interest (Figure 27). To this end, a triple transfection of the carrier, a GFP-tagged factor 1 and an RFP-tagged factor 2 would be required. If both factors interact with each other, this would result in them accumulating at the same genomic regions. In this case, this tool would allow the characterization of the effects of both factors at endogenous genomic regions.

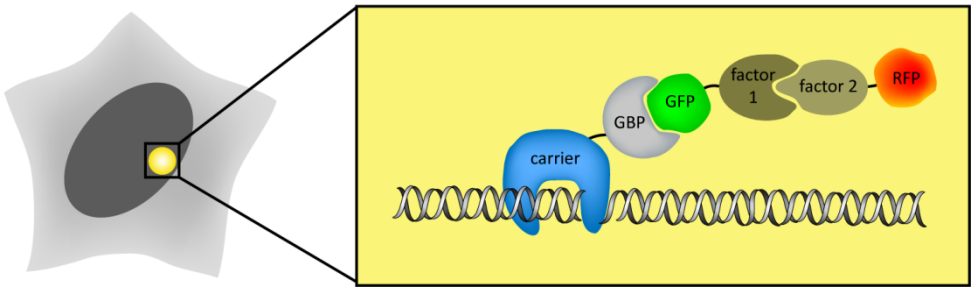

Figure 27 | Modified F2H assay with targeting to endogenous genomic regions
The targeting strategy we present can be easily expanded and combined with the F2H assay (Zolghadr et al., 2008) by co-transfection of possible interaction partners tagged to e.g. RFP. Co-localization of both GFP and RFP signals at the same region would demonstrate interaction between the two fluorescently tagged factors.

When using an endogenous protein or protein domain as a carrier, it is important to consider possible effects caused by its over-expression. For instance, the MBD domain, as well as other chromocenter binding proteins / protein domains, have an endogenous function in the cell and might be involved in the recruitment of chromatin modifying factors (Agarwal et al., 2007; Brero et al., 2005; Nan et al., 1998). I therefore propose a similar targeting strategy using an artificial protein that has no activity in the cell and does not naturally recruit any further factors. A good candidate for what so-call a "neutral carrier" would be the polydactyl zinc fingers protein MaSat, that consists of three zinc finger and binds specifically to the major satellite repeats (Lindhout et al., 2007). This protein, like the MBD domain, clearly accumulates at mouse chromocenters, however, it has more transient binding kinetics (C.S.C.-D., unpublished data), implying that its binding to major satellites is weaker than that of, e.g., the MBD. This fact can both be an advantage and drawback, since a weaker, more transient bind-

ing might be less disrupting to other processes taking place in these regions but, on the other hand, it might be too weak to actually allow the efficient recruitment of a second or third factor and / or chromatin remodeling. In any case, this tool would be a useful control for targeting strategies that use endogenous proteins / protein domains.

The novel application of TALEs (transcription activator-like effectors) for genomic targeting represents a further tool to specifically modify chromatin at particular regions (Miller et al., 2011). Originally found in the pathogenic bacterium Xanthomonas, TALEs contain a central protein domain consisting of 17.5 tandem repeats of 34 amino acids, of which only the last two are variable. These so-called hypervariable diresidues determine the DNA binding specificity of each TALE (Moscou and Bogdanove, 2009). Already shown to effectively target different enzymes to specific genomic sequences (Miller et al., 2011), TALEs could also be used to target chromatin modifiers, either directly or more flexibly via the GBP-GFP interaction, as described above. A major advantage of TALEs, when compared to zinc finger proteins, consists in their more reliable and better predictable targeting (Boch, 2011).

A further step in the specific regulation of distinct chromatin domain would be the possibility of temporally regulating the action of chromatin modifiers. Such temporal regulation could be achieved by controlling the nuclear transport of the protein of interest. Indeed, it has been shown that fusing an otherwise nuclear protein to an estrogen receptor is enough to trap it in the cytoplasma. Consequently, binding of the receptor to estrogen results in nuclear import of the fusion protein (Littlewood et al., 1995), which can then fulfill its normal role in the nucleus. The powerful combination of this tool with live-cell microscopy opens the possibility of modifying specific chromatin regions at particular cell cycle stages, an approach of special relevance when studying cell cycle dependent processes, such as DNA replication.

An important advantage of the method that I have started to develop is the fact that the results of our proposed targeting strategies can be easily quantified with automated image analysis tools and, thus, are suitable for large-scale screening of chromatin modifiers and interacting factors.

6. Discussion

The spatio-temporal regulation of DNA replication is conserved throughout metazoans and is a developmentally regulated process (Blow, 2001; Hatton et al., 1988; Hiratani et al., 2008, Simon et al., 1999). These observations demonstrate that its control cannot rely on genetic elements alone, leading to the proposal that epigenetic mechanisms are likely to influence this process (Aladjem, 2007; Mechali, 2001). When it comes to the control of replication timing in high eukaryotes, particularly in mammals, attempts to elucidate the mechanisms directly involved in defining temporal organization have been complicated by the crosstalk between the many layers of epigenetic modifications defining the chromatin state of any particular region. Thus, the question of which epigenetic marks play a direct role in defining the replication program remains open.

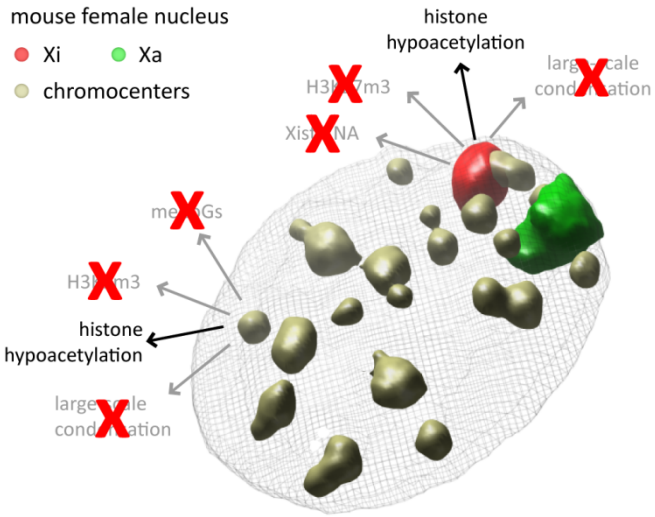

Figure 28 | Epigenetic marks directly involved in replication dynamics
Manipulation of the epigenetic hallmarks of both facultative and constitutive heterochromatic regions (the Xi and chromocenters, respectively), as well as a careful assessment of their crosstalk, allowed us to determine that the low levels of histone acetylation characteristic of both heterochromatic regions are directly linked to their replication dynamics.

At the beginning of this work, only a few studies had addressed this issue, producing seemingly contradicting results ((Bickmore and Carothers, 1995; Selig et al., 1988), see introduction). To study the effects of the epigenetic mechanisms on replication dynamics, I chose the most prominent examples of mammalian facultative and constitutive heterochromatin, the mammalian Xi and mouse chromocenters. I manipulated the epigenetic hallmarks of these regions and comprehensively analyzed the resulting effects on their replication timing. Our approach, including *in vitro*, *in situ* and *in vivo* analyses, enabled us to show that the apparently contradicting results of the above-mentioned studies can be reconciled by assessing the secondary effects of manipulating different epigenetic factors (Casas-Delucchi et al., 2011; Casas-Delucchi et al., submitted). I show that the delay in replication onset of both, facultative and constitutive heterochromatin, is a result of their histone acetylation levels (Figure 28). Here, I discuss the possible mechanisms by which histone acetylation could influence the timing of origin firing and thereby the replication program of the genome. Moreover, I make use of the

Xi as an example of transcriptionally silenced chromatin to discuss the possible effects of transcriptional activity on DNA replication dynamics.

6.1 Histone acetylation controls the inactive X chromosome replication dynamics

In the present study I demonstrate that Xi in somatic mammalian cells replicates during early-mid S-phase. The replication of most of the silenced chromosome takes place in a synchronous manner, indicating the simultaneous firing of more replication origins than in the active homologue. Furthermore, I found that these replication dynamics are controlled epigenetically. Since the close interaction between the different Xi epigenetic marks (Csankovszki et al., 2001) results in a difficulty to disrupt any of these modifications without affecting the others, I also made use of an ectopical *Xist* expression system (Wutz and Jaenisch, 2000) that permits temporal discrimination of the appearance of different modifications and their respective effect on the replication of the inactive chromosome. With this system I found that the *Xist* expressing autosome assumed the typical Xi-like synchronous replication only after cellular differentiation and global hypoacetylation of the silenced chromosome. Thus, I conclude that histone hypoacetylation is the most direct epigenetic determinant of the Xi replication mode.

Our time lapse analysis showed that the bulk Xi replicates within a narrow time frame in early-mid S-phase. The apparent contradiction to earlier studies that defined Xi as late-replicating(German, 1962; Gilbert et al., 1962; Moorhead and Defendi, 1963; Morishima et al., 1962; Petersen, 1964; Priest et al., 1967) can be clarified by carefully considering the labeling protocols used therein and, in fact, the outcomes are in agreement with ours. Using synchronized cultures pulse labeled with tritiated thymidine shortly after release of an S-phase block, would exclusively label early replicating DNA. In mitotic spreads of such pulse labeled cultures the lack of label on one of the X chromosomes was correctly interpreted as showing "non-early" replication(Petersen, 1964; Priest et al., 1967). Increasing the nucleotide pulse duration to three hours resulted in staining also the Xi (Priest et al., 1967), which indicates that replication of the presumable Xi must have started three hours after release of the cell cycle block. Schwemmle et al. (Schwemmle et al., 1989) performing cell synchronization followed by (0.5-1 hour) nucleotide pulse labeling detected no nucleotide incorporation in the Xi during the first 1-2 hours after release from G1/S block and Xi replication was detected only thereafter. This study also reevaluates a series of reports, e.g., (Latt, 1973; Willard and Breg, 1980) based on continuous labeling approaches describing a high variability in the replication sequence of the Xi. The authors could not corroborate the variation in the Xi replication sequence, which is likely a consequence of the variation in the length of the cell cycle stages. Their results fit well with our time lapse imaging and fixed cell data (Figure 8 and Supplementary Movies Xi 1 - 4). Interestingly, replication studies performed in mouse embryonic cells at

different days post coitum (dpc) show a shift from isocyclic to allocyclic replication, with delayed initiation and early cessation of the Xi replication at 6.5 dpc (Takagi, 1974; Takagi et al., 1982). In a more recent study cells were double pulse labeled with a chase of four hours in between and hybridized with an X chromosome specific paint (Visser et al., 1998). Cells that incorporated modified nucleotides during both pulses were selected, with the first pulse labeling early and the second mid/late replication structures. Indeed in this study (Figure 8), the second pulse shows a typical mid pattern, including the synchronously replicating Xi, widely excluded from the first pulse. Importantly, our data do not exclude that small regions of the Xi might be replicated asynchronously from the Xi bulk chromatin, in agreement with Hansen et al. (Hansen et al., 2010).

A second characteristic property of the Xi replication mode presented in this study is its synchronous replication. In contrast to autosomes and the active X chromosome, where a limited number of origins fire at any given time during S-phase (Camargo and Cervenka, 1982), the number of firing origins engaged in replication of Xi appeared to be concentrated within a limited period of time. This synchronous replication, already suggested in previous studies (Gilbert et al., 1962), is clearly and directly demonstrated both by our *in vivo* time lapse analysis using fluorescently tagged replication factors, as well as by nucleotide incorporation.

Since both X chromosomes contain the same DNA sequence and have been shown to utilize at least in part the same replication origins (Gomez and Brockdorff, 2004), it is clear that the synchronous replication dynamics cannot be explained genetically, suggesting that epigenetics play an important role determining the Xi replication dynamics.

An imminent question is what causes Xi to replicate synchronously within a limited time frame compared to the active homologue. Our results show that the replication dynamics of Xi is regulated epigenetically. First, I was able to show that the redundancy for *Xist* expression in the maintenance of transcriptional silencing (Csankovszki et al., 1999) is paralleled by a partial redundancy in the maintenance of the Xi replication timing. Xist RNA accumulation is the first event during the initiation of X inactivation in differentiating cells (Panning et al., 1997), hence knocking out *Xist* results in partial loss of downstream Xi modifications, such as H3K27m3 (Plath et al., 2003; Silva et al., 2003), and consequently in a partial loss of the synchronous replication pattern. Our observation that in *Xist* conditional knockout cells H3K27m3 is lost following the loss of *Xist* expression to the same degree as the Xi replication pattern, as well as increase of histone acetylation (Figure 11 and 12) indicates that the partial loss of synchronous replication was actually caused by an altered histone modification composition rather than by deficient Xist RNA accumulation *per se*. This proposal appears especially plausible insofar as cells with a “normal” Xi replication pattern showed the “normal”

elevated H3K27m3 level on Xi, although I cannot strictly rule out other potential indirect effects of the different epigenetic manipulations.

Finally, I was not only able to show that the loss of histone hypoacetylation at Xi, as a consequence of HDAC inhibition by TSA, results in a significant decrease of synchronous replication (Figure 11), but could also show that global histone hypoacetylation upon differentiation correlates with the appearance of the synchronous, early-mid Xi replication dynamics (Figure 16). Importantly, in TSA treated cells, the levels of Xist RNA (Figure 14) and H3K27m3 (Figure 11) at the inactivated chromosome were normal and both modifications were also present in transgenic ES cells prior to differentiation and appearance of the synchronous replication pattern (Figure 16). Thus Xist RNA and H3K27m3 are not sufficient to set the replication timing of the Xi and, hence, the most direct determinant of Xi replication dynamics is the level of histone acetylation.

Our observations on the Xi replication raise the question about the meaning of such distinct replication dynamics and possible parallels in other types of silenced chromatin regions. A possible consequence of the different timing of X chromosome replication, addressed in previous studies, could be that specific epigenetic marks on Xi have to be set within a limited window of time during early-mid S-phase, to limit the chromatin portion being modified(Lande-Diner et al., 2009), with distinct histone modification outcomes depending on the replication timing and ultimately influencing and/or reinforcing the transcriptional state of the replicated chromatin. ICF syndrome constitutes a striking example of the relationship between replication timing and transcriptional activity. In such cells CpG islands of the Xi are hypomethylated (Miniou et al., 1994), but only those genes that replicate asynchronously from the bulk Xi and synchronously with the Xa homologue, escape X inactivation (Hansen et al., 2000).

The synchronous replication of Xi, implying the simultaneous firing of replication origins that in the active homologue fire sequentially(Gomez and Brockdorff, 2004), resemble observations in embryos of flies and frogs previous to the onset of transcriptional activity. In *Drosophila* embryos, replication origins were shown to be regularly spaced and to fire synchronously thus permitting entire genome duplication within the extraordinarily short (3-4 minutes long) S-phase of the initial 10-13 mitotic divisions (Blumenthal et al., 1974). In *Xenopus* embryos, untranscribed DNA is replicated up to 11 times in the short time frame of 7 hours (Newport and Kirschner, 1982), requiring synchronous firing of all licensed replication origins and their regular distribution(Blow et al., 2001; Mills et al., 1989) to achieve an extremely fast completion of S-phase. Interestingly, this untranscribed chromatin is also hypoacetylated. One possibility would be that the absence of transcriptional activity/competence and

the concomitant lack of necessity of coordinating both processes might allow simultaneous replication throughout transcriptionally silenced regions (Hiratani et al., 2009).

Altogether, I speculate that the synchronous replication dynamics of Xi might represent a common replication manner to different forms of transcriptionally silent chromatin and that histone hypoacetylation is the common epigenetic denominator regulating their replication synchrony.

6.2 Histone acetylation controls replication timing of constitutive heterochromatin

In this study, I used drug treatment and mutant cell lines to comprehensively assess which epigenetic modifications are important for defining the late replicating nature of constitutive heterochromatin. By combining these approaches with quantitative microscopy, I was able to directly investigate the connection between epigenetic modifications and the spatial and temporal control of replication timing. I show that treatment with TSA, as well as knocking out *dnmt1*, results in an earlier onset of replication at chromocenters. In both cases, this effect was associated with an increase in the normal levels of histone acetylation at chromocenters (see below and Figure 29). In contrast, *Suv39h*1/2$^{-/-}$ cells with reduced levels of H3K9m3 and normal levels of histone acetylation exhibited no change in replication timing. I therefore conclude that the level of histone acetylation at a given genomic region is a major factor in determining its replication timing.

One important consideration when manipulating the epigenetic state of any genomic region is the downstream effects on chromatin structure and the binding of additional chromatin factors. This is particularly relevant with chromocenters, given that their epigenetic profile is directly related to their highly condensed nature and contributes to the recruitment of multiple proteins (Dillon and Festenstein, 2002). In this case, the methods I used to perturb the epigenetic modification on constitutive heterochromatin (i.e., TSA treatment, *dnmt1* and *Suv39h*1/2 knock-outs) all resulted in a large-scale decondensation of the chromocenters. However, only two out of the three cases promoted a shift in the replication timing of the constitutive heterochromatin. The fact that *Suv39h*1/2$^{-/-}$ cells exhibit no clear change in their replication timing indicates that the chromatin decondensation I observe here is not directly related to an alteration in replication timing. While it has been reported that an open chromatin condensation may facilitate early replication (Aladjem et al., 1995), I argue that a general decondensation on the scale that is visualized by DAPI staining *in situ* is not per se sufficient to promote early replication of heterochromatic regions. It should be noted here that while the decondensation I observed appears comparable in all three cases, it is possible that there are more subtle local differences, which cannot be detected by DAPI staining and might affect replication timing. Knocking out *Suv39h*1/2 genes also abolishes the binding of HP1 to chro-

mocenters (Lehnertz et al., 2003), indicating that this important heterochromatin determinant does not contribute to the regulation of replication timing. We, therefore, conclude that neither H3K9m3, nor chromatin condensation, nor HP1 binding, are directly involved in defining the late replication pattern observed for constitutive heterochromatin. Interestingly, knocking down HP1 in *Drosophila* affects late replication of heterochromatin, demonstrating that replication timing in mammalian cells underlies a somewhat different control mechanism as in invertebrates.

In both, TSA-treated and *dnmt1*$^{-/-}$ cells, I observe a shift in replication timing, whereby normally late replicating constitutive heterochromatin is replicated during early S-phase. TSA treatment directly promotes the hyperacetylation of histones, specifically relating this epigenetic modification to the regulation of replication timing. As DNA methylation is unaffected in TSA-treated cells, I conclude that this DNA modification does not block early replication. While DNA methylation loss is the most direct effect of knocking out *dnmt1*, our results (Figure 20), as well as previous studies (Jones et al., 1998), demonstrate that this decrease leads to elevated histone acetylation levels at chromocenters. I therefore argue that in *dnmt1*$^{-/-}$ cells, concomitant changes in the levels of histone acetylation are responsible for the shift in replication timing of constitutive heterochromatin, analogous to what I observe in TSA-treated cells. Moreover, although I do not exclude the possibility that TSA-mediated acetylation of non-histone proteins might play a role in the described shift in replication timing, our results in *dnmt1* knock-out cells demonstrate that histone hyperacetylation is sufficient to promote earlier replication onset of constitutive heterochromatin. Thus, I conclude that histone hypoacetylation facilitates late replication timing independently of both histone and DNA methylation (Figure 29). Interestingly, our results show that there is no mechanism absolutely preventing early replication of heterochromatic regions. Indeed, we have reported that in normal untreated mouse cells, a certain small percentage of the usually late-replicating centromeric regions replicate during early S-phase (Weidtkamp-Peters et al., 2006).

Ultimately, replication timing is defined by the timing of origin firing. The relative efficiency model of origin firing proposes that early origins fire more efficiently, while late origins have a low efficiency at the beginning of S-phase, which increases as S-phase progresses, thus assuring that potential gaps of unreplicated DNA are closed in a timely fashion (Rhind, 2006). In the context of this model, our data clearly points to the fact that histone acetylation plays an important role in defining the firing efficiency of origins and concomitantly the replication timing of distinct genomic regions. There are various processes leading to origin firing itself at which histone acetylation might regulate replication timing. For instance, it has been shown recently that origin firing dynamics in fission yeast can be a result of differences in the time of ORC binding at different regions (Wu and Nurse, 2009). The binding of limiting ORC factors could be enhanced at acetylated regions with an open chromatin conformation. Origin licens-

ing is another process that can be enhanced by histone acetylation, since HBO1-mediated histone acetylation in yeast has been shown to play an important role in the loading of the Mcm 2-7 complex (Miotto and Struhl, 2010), necessary for origin licensing (Takahashi et al., 2005). An increased basal level of histone acetylation may therefore facilitate origin licensing. Alternatively, histone acetylation could also play a role in the actual firing process, potentially by increasing accessibility or binding affinity to limiting firing factors, such as yeast Cdc45 (Aparicio et al., 1999; Vogelauer et al., 2002), which has been shown to increase the firing efficiency of inefficient origins (Wu and Nurse, 2009). Further experiments using high-resolution microscopy could give a more detailed insight into the structural changes resulting from histone hyperacetylation. Moreover, protein-DNA interaction profiling under different chromatin acetylation conditions could elucidate how this histone modification affects binding of licensing / firing factors to origins and how epigenetics modify chromatin metabolism.

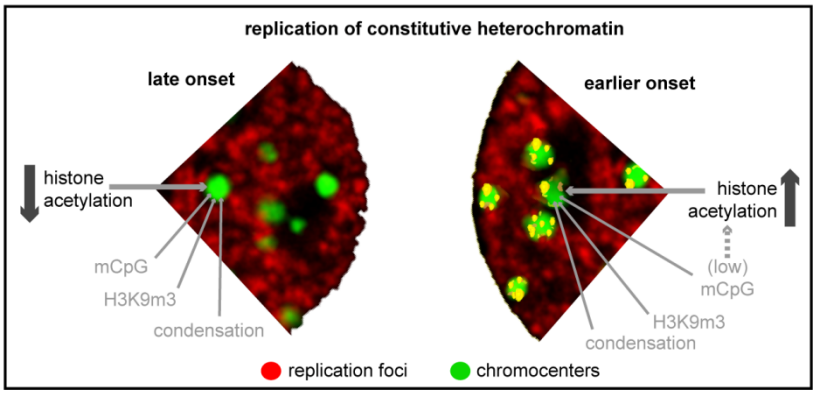

Figure 29. Summary of the effect of epigenetic changes in replication timing of constitutive heterochromatin.[17]

Histone hyperacetylation at constitutive heterochromatic regions results in earlier replication onset. While DNA methylation has and indirect effect on replication timing via histone acetylation (dashed arrow), both H3K9m3 accumulation and large-scale decondensation of chromocenters are not sufficient to disrupt late replication.

6.3 Time and time again: molecular mechanisms by which histone acetylation influences replication timing

Replication timing is ultimately defined by the timing of origin firing, which is determined by a series of molecular events that start during late mitosis and include ORC binding to potential origins, followed by recruitment of Cdc6 and Cdt1. In metazoan during G1, Cdt1 recruits HBO1, an H4-HAT with no known yeast homolog, which increases local histone acetylation.

[17] Figure taken from: Casas-Delucchi CS, van Bemmel JG, Haase S, Herce HD, Nowak D, Meilinger D, Stear JH, Leonhardt H, Cardoso MC. Histone acetylation controls replication timing of constitutive heterochromatin. Under revision.

Origins are subsequently licensed to fire by MCM loading. Origin activation occurs when Dbf4/Cdc7 and Cdk2/CyclinE phosphorylate the loaded MCMs and thereby loads pre-IC factor Cdc45, respectively. Cdc45 then interacts directly with MCM, resulting in origin unwinding, stabilization of the single strand DNA by RPA and recruitment of DNA pol α (see introduction and Figure 1 for details and references). The complexity of the multiple steps leading to origin firing offers multiple layers of possible regulatory mechanisms at which histone acetylation might play a role (Figure 30).

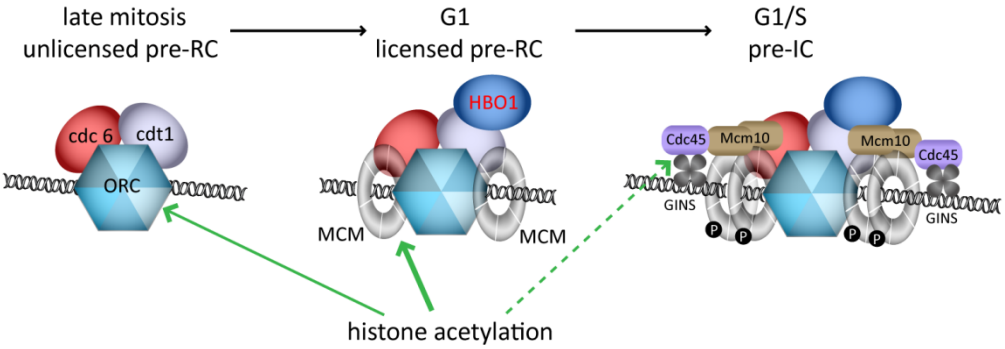

Figure 30 | Effects of histone acetylation on the different steps of origin activation.
Arrows point to the different steps leading to replication origin firing at which histone acetylation has been shown to or might play a regulatory role. Histone hyperacetylation might increase chromatin accessibility and thereby promote pre-RC formation or licensing. Indeed, the H4-HAT HBO1 has been recently shown to be required for MCM loading human cells (Miotto and Struhl, 2010). Additionally, histone acetylation might directly promote binding of pre-IC factors, such as Cdc45.

To understand how histone acetylation might be involved in defining replication timing, one needs to consider this epigenetic mark and its effects on chromatin within the context of the current knowledge on the molecular mechanisms regulating the genomic replication program. Studies in the last decade have shown that replication origins fire with different efficiencies (Hamlin et al., 2008; Lebofsky et al., 2006). Moreover, it has recently been shown that high firing efficiency strongly correlates with early origin firing (Heichinger et al., 2006). Interestingly, high firing efficiency and, hence, early replication timing have been proposed to be the consequence of preferential binding to a limiting factor, involved in the process of origin activation (Goldar et al., 2008). The existence of such a limiting factor and its role in determining firing efficiency have been supported by the observation that in *Xenopus* egg extracts, an *in vitro* system where all replication factors are present in excess, all DNA sequences replicate with approximately the same efficiency (Stanojcic et al., 2008). Similarly in *Drosophila* and *Xenopus* embryos, where origin determining, licensing and firing factors are present in excess, all available origins fire efficiently (Mechali, 2010). Furthermore, it has been suggested that the proposed limiting factor would be recycled as S-phase progresses, being released from early origins and subsequently re-used at late origins. Thus, the firing efficiency of late origins would increase during the course of S-phase. Interestingly, such molecular dynamics would

facilitate the closing of unreplicated DNA gaps and might thereby help solve the "random completion" problem (Hyrien et al., 2003). Currently, the best candidate to fulfill the role of a limiting factor appears to be the pre-IC factor Cdc45, shown to be present in limiting amounts in human cells (Pollok et al., 2007). While other pre-IC components might also be present in limiting amounts, the majority of the remaining factors, in particular the MCM proteins, are found in large excess in the nucleus and are therefore unlikely to play a limiting role in origin firing (Hyrien et al., 2003).

Interestingly, current models on replication dynamics propose that the existence of a limiting factor and differential firing efficiencies at distinct genomic regions are sufficient requirements to reconcile the seemingly contradicting phenomena of stochastic origin firing and conserved nuclear replication patterns (Rhind et al., 2010; Yang et al., 2010). Nevertheless, the exact molecular processes that eventually lead to a higher affinity of a fraction of origins for such a limiting factor have only started to be elucidated. A recent study comparing early, late and cryptic (inactive in their chromosomal context) fission yeast origins, has shown that ORC binds to early origins in mitosis earlier than to late origins (Wu and Nurse, 2009). Earlier ORC binding results in preferential pre-RC formation during G1, as measured by the levels of Mcm4 loading. Importantly, the MCM:ORC ratio has been demonstrated to be well above 1:1 *in vitro* (Bowers et al., 2004; Edwards et al., 2002), in yeast (Lei et al., 1996), as well as in animal cells (Mahbubani et al., 1997), as a result from multiple rounds of MCM loading at a single origin (Bowers et al., 2004). In fact, this so-called lateral loading might also account, at least in part, for the MCM paradox (Laskey and Madine, 2003). Importantly, higher MCM levels have been correlated with increased firing efficiency in budding yeast origins (Wyrick et al., 2001). Moreover, the efficiency of replication of DNA injected into *Xenopus* eggs has been shown to increase with the size of the injected DNA (Mechali and Kearsey, 1984), which might be a consequence of longer DNA being able to bind more MCM.

As a consequence of advanced pre-RC formation, early origins are preferentially bound by the pre-IC component Cdc45 (Wu and Nurse, 2009). Fittingly, the level of Cdc45 at a particular origin has been shown to reflect its firing efficiency (Edwards et al., 2002; Wu and Nurse, 2009). Additionally, previous studies in budding yeast also showed that the timing of Cdc45 binding differs in early and late origins (Aparicio et al., 1999).

Assuming that Cdc45 is indeed a limiting factor for replication origin firing, as a consequence of preferential binding to early origins, late origins have to wait until Cdc45 is released from early origins before they can fire. Fitting to this notion, Cdc45 over-expression advances replication of some late origins (Wu and Nurse, 2009). Interestingly, even though all MCM complexes at one origin are activated and in principle able to recruit Cdc45, only one out of ap-

proximately 24 MCM molecules actually binds Cdc45 (Edwards et al., 2002), suggesting that MCM accumulation can act cooperatively in Cdc45 recruitment. The limited Cdc45 binding might also be the result of some unknown molecular mechanism repressing Cdc45 recruitment at neighboring regions, inhibiting thereby adjacent sequences from firing in the same replication round. This so-called origin interference could thereby promote a better dispersion of firing events and reduce the probability of long unreplicated DNA gaps, as proposed in (Lucas et al., 2000). Hence, Cdc45 might play a double role in preventing long stretches of unreplicated DNA: one, by increasing late origin efficiency in the course of S-phase through its recycling from early to late origins and two, by inhibiting a too strong clustering of active origins.

Our results clearly demonstrate that replication timing is controlled epigenetically and that low levels of histone acetylation at heterochromatic regions lead to the delayed onset of replication that characterizes these regions (Casas-Delucchi et al., 2011; Casas-Delucchi et al., submitted). While manipulation of others epigenetic marks, such as Xist RNA accumulation at the Xi, histone and DNA methylation, as well as large-scale chromatin compaction did not directly affect replication timing of heterochromatin, I was able to show that increasing the normal levels of histone acetylation at both, the Xi and chromocenters, advances the onset of replication of such regions. My work illustrates the importance of addressing downstream effects of any epigenetic mark, as exemplified by the effects of disrupting the normal levels of DNA methylation at chromocenters. Such manipulation locally increases histone acetylation at constitutive heterochromatin and thereby indirectly affects replication timing of these regions. Contrastingly, histone acetylation had a clear effect on replication timing without affecting Xist RNA accumulation, histone or DNA methylation. We, therefore, propose that the levels of histone acetylation directly influence replication timing.

To directly link histone acetylation to the regulation of the replication program, we need to consider how chromatin structure could influence any of the steps leading to origin activation. In general terms, histone acetylation has been shown to decrease the level of chromatin compaction (Gorisch et al., 2005) and, thus, might enhance chromatin accessibility for different factors. Consequently, this increased accessibility might result in better ORC binding, pre-RC or pre-IC formation (Figure 31) (Gauthier and Bechhoefer, 2009). Supporting this idea, TSA-mediated histone hyperacetylation equalizes origin firing efficiency at some human loci (Kemp et al., 2005). In this context, the fact that unfavorable nucleosome positioning inhibits origin firing further demonstrates that chromatin structure plays a role in origin selection (Crampton et al., 2008; Simpson, 1990). It should be mentioned here, that my results show that large scale decondensation of chromocenters, as it results from knocking out *Suv39h*1/2, is not enough to advance replication timing of these regions (Casas-Delucchi et al., 2011; Ca-

sas-Delucchi et al., submitted). Therefore, the increase in chromatin accessibility that results from hyperacetylation must be higher than the large scale changes that cause by the loss of histone methylation.

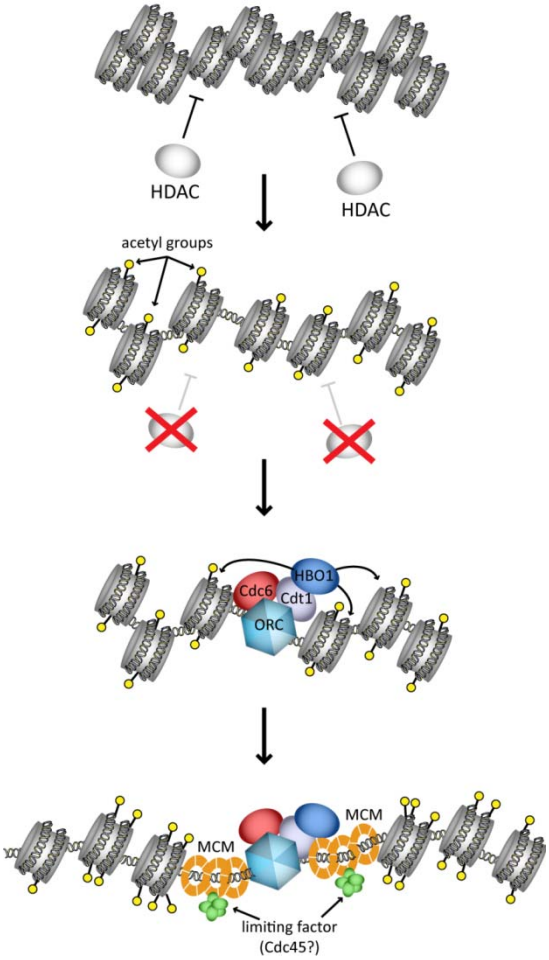

Figure 31 | Effects of HDAC inhibition on late replicating regions.
The normal histone hypoacetylated constitution of heterochromatic regions is maintained by constitutively active histone deacetylases (HDACs). If these enzymes are inhibited, e.g. by trichostatin A (TSA) treatment, heterochromatin is hyperacetylated and its structure changes to a more open conformation. This increased accessibility results in earlier origin firing, due to earlier / better binding of pre-RC and, consequently, of pre-IC factors.

Interestingly, HDAC inhibition, like knocking out HDACs or targeting HAT to particular regions (see results chapter 3 and (Knott et al., 2009; Vogelauer et al., 2002)), affects histone acetylation by changing the ratio of active HAT to HDACs globally or at specific loci. It is, therefore, conceivable that origin firing efficiency can be regulated by the local ratio of HAT to HDACs, implying that HATs could be an additional limiting factor defining origin efficiency, easily outbalanced at heterochromatic regions, where HDACs are actively recruited (Nan et al., 1998).

Interestingly, when it comes to pre-RC licensing, increased H4 acetylation by HBO1 has been shown to be a requisite for MCM loading in human cells (Miotto and Struhl, 2010). This observation suggests that the basal levels of histone acetylation could also influence the process of pre-RC licensing, where the hypoacetylated heterochromatic regions might need more cycles of HBO1-mediated acetylation than hyperacetylated euchromatic ones to achieve efficient MCM loading. This disadvantage of hypoacetylated regions for MCM loading would be further exacerbated by the preceding delay in ORC as well as Cdt1 binding and, consequently, HBO1 recruitment.

In addition, histone acetylation could also play a direct role in regulating chromatin recruitment of pre-IC factors, such as Cdc45, Mcm10 or GINS (Gauthier and Bechhoefer, 2009). Interestingly, the primase inhibitor actinomycin D, which also intercalates into DNA and might thereby induce structural changes, enhances Cdc45 binding to MCM (Edwards et al., 2002). Importantly, I do not rule out the possibility that histone acetylation could play a role by directly recruiting specific pre-RC or pre-IC factors to chromatin. It should be noted here that acetylation of non-histone proteins could also be involved in the process of origin activation. For instance, it has been demonstrated that Mcm3 is acetylated when loaded onto chromatin by the enzyme MCM3AP, although here acetylation negatively regulates replication and therefore does not explain my results (Takei et al., 2002; Takei et al., 2001). On the other hand, more recently cohesin acetylation has been proposed to play a role in replication dynamics by accelerating the replication fork. Here, acetylation of cohesin is suggested to result in structural changes from a fork-obstructing cohesin configuration to one that permits fork progression (Terret et al., 2009).

In summary, I propose a model whereby histone acetylation enhances pre-RC formation and / or licensing by increasing access of the pre-RC / pre-IC factors to chromatin (Figure 32). This preferential pre-RC formation results in an advantage for hyperacetylated origins when competing for any limiting pre-IC factor, likely Cdc45, leading to earlier origin firing. On the other hand, origins in hypoacetylated, higher compacted regions would have slower pre-RC formation dynamics and possibly even require more rounds of (HBO1-mediated) histone acetylation. This delayed pre-RC formation and licensing would represent a significant disadvantage towards early origins when competing for any limiting factor. As a consequence, origins in hypoacetylated regions would not be able to fire efficiently until the limiting factors are released from early origins later in S-phase (Figure 32).

Our model gives rise to the following predictions that can be tested experimentally: 1st during M/G1, mammalian origins would be bound differentially (both temporally and in the total amount) by ORC and / or MCM with a preference for origins situated in hyperacetylated,

euchromatic regions; 2nd this enhanced pre-RC formation / licensing results in preferential binding of a downstream pre-IC factor; 3rd at the onset of S-phase the limiting pre-IC factor, likely Cdc45, is not bound at late origins; and 4th as S-phase passes from the early to the late stage, the limiting factor becomes increasingly available for the unreplicated regions, which increases their firing efficiency and helps close unreplicated gaps.

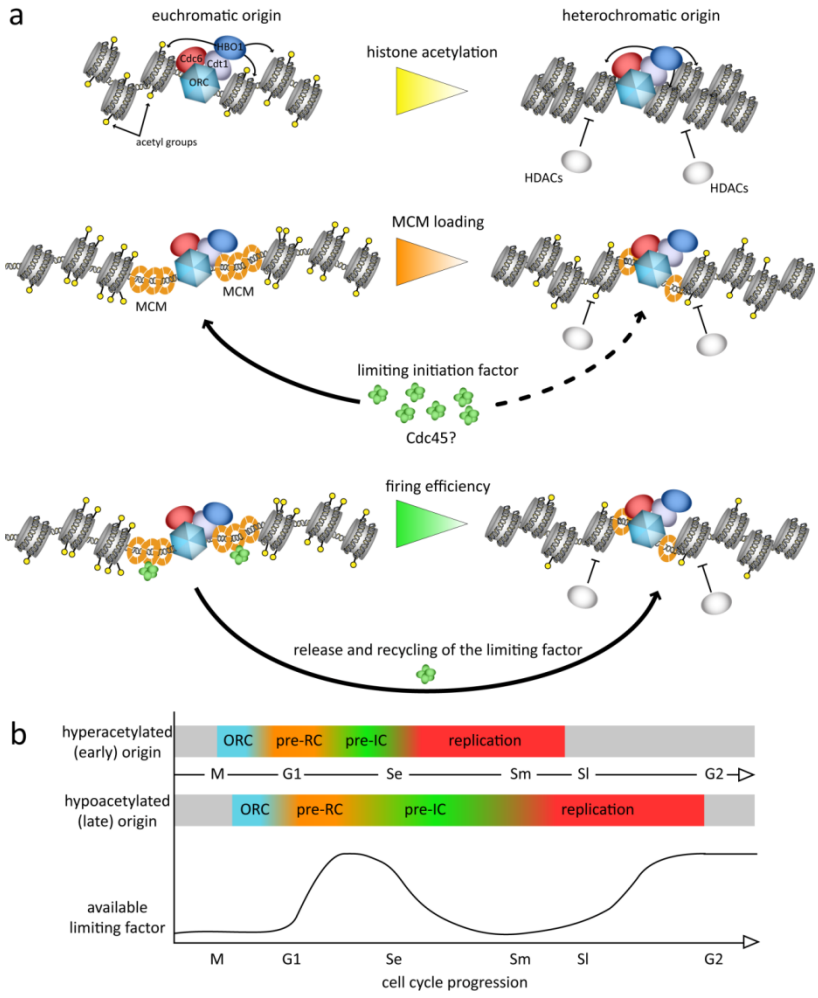

Figure 32 | Comparison of euchromatic versus heterochromatic origins in mammalian cells.
a. Histone hyperacetylation in euchromatin results in increased accessibility for pre-RC factors. I propose that this open conformation due to histone acetylation is reflected in higher levels of and / or advanced MCM loading, leading to an advantage when competing for a limiting pre-IC factor. On the other hand, heterochromatic origins are more tightly packed, so that even after HBO1-mediated histone acetylation increase, they are less accessible for pre-RC formation and therefore less prone to bind the liming factor. As a consequence, hypoacetylated origins cannot fire efficiently until the limiting factor is released from early origins. Therefore, I propose that the histone acetylation level at replication origins controls their firing efficiency. b. Temporal correlation between the molecular events at replication origins leading to firing of early (hyperacetylated) versus late (hypoacetylation) origins and their relation to the unbound fraction of the proposed limiting factor Cdc45. This time line results from my model suggesting that histone acetylation determines firing timing by regulating the order of pre-RC and / or pre-IC formation and concomitantly the likelihood of a particular origin to recruit Cdc45.

6.4 The replication program and transcriptional activity or on how a mammalian chromosome resembles fly and frog genomes

Using *in situ* and *in vivo* replication analysis of mammalian female cells from different tissues and species, I was able to study with high temporal resolution the replication dynamics of the Xi, an epigenetically silenced chromosome that constitutes the most prominent example of facultative heterochromatin (Lyon, 1961). We confirmed that, as described 50 years ago, the Xi starts replicating later than the active homologue and the autosomes (German et al., 1962; Gilbert et al., 1962; Morishima et al., 1962) and yet were able to show that the Xi is replicated still during the first half of S-phase, thereby shifting the paradigm of a late replicating Xi. Furthermore, we demonstrate that, once it starts, the replication of the bulk Xi takes only one to two hours. This extremely short time, compared to the on average ten hours long S-phase of mammalian somatic cells, results from the synchronous replication of most of the chromosome (Casas-Delucchi et al., 2011).

A fascinating example of the synchronous replication dynamics we describe for the mammalian Xi is found in early *Xenopus* and *Drosophila* embryos. Before the onset of embryonic transcription, these cells are able to undergo many rounds of genome duplication impressively fast (3 – 4 minutes per replication round in *Drosophila*, 11 cell cycles in 7 hours in *Xenopus*). This rapid genome duplication is achieved by the synchronous activation of sequence unspecific origins all over the genome with a constant distance of approximately 8-20 kb, thus ensuring that no DNA remains unreplicated when cell division starts (Blumenthal et al., 1974; Hyrien et al., 1995; Hyrien and Mechali, 1993).

The parallels between the replication dynamics in the developmentally opposite systems of early embryos of flies and frogs and the differentiated mammalian cells, as well as their correlation with a transcriptionally inactive state, suggest that there might be a causative relation between the transcriptionally silenced state and synchronous replication. In fact, it is conceivable that the transcription machinery might interfere with origin activation. The observations of Looke and colleagues (Looke et al., 2010) suggest that the transcription machinery is able to disassemble pre-RCs from chromatin and that this disassembly is reversible once the transcription machinery has left the origin. We therefore propose the following model to explain the relationship between transcriptional activity and replication (a)synchrony (Figure 32): during late M / G1 pre-RC are assembled and go through many rounds of licensing (Bowers et al., 2004), with origins in hypoacetylated regions, like the Xi, completing these processes later than those in hyperacetylated regions (see discussion above). However, during G1 there is a certain probability that in euchromatic regions, the transcription machinery collides with a fraction of the formed pre-RC, resulting in their disassembly (Looke et al., 2010). On the other hand, as the transcription machinery moves on from the respective ori-

gins, some pre-RC could still be re-assembled as long as the cell has not yet entered S-phase. After the G1 / S transition CDK and DDK activity will prevent origin licensing (Porter, 2008; Zegerman and Diffley, 2010). This transcription-driven on-and-off rate of pre-RC assembly would imply that the pre-RCs that are ready to fire during S-phase were assembled at different time points during the preceding G1 phase and reached different levels of maturation until G1 / S transition. Since the time of pre-RC formation and licensing is likely to influence the time of firing ((Wu and Nurse, 2009), see discussion above), the temporal mosaic of pre-RC at transcriptionally active regions, would be then reflected in a temporal mosaic of origin firing.

In contrast, in the hypoacetylated Xi, pre-RC formation and licensing take place later in G1, so that the replication onset in this chromosome is delayed in relation to euchromatic regions (Casas-Delucchi et al., 2011). However, the lack of transcriptional activity in this chromosome would result in a lower probability of pre-RC disassembly in G1, so that as the cell enters S-phase, most licensed pre-RC at the Xi were actually assembled within a short time interval. This simultaneous assembly and licensing of pre-RC, which in silenced regions is not affected by transcription, is subsequently reflected in the synchronous origin firing at the Xi and, therefore, in the fast replication of most of the Barr body in an extremely short time frame (Casas-Delucchi et al., 2011). Histone hypoacetylation might, therefore, represent a common mechanism to delay origin activation, maintain transcriptionally inactivity and concomitantly results in synchronous replication activation.

Additionally, a further conceivable way of achieving fast replication of the Xi, besides synchronous closely spaced origin firing, is a higher replication fork speed. Indeed, replication fork progression can be negatively affected by the transcription machinery. In fact, it has been showed that the presence of transcription complexes on the DNA strand can stall replication fork progression, especially if the DNA and RNA polymerases are exposed to head-on collision (Pomerantz and O'Donnell, 2010). This has been shown *in vitro* (Elias-Arnanz and Salas, 1997; Liu and Alberts, 1995) and, to certain extent, *in vivo* (French, 1992; Prado and Aguilera, 2005; Vilette et al., 1996), suggesting that head-on collision between RNA and DNA polymerases results in inhibition of the replication fork progression. Even though these observations correspond to prokaryotic and phage systems, they might be transferrable to eukaryotes and therefore represent a possible additional explanation for the faster completion of replication of an entire mammalian chromosome, or for that matter, of an entire fly or frog genome, when these regions are not transcriptionally active.

It should be noted that we are proposing a model to explain the role of transcriptional activity in the asynchrony of replication throughout euchromatic regions. The overall replication timing, on the other hand, has been proposed to be positively affected by transcriptional compe-

tence and the underlying chromatin state. This is most likely a more global effect of the epigenetic characteristic of transcriptionally competent regions, which concomitantly have, because of their open chromatin structure, an overall higher probability of early firing. However, at a more local, single origin, scale, transcription might actually prevent an origin from firing (Haase et al., 1994; Mesner and Hamlin, 2005; Sasaki et al., 2006) in accordance to my proposal on the negative effects of transcriptional activity on replication synchrony at euchromatic regions.

In conclusion, we propose that the lack of transcriptional activity in a particular genomic region allows the majority of all available replication origins in that same region to be licensed and activated within a short time interval, resulting in synchronous replication dynamics, as observed for the mammalian Xi and the genomes of early *Xenopus* and *Drosophila* embryos. In contrast, transcriptional activity in euchromatic regions results in a temporal mosaic of replication activation (Figure 33). Consequently, we predict that reactivation of the Xi would abolish its synchronous replication dynamics.

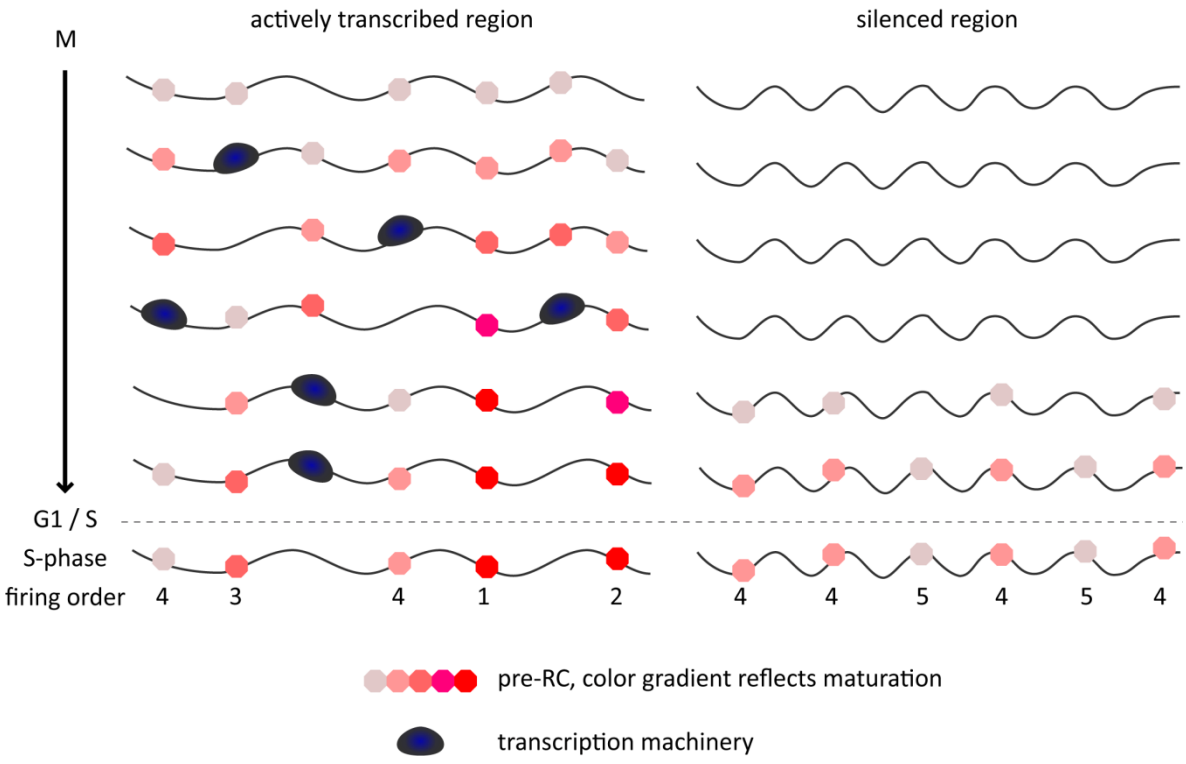

Figure 33 | Effects of transcription on replication synchrony.
Schematic representation of the temporal order of assembly, disassembly and re-assembly of pre-RC at replication origins in actively transcribed versus silenced regions. Disassembly and re-assembly of pre-RC at active regions result in a temporal mosaic of origin firing during S-phase, contrasting to the synchronous origin activation in silenced regions.

6. Perspectives

The results presented in this work lead to new exciting questions that will be basis of future studies. The predictions arising from my model on the mechanisms by which histone acetylation is likely to influence replication timing (see discussion), can be tested experimentally by assessing the chromatin binding kinetics of particular factors involved in origin determination and firing in the mammalian nucleus. These analyses should be done discriminating between hyperacetylated euchromatin versus hypoacetylated heterochromatin. In particular, we propose to study pre-RC formation kinetics, the level and duration of HBO1 binding, as well as the transient histone acetylation increase at origins. Moreover, we intend to assess the time and level of MCM loading, the availability and recruitment of Cdc45 and other firing factors, such as Mcm10 or GINS, as well as their recycling from early to late origins as S-phase progresses. To achieve these goals, we will apply our extensive molecular tools and expertise in the field of live-cell microscopy. Further, we will expand our approach by using ChIP analysis for an increased 1D spatial resolution.

Following our proposal that HAT versus HDAC activity might be an additional limiting factor determining origin firing efficiency, we further intend to take advantage of the targeting methods that we have developed (see results, chapter 3) to manipulate the ratio of HATs to HDACs at specific genomic regions. Especially the temporally regulated targeting of chromatin modifiers at defined cell cycle stages would allow us to determine whether origin firing can be manipulated by tuning histone acetylation at specific origin maturation stages.

In the case of the synchronous replication of the mammalian Xi, the next step will be to analyze in higher spatial resolution its replication dynamics. To this end, super resolution microscopy of short nucleotide pulses labeling DNA synthesis, as well as combination of replication detection and X chromosome FISH on DNA fibers would allow the analysis of the distribution of replication origins, as well as of the replication fork speed. This would answer whether the fast completion of the Xi replication is due to the synchronous activation of more origins than in the Xa, or to a higher replication fork speed.

Furthermore, high-resolution analysis of the Xi replication could be achieved by double chromatin immuno-precipitation experiments, first pulling down the inactive X, through e.g. macroH2A, and then nascent DNA. A system allowing us to discriminate between the homologues would further simplify the experiment. For this, we are going to take advantage of a MEF line with a stable inactivation of one of the X chromosomes and sufficiently frequent single nucleotide polymorphisms (SNPs) to allow the discrimination of the two homologous chromosomes.

The fact that the appearance of the Xi synchronous replication is concomitant to the irreversibility of the inactive state, suggests that this replication mode might play a role in the maintenance of the transcriptionally silenced state. On the other hand, we have proposed that the transcriptionally inactive state is a requisite for synchronous replication Therefore, it would be interesting to assess the effects of the treatments or mutation that abolish synchronous replication on Xi transcriptional silencing and assess whether abolishing synchronous replication is followed by re-activation of the Xi or whether transcriptional re-activation precedes the loss of replication synchrony.

Accompanying the quest for answers to our biological questions, we will continue developing tools that will enhance our possibilities to visualize and manipulate nuclear processes. Continuing the project on the targeting of chromatin modifiers to distinct nuclear regions, we next intend to change our current approach by using a Zinc finger major satellite DNA binding protein (Lindhout et al., 2007) instead of MBD, because this protein is itself not involved in the recruitment of further enzymes. To target chromatin modifiers to the Xi, we propose to use macroH2A. Additionally, we intend to take advantage of the estrogen receptor to trap proteins in the cytoplasma and control their nuclear import at different cell cycle stages by supplying the medium with the appropriate hormone ligand.

Finally, the next step for the development of computational tools for S-phase pattern recognition and classification, as well as colocalization analysis will be implementation and adaptation of more user-friendly and higher throughput analysis of both low and high throughput imaging. This would further allow whole genome screening of S-phase progression regulators, as well as small chemical inhibitors, with potential biomedical applications.

7. References

Aasland, R., and Stewart, A. F. (1995). The chromo shadow domain, a second chromo domain in heterochromatin-binding protein 1, HP1. Nucleic Acids Res *23*, 3168-3173.

Agarwal, N., Hardt, T., Brero, A., Nowak, D., Rothbauer, U., Becker, A., Leonhardt, H., and Cardoso, M. C. (2007). MeCP2 interacts with HP1 and modulates its heterochromatin association during myogenic differentiation. Nucleic Acids Res *35*, 5402-5408.

Aggarwal, B. D., and Calvi, B. R. (2004). Chromatin regulates origin activity in Drosophila follicle cells. Nature *430*, 372-376.

Aladjem, M. I. (2007). Replication in context: dynamic regulation of DNA replication patterns in metazoans. Nat Rev Genet *8*, 588-600.

Aladjem, M. I., Groudine, M., Brody, L. L., Dieken, E. S., Fournier, R. E., Wahl, G. M., and Epner, E. M. (1995). Participation of the human beta-globin locus control region in initiation of DNA replication. Science *270*, 815-819.

Alexandrova, O., Solovei, I., Cremer, T., and David, C. N. (2003). Replication labeling patterns and chromosome territories typical of mammalian nuclei are conserved in the early metazoan Hydra. Chromosoma *112*, 190-200.

Aparicio, O. M., Stout, A. M., and Bell, S. P. (1999). Differential assembly of Cdc45p and DNA polymerases at early and late origins of DNA replication. Proc Natl Acad Sci U S A *96*, 9130-9135.

Aparicio, O. M., Weinstein, D. M., and Bell, S. P. (1997). Components and dynamics of DNA replication complexes in S. cerevisiae: redistribution of MCM proteins and Cdc45p during S phase. Cell *91*, 59-69.

Aran, D., Toperoff, G., Rosenberg, M., and Hellman, A. (2011). Replication timing-related and gene body-specific methylation of active human genes. Hum Mol Genet *20*, 670-680.

Audit, B., Zaghloul, L., Vaillant, C., Chevereau, G., d'Aubenton-Carafa, Y., Thermes, C., and Arneodo, A. (2009). Open chromatin encoded in DNA sequence is the signature of 'master' replication origins in human cells. Nucleic Acids Res *37*, 6064-6075.

Baddeley, D., Chagin, V. O., Schermelleh, L., Martin, S., Pombo, A., Carlton, P. M., Gahl, A., Domaing, P., Birk, U., Leonhardt, H*., et al.* (2010). Measurement of replication structures at the nanometer scale using super-resolution light microscopy. Nucleic Acids Res *38*, e8.

Barr, M., and Bertram, E. (1949). A morphological distinction between neurones of the male and female, and the behavior of the nucleolar satellite during accelerated nucleoprotein synthesis. Nature *163*, 676-677.

Bell, S. P., and Dutta, A. (2002). DNA replication in eukaryotic cells. Annu Rev Biochem *71*, 333-374.

Berger, S. L. (2007). The complex language of chromatin regulation during transcription. Nature *447*, 407-412.

Bickmore, W. A., and Carothers, A. D. (1995). Factors affecting the timing and imprinting of replication on a mammalian chromosome. J Cell Sci *108 (Pt 8)*, 2801-2809.

Blow, J. J. (2001). Control of chromosomal DNA replication in the early Xenopus embryo. Embo J *20*, 3293-3297.

Blow, J. J., Gillespie, P. J., Francis, D., and Jackson, D. A. (2001). Replication origins in Xenopus egg extract Are 5-15 kilobases apart and are activated in clusters that fire at different times. J Cell Biol *152*, 15-25.

Blumenthal, A. B., Kriegstein, H. J., and Hogness, D. S. (1974). The units of DNA replication in Drosophila melanogaster chromosomes. Cold Spring Harb Symp Quant Biol *38*, 205-223.

Boch, J. (2011). TALEs of genome targeting. Nat Biotechnol *29*, 135-136.

Bousset, K., and Diffley, J. F. (1998). The Cdc7 protein kinase is required for origin firing during S phase. Genes Dev *12*, 480-490.

Bowers, J. L., Randell, J. C., Chen, S., and Bell, S. P. (2004). ATP hydrolysis by ORC catalyzes reiterative Mcm2-7 assembly at a defined origin of replication. Mol Cell *16*, 967-978.

Braunstein, J. D., Schulze, D., DelGiudice, T., Furst, A., and Schildkraut, C. L. (1982). The temporal order of replication of murine immunoglobulin heavy chain constant region sequences corresponds to their linear order in the genome. Nucleic Acids Res *10*, 6887-6902.

Brero, A., Easwaran, H. P., Nowak, D., Grunewald, I., Cremer, T., Leonhardt, H., and Cardoso, M. C. (2005). Methyl CpG-binding proteins induce large-scale chromatin reorganization during terminal differentiation. J Cell Biol *169*, 733-743.

Brockdorff, N., Ashworth, A., Kay, G. F., Cooper, P., Smith, S., McCabe, V. M., Norris, D. P., Penny, G. D., Patel, D., and Rastan, S. (1991). Conservation of position and exclusive expression of mouse Xist from the inactive X chromosome. Nature *351*, 329-331.

Cadoret, J. C., Meisch, F., Hassan-Zadeh, V., Luyten, I., Guillet, C., Duret, L., Quesneville, H., and Prioleau, M. N. (2008). Genome-wide studies highlight indirect links between human replication origins and gene regulation. Proc Natl Acad Sci U S A *105*, 15837-15842.

Calvi, B. R., Lilly, M. A., and Spradling, A. C. (1998). Cell cycle control of chorion gene amplification. Genes Dev *12*, 734-744.

Camargo, M., and Cervenka, J. (1982). Patterns of DNA replication of human chromosomes. II. Replication map and replication model. Am J Hum Genet *34*, 757-780.

Campbell, J. L. (1986). Eukaryotic DNA replication. Annu Rev Biochem *55*, 733-771.

Cardoso, M. C., Joseph, C., Rahn, H. P., Reusch, R., Nadal-Ginard, B., and Leonhardt, H. (1997). Mapping and use of a sequence that targets DNA ligase I to sites of DNA replication in vivo. J Cell Biol *139*, 579-587.

Cardoso, M. C., Leonhardt, H., and Nadal-Ginard, B. (1993). Reversal of terminal differentiation and control of DNA replication: cyclin A and Cdk2 specifically localize at subnuclear sites of DNA replication. Cell *74*, 979-992.

Casas-Delucchi, C. S., Brero, A., Rahn, H. P., Solovei, I., Wutz, A., Cremer, T., Leonhardt, H., and Cardoso, M. C. (2011). Histone acetylation controls the inactive X chromosome replication dynamics. Nat Commun *2*, 222 doi: 210.1038/ncomm1218.

Casas-Delucchi, C. S., van Bemmel, J. G., Haase, S., Herce, H. D., Nowak, D., Meilinger, D., Stear, J. H., Leonhardt, H., and Cardoso, M. C. (submitted). Histone acetylation controls replication timing of constitutive heterochromatin.

Chadwick, B. P., and Willard, H. F. (2003). Barring gene expression after XIST: maintaining facultative heterochromatin on the inactive X. Semin Cell Dev Biol *14*, 359-367.

Cheng, L. Z., Workman, J. L., Kingston, R. E., and Kelly, T. J. (1992). Regulation of DNA replication in vitro by the transcriptional activation domain of GAL4-VP16. Proc Natl Acad Sci U S A *89*, 589-593.

Chow, J., and Heard, E. (2009). X inactivation and the complexities of silencing a sex chromosome. Curr Opin Cell Biol *21*, 359-366.

Clemson, C. M., McNeil, J. A., Willard, H. F., and Lawrence, J. B. (1996). XIST RNA paints the inactive X chromosome at interphase: evidence for a novel RNA involved in nuclear/chromosome structure. J Cell Biol *132*, 259-275.

Cohen, S. M., Chastain, P. D., 2nd, Cordeiro-Stone, M., and Kaufman, D. G. (2009). DNA replication and the GINS complex: localization on extended chromatin fibers. Epigenetics Chromatin *2*, 6.

Costanzi, C., and Pehrson, J. R. (1998). Histone macroH2A1 is concentrated in the inactive X chromosome of female mammals. Nature *393*, 599-601.

Craig, J. M., and Bickmore, W. A. (1993). Chromosome bands--flavours to savour. Bioessays *15*, 349-354.

Crampton, A., Chang, F., Pappas, D. L., Jr., Frisch, R. L., and Weinreich, M. (2008). An ARS element inhibits DNA replication through a SIR2-dependent mechanism. Mol Cell *30*, 156-166.

Cremer, M., Müller, S., Köhler, D., Brero, A., and Solovei, I. (2006). Cell preparation and multicolor FISH in 3D preserved cultured mammalian cells. Cold Spring Harb Prot *doi:10.1101/pdb.prot4723*.

Cremer, T., and Cremer, C. (2001). Chromosome territories, nuclear architecture and gene regulation in mammalian cells. Nat Rev Genet *2*, 292-301.

Csankovszki, G., Nagy, A., and Jaenisch, R. (2001). Synergism of Xist RNA, DNA methylation, and histone hypoacetylation in maintaining X chromosome inactivation. J Cell Biol *153*, 773-784.

Csankovszki, G., Panning, B., Bates, B., Pehrson, J. R., and Jaenisch, R. (1999). Conditional deletion of Xist disrupts histone macroH2A localization but not maintenance of X inactivation. Nat Genet *22*, 323-324.

Danis, E., Brodolin, K., Menut, S., Maiorano, D., Girard-Reydet, C., and Mechali, M. (2004). Specification of a DNA replication origin by a transcription complex. Nat Cell Biol *6*, 721-730.

DePamphilis, M. L. (2005). Cell cycle dependent regulation of the origin recognition complex. Cell Cycle *4*, 70-79.

Dillon, N., and Festenstein, R. (2002). Unravelling heterochromatin: competition between positive and negative factors regulates accessibility. Trends Genet *18*, 252-258.

Donaldson, A. D. (2005). Shaping time: chromatin structure and the DNA replication programme. Trends Genet *21*, 444-449.

Donaldson, A. D., Fangman, W. L., and Brewer, B. J. (1998). Cdc7 is required throughout the yeast S phase to activate replication origins. Genes Dev *12*, 491-501.

Donovan, S., Harwood, J., Drury, L. S., and Diffley, J. F. (1997). Cdc6p-dependent loading of Mcm proteins onto pre-replicative chromatin in budding yeast. Proc Natl Acad Sci U S A *94*, 5611-5616.

Drouin, R., Lemieux, N., and Richer, C. L. (1990). Analysis of DNA replication during S-phase by means of dynamic chromosome banding at high resolution. Chromosoma *99*, 273-280.

Dutta, A., and Bell, S. P. (1997). Initiation of DNA replication in eukaryotic cells. Annu Rev Cell Dev Biol *13*, 293-332.

Eaton, M. L., Galani, K., Kang, S., Bell, S. P., and MacAlpine, D. M. (2010). Conserved nucleosome positioning defines replication origins. Genes Dev *24*, 748-753.

Eaton, M. L., Prinz, J. A., Macalpine, H. K., Tretyakov, G., Kharchenko, P. V., and Macalpine, D. M. (2011). Chromatin signatures of the Drosophila replication program. Genome Res *21*, 164-174.

Edwards, M. C., Tutter, A. V., Cvetic, C., Gilbert, C. H., Prokhorova, T. A., and Walter, J. C. (2002). MCM2-7 complexes bind chromatin in a distributed pattern surrounding the origin recognition complex in Xenopus egg extracts. J Biol Chem *277*, 33049-33057.

Elias-Arnanz, M., and Salas, M. (1997). Bacteriophage phi29 DNA replication arrest caused by codirectional collisions with the transcription machinery. Embo J *16*, 5775-5783.

Felsenfeld, G., and Groudine, M. (2003). Controlling the double helix. Nature *421*, 448-453.

Ferguson, B. M., and Fangman, W. L. (1992). A position effect on the time of replication origin activation in yeast. Cell *68*, 333-339.

Field, Y., Kaplan, N., Fondufe-Mittendorf, Y., Moore, I. K., Sharon, E., Lubling, Y., Widom, J., and Segal, E. (2008). Distinct modes of regulation by chromatin encoded through nucleosome positioning signals. PLoS Comput Biol *4*, e1000216.

Forsburg, S. L. (2004). Eukaryotic MCM proteins: beyond replication initiation. Microbiol Mol Biol Rev *68*, 109-131.

French, S. (1992). Consequences of replication fork movement through transcription units in vivo. Science *258*, 1362-1365.

Friedman, K. L., Diller, J. D., Ferguson, B. M., Nyland, S. V., Brewer, B. J., and Fangman, W. L. (1996). Multiple determinants controlling activation of yeast replication origins late in S phase. Genes Dev *10*, 1595-1607.

Gambus, A., Jones, R. C., Sanchez-Diaz, A., Kanemaki, M., van Deursen, F., Edmondson, R. D., and Labib, K. (2006). GINS maintains association of Cdc45 with MCM in replisome progression complexes at eukaryotic DNA replication forks. Nat Cell Biol *8*, 358-366.

Gauthier, M. G., and Bechhoefer, J. (2009). Control of DNA replication by anomalous reaction-diffusion kinetics. Phys Rev Lett *102*, 158104.

German, J. I. (1962). DNA synthesis in human chromosomes. Tr New York Acad Sc *24*, 395-407.

German, J. L., 3rd, Bearn, A. G., and Mc, G. J. (1962). Chromosomal studies of three hermaphrodites. Am J Med *33*, 83-87.

Ghosh, D. (2005). Nonparametric methods for analyzing replication origins in genomewide data. Funct Integr Genomics *5*, 28-31.

Gilbert, C. W., Muldal, S., Lajtha, L. G., and Rowley, J. (1962). Time-sequence of human chromosome duplication. Nature *195*, 869-873.

Gilbert, D. M. (2001). Making sense of eukaryotic DNA replication origins. Science *294*, 96-100.

Gilbert, D. M. (2002). Replication timing and transcriptional control: beyond cause and effect. Curr Opin Cell Biol *14*, 377-383.

Goldar, A., Labit, H., Marheineke, K., and Hyrien, O. (2008). A dynamic stochastic model for DNA replication initiation in early embryos. PLoS One *3*, e2919.

Gomez, M., and Brockdorff, N. (2004). Heterochromatin on the inactive X chromosome delays replication timing without affecting origin usage. Proc Natl Acad Sci U S A *101*, 6923-6928.

Goren, A., Tabib, A., Hecht, M., and Cedar, H. (2008). DNA replication timing of the human beta-globin domain is controlled by histone modification at the origin. Genes Dev *22*, 1319-1324.

Görisch, S. M., and Cardoso, M. C. (2006). PCNA and DNA Replication (I), In In Profilerating Cell Nuclear Antigen, H. Lee, and M. Szyf, eds. (Research SignPost), pp. 51-70.

Gorisch, S. M., Sporbert, A., Stear, J. H., Grunewald, I., Nowak, D., Warbrick, E., Leonhardt, H., and Cardoso, M. C. (2008). Uncoupling the replication machinery: replication fork progression in the absence of processive DNA synthesis. Cell Cycle *7*, 1983-1990.

Gorisch, S. M., Wachsmuth, M., Toth, K. F., Lichter, P., and Rippe, K. (2005). Histone acetylation increases chromatin accessibility. J Cell Sci *118*, 5825-5834.

Gregoire, D., Brodolin, K., and Mechali, M. (2006). HoxB domain induction silences DNA replication origins in the locus and specifies a single origin at its boundary. EMBO Rep *7*, 812-816.

Gribnau, J., Hochedlinger, K., Hata, K., Li, E., and Jaenisch, R. (2003). Asynchronous replication timing of imprinted loci is independent of DNA methylation, but consistent with differential subnuclear localization. Genes Dev *17*, 759-773.

Haase, S. B., Heinzel, S. S., and Calos, M. P. (1994). Transcription inhibits the replication of autonomously replicating plasmids in human cells. Mol Cell Biol *14*, 2516-2524.

Hamlin, J. L., Mesner, L. D., Lar, O., Torres, R., Chodaparambil, S. V., and Wang, L. (2008). A revisionist replicon model for higher eukaryotic genomes. J Cell Biochem *105*, 321-329.

Hansen, R. S., Stoger, R., Wijmenga, C., Stanek, A. M., Canfield, T. K., Luo, P., Matarazzo, M. R., D'Esposito, M., Feil, R., Gimelli, G.*, et al.* (2000). Escape from gene silencing in ICF syndrome: evidence for advanced replication time as a major determinant. Hum Mol Genet *9*, 2575-2587.

Hansen, R. S., Thomas, S., Sandstrom, R., Canfield, T. K., Thurman, R. E., Weaver, M., Dorschner, M. O., Gartler, S. M., and Stamatoyannopoulos, J. A. (2010). Sequencing newly replicated DNA reveals widespread plasticity in human replication timing. Proc Natl Acad Sci U S A *107*, 139-144.

Harvey, K. J., and Newport, J. (2003). Metazoan origin selection: origin recognition complex chromatin binding is regulated by CDC6 recruitment and ATP hydrolysis. J Biol Chem *278*, 48524-48528.

Hatton, K. S., Dhar, V., Brown, E. H., Iqbal, M. A., Stuart, S., Didamo, V. T., and Schildkraut, C. L. (1988). Replication program of active and inactive multigene families in mammalian cells. Mol Cell Biol *8*, 2149-2158.

Hayashi, M., Katou, Y., Itoh, T., Tazumi, A., Yamada, Y., Takahashi, T., Nakagawa, T., Shirahige, K., and Masukata, H. (2007). Genome-wide localization of pre-RC sites and identification of replication origins in fission yeast. Embo J *26*, 1327-1339.

Hayflick, L. (1961). The establishment of a line (WISH) of human amnion cells in continuous cultivation. Exp Cell Res *23*, 14-20.

Heichinger, C., Penkett, C. J., Bahler, J., and Nurse, P. (2006). Genome-wide characterization of fission yeast DNA replication origins. Embo J *25*, 5171-5179.

Heitz, E. (1928). Das Heterochromatin der Moose. I. Jahrbücher für wissenschaftlitsche Botanik *69*, 762-818.

Hendrich, B., and Bird, A. (1998). Identification and characterization of a family of mammalian methyl-CpG binding proteins. Mol Cell Biol *18*, 6538-6547.

Herzing, L. B., Romer, J. T., Horn, J. M., and Ashworth, A. (1997). Xist has properties of the X-chromosome inactivation centre. Nature *386*, 272-275.

Hiratani, I., and Gilbert, D. M. (2009). Replication timing as an epigenetic mark. Epigenetics *4*, 93-97.

Hiratani, I., Ryba, T., Itoh, M., Yokochi, T., Schwaiger, M., Chang, C. W., Lyou, Y., Townes, T. M., Schubeler, D., and Gilbert, D. M. (2008). Global reorganization of replication domains during embryonic stem cell differentiation. PLoS Biol *6*, e245.

Hiratani, I., Takebayashi, S., Lu, J., and Gilbert, D. M. (2009). Replication timing and transcriptional control: beyond cause and effect--part II. Curr Opin Genet Dev *19*, 142-149.

Homesley, L., Lei, M., Kawasaki, Y., Sawyer, S., Christensen, T., and Tye, B. K. (2000). Mcm10 and the MCM2-7 complex interact to initiate DNA synthesis and to release replication factors from origins. Genes Dev *14*, 913-926.

Huberman, J. A., and Riggs, A. D. (1966). Autoradiography of chromosomal DNA fibers from Chinese hamster cells. Proc Natl Acad Sci U S A *55*, 599-606.

Hubscher, U., Maga, G., and Spadari, S. (2002). Eukaryotic DNA polymerases. Annu Rev Biochem *71*, 133-163.

Hyrien, O., Marheineke, K., and Goldar, A. (2003). Paradoxes of eukaryotic DNA replication: MCM proteins and the random completion problem. Bioessays *25*, 116-125.

Hyrien, O., Maric, C., and Mechali, M. (1995). Transition in specification of embryonic metazoan DNA replication origins. Science *270*, 994-997.

Hyrien, O., and Mechali, M. (1993). Chromosomal replication initiates and terminates at random sequences but at regular intervals in the ribosomal DNA of Xenopus early embryos. Embo J *12*, 4511-4520.

Iizuka, M., Matsui, T., Takisawa, H., and Smith, M. M. (2006). Regulation of replication licensing by acetyltransferase Hbo1. Mol Cell Biol *26*, 1098-1108.

Iizuka, M., and Stillman, B. (1999). Histone acetyltransferase HBO1 interacts with the ORC1 subunit of the human initiator protein. J Biol Chem *274*, 23027-23034.

Jentsch, I., Adler, I. D., Carter, N. P., and Speicher, M. R. (2001). Karyotyping mouse chromosomes by multiplex-FISH (M-FISH). Chromosome Res *9*, 211-214.

Jeppesen, P., Mitchell, A., Turner, B., and Perry, P. (1992). Antibodies to defined histone epitopes reveal variations in chromatin conformation and underacetylation of centric heterochromatin in human metaphase chromosomes. Chromosoma *101*, 322-332.

Jeppesen, P., and Turner, B. M. (1993). The inactive X chromosome in female mammals is distinguished by a lack of histone H4 acetylation, a cytogenetic marker for gene expression. Cell *74*, 281-289.

Jones, K. W. (1970). Chromosomal and nuclear location of mouse satellite DNA in individual cells. Nature *225*, 912-915.

Jones, P. L., Veenstra, G. J., Wade, P. A., Vermaak, D., Kass, S. U., Landsberger, N., Strouboulis, J., and Wolffe, A. P. (1998). Methylated DNA and MeCP2 recruit histone deacetylase to repress transcription. Nat Genet *19*, 187-191.

Kamimura, Y., Tak, Y. S., Sugino, A., and Araki, H. (2001). Sld3, which interacts with Cdc45 (Sld4), functions for chromosomal DNA replication in Saccharomyces cerevisiae. Embo J *20*, 2097-2107.

Kanemaki, M., and Labib, K. (2006). Distinct roles for Sld3 and GINS during establishment and progression of eukaryotic DNA replication forks. Embo J *25*, 1753-1763.

Karnani, N., Taylor, C., Malhotra, A., and Dutta, A. (2007). Pan-S replication patterns and chromosomal domains defined by genome-tiling arrays of ENCODE genomic areas. Genome Res *17*, 865-876.

Kemp, M. G., Ghosh, M., Liu, G., and Leffak, M. (2005). The histone deacetylase inhibitor trichostatin A alters the pattern of DNA replication origin activity in human cells. Nucleic Acids Res *33*, 325-336.

Keohane, A. M., O'Neill L, P., Belyaev, N. D., Lavender, J. S., and Turner, B. M. (1996). X-Inactivation and histone H4 acetylation in embryonic stem cells. Dev Biol *180*, 618-630.

Knott, S. R., Viggiani, C. J., Tavare, S., and Aparicio, O. M. (2009). Genome-wide replication profiles indicate an expansive role for Rpd3L in regulating replication initiation timing or efficiency, and reveal genomic loci of Rpd3 function in Saccharomyces cerevisiae. Genes Dev *23*, 1077-1090.

Kohlmaier, A., Savarese, F., Lachner, M., Martens, J., Jenuwein, T., and Wutz, A. (2004). A chromosomal memory triggered by Xist regulates histone methylation in X inactivation. PLoS Biol *2*, E171.

Labib, K., and Diffley, J. F. (2001). Is the MCM2-7 complex the eukaryotic DNA replication fork helicase? Curr Opin Genet Dev *11*, 64-70.

Lande-Diner, L., Zhang, J., Ben-Porath, I., Amariglio, N., Keshet, I., Hecht, M., Azuara, V., Fisher, A. G., Rechavi, G., and Cedar, H. (2007). Role of DNA methylation in stable gene repression. J Biol Chem *282*, 12194-12200.

Lande-Diner, L., Zhang, J., and Cedar, H. (2009). Shifts in replication timing actively affect histone acetylation during nucleosome reassembly. Mol Cell *34*, 767-774.

Laskey, R. A., and Madine, M. A. (2003). A rotary pumping model for helicase function of MCM proteins at a distance from replication forks. EMBO Rep *4*, 26-30.

Latt, S. A. (1973). Microfluorometric detection of deoxyribonucleic acid replication in human metaphase chromosomes. Proc Natl Acad Sci U S A *70*, 3395-3399.

Lebofsky, R., Heilig, R., Sonnleitner, M., Weissenbach, J., and Bensimon, A. (2006). DNA replication origin interference increases the spacing between initiation events in human cells. Mol Biol Cell *17*, 5337-5345.

Lehnertz, B., Ueda, Y., Derijck, A. A., Braunschweig, U., Perez-Burgos, L., Kubicek, S., Chen, T., Li, E., Jenuwein, T., and Peters, A. H. (2003). Suv39h-mediated histone H3 lysine 9 methylation directs DNA methylation to major satellite repeats at pericentric heterochromatin. Curr Biol *13*, 1192-1200.

Lei, M., Kawasaki, Y., and Tye, B. K. (1996). Physical interactions among Mcm proteins and effects of Mcm dosage on DNA replication in Saccharomyces cerevisiae. Mol Cell Biol *16*, 5081-5090.

Leonhardt, H., Rahn, H. P., Weinzierl, P., Sporbert, A., Cremer, T., Zink, D., and Cardoso, M. C. (2000). Dynamics of DNA replication factories in living cells. J Cell Biol *149*, 271-280.

Lewis, J. D., Meehan, R. R., Henzel, W. J., Maurer-Fogy, I., Jeppesen, P., Klein, F., and Bird, A. (1992). Purification, sequence, and cellular localization of a novel chromosomal protein that binds to methylated DNA. Cell *69*, 905-914.

Li, E., Beard, C., and Jaenisch, R. (1993). Role for DNA methylation in genomic imprinting. Nature *366*, 362-365.

Li, F., Chen, J., Solessio, E., and Gilbert, D. M. (2003). Spatial distribution and specification of mammalian replication origins during G1 phase. J Cell Biol *161*, 257-266.

Li, J., Santoro, R., Koberna, K., and Grummt, I. (2005). The chromatin remodeling complex NoRC controls replication timing of rRNA genes. Embo J *24*, 120-127.

Li, J. J., and Kelly, T. J. (1984). Simian virus 40 DNA replication in vitro. Proc Natl Acad Sci U S A *81*, 6973-6977.

Lindhout, B. I., Fransz, P., Tessadori, F., Meckel, T., Hooykaas, P. J., and van der Zaal, B. J. (2007). Live cell imaging of repetitive DNA sequences via GFP-tagged polydactyl zinc finger proteins. Nucleic Acids Res *35*, e107.

Lipford, J. R., and Bell, S. P. (2001). Nucleosomes positioned by ORC facilitate the initiation of DNA replication. Mol Cell *7*, 21-30.

Littlewood, T. D., Hancock, D. C., Danielian, P. S., Parker, M. G., and Evan, G. I. (1995). A modified oestrogen receptor ligand-binding domain as an improved switch for the regulation of heterologous proteins. Nucleic Acids Res *23*, 1686-1690.

Liu, B., and Alberts, B. M. (1995). Head-on collision between a DNA replication apparatus and RNA polymerase transcription complex. Science *267*, 1131-1137.

Looke, M., Reimand, J., Sedman, T., Sedman, J., Jarvinen, L., Varv, S., Peil, K., Kristjuhan, K., Vilo, J., and Kristjuhan, A. (2010). Relicensing of transcriptionally inactivated replication origins in budding yeast. J Biol Chem *285*, 40004-40011.

Lu, Z. H., Sittman, D. B., Romanowski, P., and Leno, G. H. (1998). Histone H1 reduces the frequency of initiation in Xenopus egg extract by limiting the assembly of prereplication complexes on sperm chromatin. Mol Biol Cell *9*, 1163-1176.

Lucas, I., Chevrier-Miller, M., Sogo, J. M., and Hyrien, O. (2000). Mechanisms ensuring rapid and complete DNA replication despite random initiation in Xenopus early embryos. J Mol Biol *296*, 769-786.

Lucas, I., Palakodeti, A., Jiang, Y., Young, D. J., Jiang, N., Fernald, A. A., and Le Beau, M. M. (2007). High-throughput mapping of origins of replication in human cells. EMBO Rep *8*, 770-777.

Lunyak, V. V., Ezrokhi, M., Smith, H. S., and Gerbi, S. A. (2002). Developmental changes in the Sciara II/9A initiation zone for DNA replication. Mol Cell Biol *22*, 8426-8437.

Lyon, M. F. (1961). Gene action in the X-chromosome of the mouse (Mus musculus L.). Nature *190*, 372-373.

MacAlpine, D. M., Rodriguez, H. K., and Bell, S. P. (2004). Coordination of replication and transcription along a Drosophila chromosome. Genes Dev *18*, 3094-3105.

Mahbubani, H. M., Chong, J. P., Chevalier, S., Thommes, P., and Blow, J. J. (1997). Cell cycle regulation of the replication licensing system: involvement of a Cdk-dependent inhibitor. J Cell Biol *136*, 125-135.

Maiorano, D., Lemaitre, J. M., and Mechali, M. (2000). Stepwise regulated chromatin assembly of MCM2-7 proteins. J Biol Chem *275*, 8426-8431.

Maison, C., and Almouzni, G. (2004). HP1 and the dynamics of heterochromatin maintenance. Nat Rev Mol Cell Biol *5*, 296-304.

Maric, C., Benard, M., and Pierron, G. (2003). Developmentally regulated usage of Physarum DNA replication origins. EMBO Rep *4*, 474-478.

Masata, M., Juda, P., Raska, O., Cardoso, M. C., and Raska, I. (2011). A fraction of MCM 2 proteins remain associated with replication foci during a major part of S phase. Fol Biol *57*, 3-11.

Masumoto, H., Sugino, A., and Araki, H. (2000). Dpb11 controls the association between DNA polymerases alpha and epsilon and the autonomously replicating sequence region of budding yeast. Mol Cell Biol *20*, 2809-2817.

Maya-Mendoza, A., Olivares-Chauvet, P., Shaw, A., and Jackson, D. A. (2010). S phase progression in human cells is dictated by the genetic continuity of DNA foci. PLoS Genet *6*, e1000900.

McGarry, T. J., and Kirschner, M. W. (1998). Geminin, an inhibitor of DNA replication, is degraded during mitosis. Cell *93*, 1043-1053.

McNairn, A. J., and Gilbert, D. M. (2003). Epigenomic replication: linking epigenetics to DNA replication. Bioessays *25*, 647-656.

Mechali, M. (2001). DNA replication origins: from sequence specificity to epigenetics. Nat Rev Genet *2*, 640-645.

Mechali, M. (2010). Eukaryotic DNA replication origins: many choices for appropriate answers. Nat Rev Mol Cell Biol *11*, 728-738.

Mechali, M., and Kearsey, S. (1984). Lack of specific sequence requirement for DNA replication in Xenopus eggs compared with high sequence specificity in yeast. Cell *38*, 55-64.

Merchant, A. M., Kawasaki, Y., Chen, Y., Lei, M., and Tye, B. K. (1997). A lesion in the DNA replication initiation factor Mcm10 induces pausing of elongation forks through chromosomal replication origins in Saccharomyces cerevisiae. Mol Cell Biol *17*, 3261-3271.

Mesner, L. D., and Hamlin, J. L. (2005). Specific signals at the 3' end of the DHFR gene define one boundary of the downstream origin of replication. Genes Dev *19*, 1053-1066.

Miller, J. C., Tan, S., Qiao, G., Barlow, K. A., Wang, J., Xia, D. F., Meng, X., Paschon, D. E., Leung, E., Hinkley, S. J.*, et al.* (2011). A TALE nuclease architecture for efficient genome editing. Nat Biotechnol *29*, 143-148.

Mills, A. D., Blow, J. J., White, J. G., Amos, W. B., Wilcock, D., and Laskey, R. A. (1989). Replication occurs at discrete foci spaced throughout nuclei replicating in vitro. Journal of Cell Science *94*, 471-477.

Minami, H., Takahashi, J., Suto, A., Saitoh, Y., and Tsutsumi, K. (2006). Binding of AlF-C, an Orc1-binding transcriptional regulator, enhances replicator activity of the rat aldolase B origin. Mol Cell Biol *26*, 8770-8780.

Miniou, P., Jeanpierre, M., Blanquet, V., Sibella, V., Bonneau, D., Herbelin, C., Fischer, A., Niveleau, A., and Viegas-Pequignot, E. (1994). Abnormal methylation pattern in constitutive and facultative (X inactive chromosome) heterochromatin of ICF patients. Hum Mol Genet *3*, 2093-2102.

Miotto, B., and Struhl, K. (2010). HBO1 histone acetylase activity is essential for DNA replication licensing and inhibited by Geminin. Mol Cell *37*, 57-66.

Mizushima, T., Takahashi, N., and Stillman, B. (2000). Cdc6p modulates the structure and DNA binding activity of the origin recognition complex in vitro. Genes Dev *14*, 1631-1641.

Monkhorst, K., de Hoon, B., Jonkers, I., Mulugeta Achame, E., Monkhorst, W., Hoogerbrugge, J., Rentmeester, E., Westerhoff, H. V., Grosveld, F., Grootegoed, J. A., and Gribnau, J. (2009). The probability to initiate X chromosome inactivation is determined by the X to autosomal ratio and X chromosome specific allelic properties. PLoS One *4*, e5616.

Moorhead, P. S., and Defendi, V. (1963). Asynchrony of DNA synthesis in chromosomes of human diploid cells. J Cell Biol *16*, 202-209.

Morishima, A., Grumbach, M. M., and Taylor, J. H. (1962). Asynchronous duplication of human chromosomes and the origin of sex chromatin. Proc Natl Acad Sci U S A *48*, 756-763.

Moscou, M. J., and Bogdanove, A. J. (2009). A simple cipher governs DNA recognition by TAL effectors. Science *326*, 1501.

Nakamura, H., Morita, T., and Sato, C. (1986). Structural organizations of replicon domains during DNA synthetic phase in the mammalian nucleus. Exp Cell Res *165*, 291-297.

Nakayasu, H., and Berezney, R. (1989). Mapping replicational sites in the eucaryotic cell nucleus. J Cell Biol *108*, 1-11.

Nan, X., Ng, H. H., Johnson, C. A., Laherty, C. D., Turner, B. M., Eisenman, R. N., and Bird, A. (1998). Transcriptional repression by the methyl-CpG-binding protein MeCP2 involves a histone deacetylase complex. Nature *393*, 386-389.

Newport, J., and Kirschner, M. (1982). A major developmental transition in early Xenopus embryos: I. characterization and timing of cellular changes at the midblastula stage. Cell *30*, 675-686.

Norio, P., Kosiyatrakul, S., Yang, Q., Guan, Z., Brown, N. M., Thomas, S., Riblet, R., and Schildkraut, C. L. (2005). Progressive activation of DNA replication initiation in large domains of the immunoglobulin heavy chain locus during B cell development. Mol Cell *20*, 575-587.

Norris, D. P., Brockdorff, N., and Rastan, S. (1991). Methylation status of CpG-rich islands on active and inactive mouse X chromosomes. Mamm Genome *1*, 78-83.

Nossal, N. G. (1992). Protein-protein interactions at a DNA replication fork: bacteriophage T4 as a model. Faseb J *6*, 871-878.

O'Keefe, R. T., Henderson, S. C., and Spector, D. L. (1992). Dynamic organization of DNA replication in mammalian cell nuclei: spatially and temporally defined replication of chromosome-specific alpha-satellite DNA sequences. J Cell Biol *116*, 1095-1110.

Ohta, S., Tatsumi, Y., Fujita, M., Tsurimoto, T., and Obuse, C. (2003). The ORC1 cycle in human cells: II. Dynamic changes in the human ORC complex during the cell cycle. J Biol Chem *278*, 41535-41540.

Otsu, N. (1979). A threshold selection method from gray-level histograms. IEEE Trans Sys, Man, Cyber *9*, 62-66.

Pacek, M., Tutter, A. V., Kubota, Y., Takisawa, H., and Walter, J. C. (2006). Localization of MCM2-7, Cdc45, and GINS to the site of DNA unwinding during eukaryotic DNA replication. Mol Cell *21*, 581-587.

Palzkill, T. G., and Newlon, C. S. (1988). A yeast replication origin consists of multiple copies of a small conserved sequence. Cell *53*, 441-450.

Panning, B., Dausman, J., and Jaenisch, R. (1997). X chromosome inactivation is mediated by Xist RNA stabilization. Cell *90*, 907-916.

Pasero, P., Duncker, B. P., Schwob, E., and Gasser, S. M. (1999). A role for the Cdc7 kinase regulatory subunit Dbf4p in the formation of initiation-competent origins of replication. Genes Dev *13*, 2159-2176.

Patel, P. K., Arcangioli, B., Baker, S. P., Bensimon, A., and Rhind, N. (2006). DNA replication origins fire stochastically in fission yeast. Mol Biol Cell *17*, 308-316.

Peters, A. H., O'Carroll, D., Scherthan, H., Mechtler, K., Sauer, S., Schofer, C., Weipoltshammer, K., Pagani, M., Lachner, M., Kohlmaier, A*., et al.* (2001). Loss of the Suv39h histone methyltransferases impairs mammalian heterochromatin and genome stability. Cell *107*, 323-337.

Petersen, A. J. (1964). DNA Synthesis and Chromosomal Asynchrony: Induced Parasynchronous DNA Synthesis in Human Leucocyte Cultures and Chromosomal Asynchrony in the Early S Phase. J Cell Biol *23*, 651-654.

Pfeifer, G. P., Tanguay, R. L., Steigerwald, S. D., and Riggs, A. D. (1990). In vivo footprint and methylation analysis by PCR-aided genomic sequencing: comparison of active and inactive X chromosomal DNA at the CpG island and promoter of human PGK-1. Genes Dev *4*, 1277-1287.

Plath, K., Fang, J., Mlynarczyk-Evans, S. K., Cao, R., Worringer, K. A., Wang, H., de la Cruz, C. C., Otte, A. P., Panning, B., and Zhang, Y. (2003). Role of histone H3 lysine 27 methylation in X inactivation. Science *300*, 131-135.

Pollok, S., Bauerschmidt, C., Sanger, J., Nasheuer, H. P., and Grosse, F. (2007). Human Cdc45 is a proliferation-associated antigen. Febs J *274*, 3669-3684.

Pomerantz, R. T., and O'Donnell, M. (2010). Direct restart of a replication fork stalled by a head-on RNA polymerase. Science *327*, 590-592.

Pope, B. D., Hiratani, I., and Gilbert, D. M. (2010). Domain-wide regulation of DNA replication timing during mammalian development. Chromosome Res *18*, 127-136.

Popova, E. Y., Krauss, S. W., Short, S. A., Lee, G., Villalobos, J., Etzell, J., Koury, M. J., Ney, P. A., Chasis, J. A., and Grigoryev, S. A. (2009). Chromatin condensation in terminally differentiating mouse erythroblasts does not involve special architectural proteins but depends on histone deacetylation. Chromosome Res *17*, 47-64.

Porter, A. C. (2008). Preventing DNA over-replication: a Cdk perspective. Cell Div *3*, 3.

Prado, F., and Aguilera, A. (2005). Impairment of replication fork progression mediates RNA polII transcription-associated recombination. Embo J *24*, 1267-1276.

Priest, J. H., Heady, J. E., and Priest, R. E. (1967). Delayed Onset of Replication of Human X Chromosomes. J Cell Biol *35*, 483-487.

Pryde, F., Jain, D., Kerr, A., Curley, R., Mariotti, F. R., and Vogelauer, M. (2009). H3 k36 methylation helps determine the timing of cdc45 association with replication origins. PLoS One *4*, e5882.

Rabbitts, P., Impey, H., Heppell-Parton, A., Langford, C., Tease, C., Lowe, N., Bailey, D., Ferguson-Smith, M., and Carter, N. (1995). Chromosome specific paints from a high resolution flow karyotype of the mouse. Nat Genet *9*, 369-375.

Raghuraman, M. K., and Brewer, B. J. (2010). Molecular analysis of the replication program in unicellular model organisms. Chromosome Res *18*, 19-34.

Raghuraman, M. K., Winzeler, E. A., Collingwood, D., Hunt, S., Wodicka, L., Conway, A., Lockhart, D. J., Davis, R. W., Brewer, B. J., and Fangman, W. L. (2001). Replication dynamics of the yeast genome. Science *294*, 115-121.

Rhind, N. (2006). DNA replication timing: random thoughts about origin firing. Nat Cell Biol *8*, 1313-1316.

Rhind, N., Yang, S. C., and Bechhoefer, J. (2010). Reconciling stochastic origin firing with defined replication timing. Chromosome Res *18*, 35-43.

Rothbauer, U., Zolghadr, K., Muyldermans, S., Schepers, A., Cardoso, M. C., and Leonhardt, H. (2008). A versatile nanotrap for biochemical and functional studies with fluorescent fusion proteins. Mol Cell Proteomics *7*, 282-289.

Rountree, M. R., Bachman, K. E., and Baylin, S. B. (2000). DNMT1 binds HDAC2 and a new corepressor, DMAP1, to form a complex at replication foci. Nat Genet *25*, 269-277.

Sadoni, N., Cardoso, M. C., Stelzer, E. H., Leonhardt, H., and Zink, D. (2004). Stable chromosomal units determine the spatial and temporal organization of DNA replication. J Cell Sci *117*, 5353-5365.

Saha, S., Shan, Y., Mesner, L. D., and Hamlin, J. L. (2004). The promoter of the Chinese hamster ovary dihydrofolate reductase gene regulates the activity of the local origin and helps define its boundaries. Genes Dev *18*, 397-410.

Salic, A., and Mitchison, T. J. (2008). A chemical method for fast and sensitive detection of DNA synthesis in vivo. Proc Natl Acad Sci U S A *105*, 2415-2420.

Santoro, R., Li, J., and Grummt, I. (2002). The nucleolar remodeling complex NoRC mediates heterochromatin formation and silencing of ribosomal gene transcription. Nat Genet *32*, 393-396.

Sasaki, T., Ramanathan, S., Okuno, Y., Kumagai, C., Shaikh, S. S., and Gilbert, D. M. (2006). The Chinese hamster dihydrofolate reductase replication origin decision point follows activation of transcription and suppresses initiation of replication within transcription units. Mol Cell Biol *26*, 1051-1062.

Schepers, A., and Papior, P. (2010). Why are we where we are? Understanding replication origins and initiation sites in eukaryotes using ChIP-approaches. Chromosome Res *18*, 63-77.

Schermelleh, L., Carlton, P. M., Haase, S., Shao, L., Winoto, L., Kner, P., Burke, B., Cardoso, M. C., Agard, D. A., Gustafsson, M. G.*, et al.* (2008). Subdiffraction multicolor imaging of the nuclear periphery with 3D structured illumination microscopy. Science *320*, 1332-1336.

Schubeler, D., Lorincz, M. C., Cimbora, D. M., Telling, A., Feng, Y. Q., Bouhassira, E. E., and Groudine, M. (2000). Genomic targeting of methylated DNA: influence of methylation on transcription, replication, chromatin structure, and histone acetylation. Mol Cell Biol *20*, 9103-9112.

Schwaiger, M., Kohler, H., Oakeley, E. J., Stadler, M. B., and Schubeler, D. (2010). Heterochromatin protein 1 (HP1) modulates replication timing of the Drosophila genome. Genome Res *20*, 771-780.

Schwaiger, M., and Schubeler, D. (2006). A question of timing: emerging links between transcription and replication. Curr Opin Genet Dev *16*, 177-183.

Schwaiger, M., Stadler, M. B., Bell, O., Kohler, H., Oakeley, E. J., and Schubeler, D. (2009). Chromatin state marks cell-type- and gender-specific replication of the Drosophila genome. Genes Dev *23*, 589-601.

Schwemmle, S., Mehnert, K., and Vogel, W. (1989). How does inactivation change timing of replication in the human X chromosome? Hum Genet *83*, 26-32.

Schwob, E., de Renty, C., Coulon, V., Gostan, T., Boyer, C., Camet-Gabut, L., and Amato, C. (2009). Use of DNA combing for studying DNA replication in vivo in yeast and mammalian cells. Methods Mol Biol *521*, 673-687.

Selig, S., Ariel, M., Goitein, R., Marcus, M., and Cedar, H. (1988). Regulation of mouse satellite DNA replication time. Embo J *7*, 419-426.

Sequeira-Mendes, J., Diaz-Uriarte, R., Apedaile, A., Huntley, D., Brockdorff, N., and Gomez, M. (2009). Transcription initiation activity sets replication origin efficiency in mammalian cells. PLoS Genet *5*, e1000446.

Sheu, Y. J., and Stillman, B. (2010). The Dbf4-Cdc7 kinase promotes S phase by alleviating an inhibitory activity in Mcm4. Nature *463*, 113-117.

Shin, J. H., Grabowski, B., Kasiviswanathan, R., Bell, S. D., and Kelman, Z. (2003). Regulation of minichromosome maintenance helicase activity by Cdc6. J Biol Chem *278*, 38059-38067.

Silva, J., Mak, W., Zvetkova, I., Appanah, R., Nesterova, T. B., Webster, Z., Peters, A. H., Jenuwein, T., Otte, A. P., and Brockdorff, N. (2003). Establishment of histone h3 methylation on the inactive X chromosome requires transient recruitment of Eed-Enx1 polycomb group complexes. Dev Cell *4*, 481-495.

Simon, I., Tenzen, T., Reubinoff, B. E., Hillman, D., McCarrey, J. R., and Cedar, H. (1999). Asynchronous replication of imprinted genes is established in the gametes and maintained during development. Nature *401*, 929-932.

Simpson, R. T. (1990). Nucleosome positioning can affect the function of a cis-acting DNA element in vivo. Nature *343*, 387-389.

Sporbert, A., Domaing, P., Leonhardt, H., and Cardoso, M. C. (2005). PCNA acts as a stationary loading platform for transiently interacting Okazaki fragment maturation proteins. Nucleic Acids Res *33*, 3521-3528.

Sporbert, A., Gahl, A., Ankerhold, R., Leonhardt, H., and Cardoso, M. C. (2002). DNA polymerase clamp shows little turnover at established replication sites but sequential de novo assembly at adjacent origin clusters. Mol Cell *10*, 1355-1365.

Stanojcic, S., Lemaitre, J. M., Brodolin, K., Danis, E., and Mechali, M. (2008). In Xenopus egg extracts, DNA replication initiates preferentially at or near asymmetric AT sequences. Mol Cell Biol *28*, 5265-5274.

Stinchcomb, D. T., Struhl, K., and Davis, R. W. (1979). Isolation and characterisation of a yeast chromosomal replicator. Nature *282*, 39-43.

Su, I. H., Basavaraj, A., Krutchinsky, A. N., Hobert, O., Ullrich, A., Chait, B. T., and Tarakhovsky, A. (2003). Ezh2 controls B cell development through histone H3 methylation and Igh rearrangement. Nat Immunol *4*, 124-131.

Taddei, A., Maison, C., Roche, D., and Almouzni, G. (2001). Reversible disruption of pericentric heterochromatin and centromere function by inhibiting deacetylases. Nat Cell Biol *3*, 114-120.

Takagi, N. (1974). Differentiation of X chromosomes in early female mouse embryos. Exp Cell Res *86*, 127-135.

Takagi, N., Sugawara, O., and Sasaki, M. (1982). Regional and temporal changes in the pattern of X-chromosome replication during the early post-implantation development of the female mouse. Chromosoma *85*, 275-286.

Takahashi, T. S., Wigley, D. B., and Walter, J. C. (2005). Pumps, paradoxes and ploughshares: mechanism of the MCM2-7 DNA helicase. Trends Biochem Sci *30*, 437-444.

Takei, Y., Assenberg, M., Tsujimoto, G., and Laskey, R. (2002). The MCM3 acetylase MCM3AP inhibits initiation, but not elongation, of DNA replication via interaction with MCM3. J Biol Chem *277*, 43121-43125.

Takei, Y., Swietlik, M., Tanoue, A., Tsujimoto, G., Kouzarides, T., and Laskey, R. (2001). MCM3AP, a novel acetyltransferase that acetylates replication protein MCM3. EMBO Rep *2*, 119-123.

Tardat, M., Brustel, J., Kirsh, O., Lefevbre, C., Callanan, M., Sardet, C., and Julien, E. (2010). The histone H4 Lys 20 methyltransferase PR-Set7 regulates replication origins in mammalian cells. Nat Cell Biol *12*, 1086-1093.

Taylor, J. H. (1960). Asynchronous duplication of chromosomes in cultured cells of Chinese hamster. J Biophys Biochem Cytol *7*, 455-464.

Terret, M. E., Sherwood, R., Rahman, S., Qin, J., and Jallepalli, P. V. (2009). Cohesin acetylation speeds the replication fork. Nature *462*, 231-234.

Theis, J. F., Dershowitz, A., Irene, C., Maciariello, C., Tobin, M. L., Liberi, G., Tabrizifard, S., Korus, M., Fabiani, L., and Newlon, C. S. (2007). Identification of mutations that decrease the stability of a fragment of Saccharomyces cerevisiae chromosome III lacking efficient replicators. Genetics *177*, 1445-1458.

Unnikrishnan, A., Gafken, P. R., and Tsukiyama, T. (2010). Dynamic changes in histone acetylation regulate origins of DNA replication. Nat Struct Mol Biol *17*, 430-437.

Vilette, D., Ehrlich, S. D., and Michel, B. (1996). Transcription-induced deletions in plasmid vectors: M13 DNA replication as a source of instability. Mol Gen Genet *252*, 398-403.

Vissel, B., and Choo, K. H. (1989). Mouse major (gamma) satellite DNA is highly conserved and organized into extremely long tandem arrays: implications for recombination between non-homologous chromosomes. Genomics *5*, 407-414.

Visser, A. E., Eils, R., Jauch, A., Little, G., Bakker, P. J., Cremer, T., and Aten, J. A. (1998). Spatial distributions of early and late replicating chromatin in interphase chromosome territories. Exp Cell Res *243*, 398-407.

Vogelauer, M., Rubbi, L., Lucas, I., Brewer, B. J., and Grunstein, M. (2002). Histone acetylation regulates the time of replication origin firing. Mol Cell *10*, 1223-1233.

Walter, J., and Newport, J. (2000). Initiation of eukaryotic DNA replication: origin unwinding and sequential chromatin association of Cdc45, RPA, and DNA polymerase alpha. Mol Cell *5*, 617-627.

Watanabe, Y., Fujiyama, A., Ichiba, Y., Hattori, M., Yada, T., Sakaki, Y., and Ikemura, T. (2002). Chromosome-wide assessment of replication timing for human chromosomes 11q and 21q: disease-related genes in timing-switch regions. Hum Mol Genet *11*, 13-21.

Wei, X., Samarabandu, J., Devdhar, R. S., Siegel, A. J., Acharya, R., and Berezney, R. (1998). Segregation of transcription and replication sites into higher order domains. Science *281*, 1502-1506.

Weidtkamp-Peters, S., Rahn, H. P., Cardoso, M. C., and Hemmerich, P. (2006). Replication of centromeric heterochromatin in mouse fibroblasts takes place in early, middle, and late S phase. Histochem Cell Biol *125*, 91-102.

Weinreich, M., Palacios DeBeer, M. A., and Fox, C. A. (2004). The activities of eukaryotic replication origins in chromatin. Biochim Biophys Acta *1677*, 142-157.

Willard, H. F., and Breg, W. R. (1980). Human X chromosomes: synchrony of DNA replication in diploid and triploid fibroblasts with multiple active or inactive X chromosomes. Somatic Cell Genet *6*, 187-198.

Wong, P. G., Glozak, M. A., Cao, T. V., Vaziri, C., Seto, E., and Alexandrow, M. (2010). Chromatin unfolding by Cdt1 regulates MCM loading via opposing functions of HBO1 and HDAC11-geminin. Cell Cycle *9*, 4351-4363.

Woodfine, K., Fiegler, H., Beare, D. M., Collins, J. E., McCann, O. T., Young, B. D., Debernardi, S., Mott, R., Dunham, I., and Carter, N. P. (2004). Replication timing of the human genome. Hum Mol Genet *13*, 191-202.

Wu, P. Y., and Nurse, P. (2009). Establishing the program of origin firing during S phase in fission Yeast. Cell *136*, 852-864.

Wu, R., Singh, P. B., and Gilbert, D. M. (2006). Uncoupling global and fine-tuning replication timing determinants for mouse pericentric heterochromatin. J Cell Biol *174*, 185-194.

Wutz, A., and Jaenisch, R. (2000). A shift from reversible to irreversible X inactivation is triggered during ES cell differentiation. Mol Cell *5*, 695-705.

Wyrick, J. J., Aparicio, J. G., Chen, T., Barnett, J. D., Jennings, E. G., Young, R. A., Bell, S. P., and Aparicio, O. M. (2001). Genome-wide distribution of ORC and MCM proteins in S. cerevisiae: high-resolution mapping of replication origins. Science *294*, 2357-2360.

Yang, S. C., Rhind, N., and Bechhoefer, J. (2010). Modeling genome-wide replication kinetics reveals a mechanism for regulation of replication timing. Mol Syst Biol *6*, 404.

Yompakdee, C., and Huberman, J. A. (2004). Enforcement of late replication origin firing by clusters of short G-rich DNA sequences. J Biol Chem *279*, 42337-42344.

Zappulla, D. C., Sternglanz, R., and Leatherwood, J. (2002). Control of replication timing by a transcriptional silencer. Curr Biol *12*, 869-875.

Zegerman, P., and Diffley, J. F. (2010). Checkpoint-dependent inhibition of DNA replication initiation by Sld3 and Dbf4 phosphorylation. Nature *467*, 474-478.

Zhou, J., Chau, C. M., Deng, Z., Shiekhattar, R., Spindler, M. P., Schepers, A., and Lieberman, P. M. (2005). Cell cycle regulation of chromatin at an origin of DNA replication. Embo J *24*, 1406-1417.

Zhou, J., Ermakova, O. V., Riblet, R., Birshtein, B. K., and Schildkraut, C. L. (2002). Replication and subnuclear location dynamics of the immunoglobulin heavy-chain locus in B-lineage cells. Mol Cell Biol *22*, 4876-4889.

Zinner, R., Teller, K., Versteeg, R., Cremer, T., and Cremer, M. (2007). Biochemistry meets nuclear architecture: multicolor immuno-FISH for co-localization analysis of chromosome segments and differentially expressed gene loci with various histone methylations. Adv Enzyme Regul *47*, 223-241.

Zolghadr, K., Mortusewicz, O., Rothbauer, U., Kleinhans, R., Goehler, H., Wanker, E. E., Cardoso, M. C., and Leonhardt, H. (2008). A fluorescent two-hybrid assay for direct visualization of protein interactions in living cells. Mol Cell Proteomics *7*, 2279-2287.

Zou, L., and Stillman, B. (2000). Assembly of a complex containing Cdc45p, replication protein A, and Mcm2p at replication origins controlled by S-phase cyclin-dependent kinases and Cdc7p-Dbf4p kinase. Mol Cell Biol *20*, 3086-3096.

8. Annex

Abbreviations

aa	amino acids
AAA+	ATPases associated with a variety of cellular activities
ac	acetylated
ACS	autonomous consensus sequence
ARS	autonomous replication sequence
BrdU	5-bromo-2'-deoxyuridine
Cdc	cell division control protein
Cdt1	chromatin licensing and DNA replication factor 1
CDK	cyclin dependent kinase
ChIP	chromatin immuno-precipitation
DDK	Dbf4-dependent kinase
DHFR	dihydrofolate reductase
DNA	deoxyribonucleic acid
Dnmt	DNA methyltransferase
EdU	5-ethynyl-2'-deoxyuridine
GFP	green fluorescent protein
GINS	Go, Ichi, Nii, and San replication complex (five, one, two, and three in Japanese)
HAT	histone acetyl transferase
HBO1	human acetylase binding to ORC1
HDAC	histone deacetylase
kb	kilo base pair
MaSat	major satellite repeat binder
MBD	5' methylcytosine binding domain
MBT	mid-blastula transition
MCM	Mcm2-7 complex
Mcm	minichromosome maintenance protein
me	methylation
MEF	mouse embryonic fibroblasts
NoRC	nucleolar remodeling complex
ORC	origin recognition complex
PCNA	proliferating cell nuclear anti-gen
Pol	polymerase
pre-RC	pre-replicative complex
RFC	replication factor C
RPA	replication protein A
RT	room temperature
Se / Sm / Sl	early / mid / late S-phase
Sld3	synthetic lethal mutations with dbp11-1
SNP	single nucleotide polymorphism
TSA	trichostatin A
WT	wild type
Xa / Xi	active / inactive X chromosome
Xist	X inactive specific transcript

Acknowledgements

In the first place, I would like to thank my Doktormutter M. Cristina Cardoso. There are certainly innumerable reasons why I am grateful to Cristina, but above all, I would like to express my gratitude to her for challenging me to become a better scientist at every single step of the way. The years I have spent working with her have been full of excitement and I wouldn't want to miss any part of it. Thank you for always having an open ear and for taking such good care of us. I cannot imagine having had a better supervisor than you!

For agreeing to be the second corrector of this thesis, I would like to say thanks to Prof. Adam Bertl. For his advice in and out of the lab, his sense of humor and all the time he spent teaching me how to write, I would like to thank Jeff Stear. Also, I'd like to say thanks to Heinrich Leonhardt for his advice, his interest in my projects and the time he invested in them.

Very special thanks go to Annette Becker for being my biochemical advisor and, most importantly, for her good heart and for always just being who she is, to Henry Herce for his enthusiasm in my work and for always being ready to share a good bottle of wine, to Sebastian Haase for his endearing nature and for introducing me into the world of Python and to Anne Lehmkuhl for her kindness and for always being ready to help and making it seem like it was nothing.

For a great working atmosphere and for making the lab a place I love to be in, I'd like to thank the whole Cardoso lab: Alex, Bianca, Britta, Franziska, Jenny, Laurence, Lena, Manuela, Marius, Vadim, Valentina, as well as all Berliner members of our lab at the MDC. I would also like to mention my undergraduate students, Janine Bolius and Güler Iren, for their excellent work and for being a great help.

I am indebted to the people from the LMU who were always ready to share their expertise, advise, materials, equipment and even to let me crash on their couch: Marion Cremer, Irina Solovei, Sandro Brero, Jens Nagel, Andreas Zunhammer, Hilmar Strickfaden, Lothar Schermelleh, Andreas Maiser, Fabio Spada, Daniela Meilinger, Tina Freisinger and, especially, Prof. Thomas Cremer for being a scientific role model for me since my very first day as a Biology student.

I would like to try to put into words my immense gratitude and love for my family, especially my dad, my mom and my sister, the source of anything good in me: everything I ever achieve, I will always owe to you. Para la Mámele y el Pápele: por ser el mejor ejemplo de que lo que realmente importa no está en libros, ni revistas. And finally, for Andreas, my best friend in the whole wide world and my sunshine no matter what. *Trami dui*.

Declaration – Ehrenwörtliche Erklärung

Ich erkläre hiermit ehrenwörtlich, dass ich die vorliegende Arbeit selbstständig angefertigt habe. Sämtliche aus fremden Quellen direkt oder indirekt übernommenen Gedanken sind als solche kenntlich gemacht.
Die Arbeit wurde bisher keiner anderen Prüfungsbehörde vorgelegt und noch nicht veröffentlicht.

Darmstadt, den 08. April 2011

Corella S. Casas Delucchi

Curriculum vitæ

Name:	Corella S. Casas Delucchi
Date of birth:	20.09.1981
Place of birth:	Lima, Peru
Address:	Technische Universität Darmstadt
	Schnittspahnstrasse 10
	64287 Darmstadt, Germany

Education

2000	Abitur / A-levels (final grade: 1.3)
	Deutsche Schule Alexander von Humboldt – Lima, Peru
2001 – 2006	Diplom Biologie (final grade: 1.1)
	Ludwig-Maximilians-Universität München – Munich, Germany
Feb. – Oct. 2006	Diploma thesis under supervision of Prof. T. Cremer: "Structural and positional changes accompanying *Xist*-mediated whole chromosome inactivation" (grade: 1.0)
May 2007 – Apr. 2011	PhD thesis under supervision of Prof. M. C. Cardoso
	Max Delbrück Center for Molecular Medicine, Berlin, Germany
	Technische Universität Darmstadt, Darmstadt, Germany

Positions and teaching

June 2006	Supervision of practical courses of neurobiology, LMU
Feb. – Apr. 2007	Assistant scientist position in the group of Prof. Thomas Cremer, LMU
2009 – 2011	Supervision of basic and advanced practical courses of cell biology, TUD
	Supervision of students during research practical course and diploma work, TUD
Nov. 2010	Project planning and supervision of school students selected for the Merck Erfinderlabor, TUD

List of publications

Casas-Delucchi CS, Brero A, Rahn HP, Solovei I, Wutz A, Cremer T, Leonhardt H, Cardoso MC (2011) Histone acetylation controls the inactive X chromosome replication dynamics. Nature Communications 2:222, doi 10.1038/ncomms1218

Kirchhofer A, Helma J, Schmidthals K, Frauer C, Cui S, Karcher A, Pellis M, Muyldermans S, **Casas-Delucchi CS**, Cardoso MC, Leonhardt H, Hopfner KP, Rothbauer U. (2010) Modulation of protein properties in living cells using nanobodies. Nature Structure and Molecular Biology 17, 133–138

Jaeger S, Palaniappan K, **Casas-Delucchi CS**, Cardoso MC. Classification of cell cycle phases in 3D confocal microscopy using PCNA and chromocenter features. (2010) ICVGIP'10 Proceedings of the Seventh Indian Conference on Computer Vision, Graphics and Image Processing. doi 10.1145/1924559. 1924614

Casas-Delucchi CS, van Bemmel JG, Haase S, Herce HD, Nowak D, Meilinger D, Stear JH, Leonhardt H, Cardoso MC. Histone acetylation controls replication timing of constitutive heterochromatin. *Under revision*.

Herce HD, **Casas-Delucchi CS**, Cardoso MC. Image co-localization and spatial correlation of objects in multicolor images as a measure of interactions between bio-molecules. *In preparation*.

Piebes DGE, MC Brink MC, Luijsterburg MS, de Groote ML, **Casas-Delucchi CS**, van Driel R, Rots MG, Cardoso MC, Verschure PJ. MeCP2 revisited: chromatin decondensation and HP1γ displacement without transcriptional activation. *In preparation*.

Teller K, Illner D, **Casas-Delucchi CS**, Thamm S, Joffe B, Cremer T, Cremer M. Large scale folding structure of the active and inactive X in human fibroblasts. *In preparation*.

Conference contributions

2nd MC-GARD Meeting on Higher Order Genome Architecture: Interplay among genetics, epigenetics and non-coding RNAs, Madrid (Spain) May 4 – 7, 2008

Poster: "Chromosome territories and nuclear architecture: a study using native and transgenic XIST inactivation "
Poster: "Epigenetic Control of Heterochromatin Replication"

XX International Congress of Genetics, Berlin (Germany); July 12 – 17, 2008

Poster: "Epigenetic Control of Heterochromatin Replication"

3rd MC-GARD Meeting on Higher Order Genome Architecture: Higher order genome architecture, Edinburgh (Scotland) April 1 – 5, 2009

Oral presentation: "Epigenetic Control of Heterochromatin Replication"

EMBO Meeting on Nuclear Structure and Dynamics, Isle sur la Sorgue (France) Sep 30-Oct 4, 2009

Poster: "Epigenetic Control of Heterochromatin Replication"

3rd Intl Congress on Stem Cells and Tissue Formation, Dresden (Germany) July 11 – 14, 2010
Poster: "Histone acetylation controls the synchronous replication of the inactive X chromosome"

International Summer School: From Pluripotency to Senescence. Molecular Mechanisms of Development, Disease and Ageing, Island of Spetses (Greece) Aug 21 – 30 2010

Poster prize and oral presentation: "Histone acetylation controls the synchronous replication of the inactive X chromosome"

Index of electronic supplementary material

Supplementary movies:

1 Histone acetylation controls the inactive X chromosome replication dynamics

Movies Xi 1 – 4: Dynamics of DNA replication visualized by GFP-PCNA.

2 Histone acetylation controls replication timing of constitutive heterochromatin

Movies CC 1 – 2: Time lapses of control (Movie 1) and treated (Movie 2) WT MEF progressing through S-phase.